STRUCTURAL ANALYSIS, EVALUATION AND STRENGTHENING OF THE TEMPLE OF AUGUSTUS IN ANKARA

A THESIS SUBMITTED TO
THE GRADUATE SCHOOL OF NATURAL AND APPLIED SCIENCES
OF
MIDDLE EAST TECHNICAL UNIVERSITY

BY

BURAK UÇAK

IN PARTIAL FULFILLMENT OF THE REQUIREMENTS
FOR
THE DEGREE OF MASTER OF SCIENCE
IN
CIVIL ENGINEERING

FEBRUARY 2016

Approval of the thesis:

STRUCTURAL ANALYSIS, EVALUATION AND STRENGTHENING OF THE TEMPLE OF AUGUSTUS IN ANKARA

submitted by **BURAK UÇAK** in partial fulfillment of the requirements for the degree of **Master of Science in Civil Engineering Department, Middle East Technical University** by,

Prof. Dr. Gülbin Dural Ünver
Dean, Graduate School of **Natural and Applied Sciences** _____

Prof. Dr. İsmail Özgür Yaman
Head of Department, **Civil Engineering** _____

Prof. Dr. Ahmet Türer
Supervisor, **Civil Engineering Dept., METU** _____

Examining Committee Members:

Prof. Dr. Altuğ Murat Erberik
Civil Engineering Dept., METU _____

Prof. Dr. Ahmet Türer
Civil Engineering Dept., METU _____

Prof. Dr. Oğuzhan Hasançebi
Civil Engineering Dept., METU _____

Prof. Dr. Neriman Şahin Güçhan
Architecture Dept., METU _____

Asst. Prof. Dr. Burcu Güldür
Civil Engineering Dept., Hacettepe University _____

Date: 01.02.2016

I hereby declare that all information in this document has been obtained and presented in accordance with academic rules and ethical conduct. I also declare that, as required by these rules and conduct, I have fully citied and referenced all material and results that are not original to this work.

Name, Last name : BURAK UÇAK

Signature :

ABSTRACT

STRUCTURAL ANALYSIS, EVALUATION AND STRENGTHENING OF THE TEMPLE OF AUGUSTUS IN ANKARA

Uçak, Burak
M.S., Department of Civil Engineering
Supervisor: Prof. Dr. Ahmet Türer
February 2016, 133 pages

The temple of Augustus in Ankara has stood as a keeper and witness of the region's historical past for hundreds of years from the time of Galatians and Romans. Bearer of the sign of ancient times not only as carved on its walls but also with its architectural and structural features, this monument now is in the need of engineering intervention to cope with the risk of collapse. Consequently, its structural behavior was analyzed using nonlinear discrete element modeling and linear finite element modeling and several relevant strengthening methods were proposed within this study. Initially, the structure was tested for its ambient vibration characteristics to compare against the analytical model for calibration and its earthquake resistance capacity was investigated with calibrated linear elastic and discrete element analytical models. Measurements recorded by long term structural health monitoring devices previously installed on the structure were also collected and post-processed. Finally, four different strengthening methods divided into two main groups, prepared with "minimum possible intervention" principle in mind, were proposed and their contribution to overall seismic resistance was evaluated.

Keywords: Temple of Augustus, Monumentum Ancyranum, Historical Masonry Structures, Discrete Element Modelling, Structural Health Monitoring, Strengthening

ÖZ

ANKARA AGUSTUS TAPINAĞININ YAPISAL ANALİZİ,
DEĞERLENDİRMESİ VE GÜÇLENDİRİLMESİ

Uçak, Burak
Yüksek Lisans, İnşaat Mühendisliği Bölümü
Tez Yöneticisi: Prof. Dr. Ahmet Türer
Şubat 2016, 133 sayfa

Ankara Agustus Tapınağı, Galatyalıların ve Romalıların devrinden beri yüzyıllardır bölgenin tarihi geçmişine muhafızlık ve tanıklık etmiştir. Kadim zamanların izini yalnızca duvarlarına kazınmış olarak değil, aynı zamanda mimari ve yapısal özellikleri ile üzerinde taşıyan bu anıt, bugün, yıkılma tehlikesi ile başa çıkabilmek için mühendislik müdahalesine ihtiyaç duymaktadır. Bu doğrultuda, bu çalışma neticesinde anıtın yapısal davranışı doğrusal olmayan ayrık eleman ve doğrusal sonlu eleman modelleri kullanılarak çözümlenmiş ve bunlara uygun çeşitli güçlendirme yöntemleri önerilmiştir. İlk aşamada yapı, oluşturulan analitik modellerle karşılaştırmak üzere ortam titreşimi özellikleri açısından test edilmiş ve depreme dayanım hususundaki yeterliliği bu test sonuçlarından çıkartılan veri ile ayarlanarak doğrulanmış doğrusal-elastik ve ayrık eleman analitik modelleri ile incelenmiştir. Yapıya daha önce yerleştirilmiş olan uzun vadeli yapısal sağlık izleme cihazları tarafından kaydedilen ölçümler de ayrıca toplanmış ve işlenerek gözden geçirilmiştir. Sonuçta, "mümkün olan en az müdahale" ilkesi göz önünde bulundurularak iki ana grup altında toplanmış dört güçlendirme yöntemi önerilmiş ve bunların yapının genel deprem dayanımına olan katkısı değerlendirilmiştir.

Anahtar Kelimeler: Agustus Tapınağı, Monumentum Ancyranum, Tarihi Yığma Yapılar, Ayrık Eleman Modelleme Yöntemi, Yapısal Sağlık İzleme, Güçlendirme

To Preservation of History

ACKNOWLEDGEMENTS

This thesis was completed under the supervision of Prof. Dr. Ahmet Türer. First and foremost, I would like to offer him my deepest gratitudes not only for his support and guidance during the course of this work, but also for presenting me with the opportunity to work on this study which brought my profession, civil engineering, together with my enthusiasm, history and archeology.

I also would like to extend my thanks to Assoc. Prof. Zeynep Gülerce for her advice in the very important ground motion selection process, Asst. Prof. Dr. Özgür Kurç for reserving me a part of the computer cluster for my extremely time consuming discrete element method analyses and Research Assistant Utku Albostan for his helping hand during this process. Evaluations and contributions of the thesis committee are also gratefully acknowledged.

I wish to express my gratefulness to my parents, Ahmet Uçak and Nazmiye Uçak, along with my sister, Ceren Aslaner and her spouse, Levent Aslaner, for their endless encouragements and moral support.

I gratefully acknowledge Uğurcan Özçamur and Barış Ünal for their assistance and patience throughout my studies, and my beloved Gözde Güney Doğan for her optimism and support. Similarly, I would like to thank Berke Sayın, Barış Güner, Batuhan İşcan and all my workmates for their motivation and tolerance.

TABLE OF CONTENTS

LIST OF TABLES

LIST OF FIGURES

CHAPTER 1

INTRODUCTION

This chapter aims to describe the Monumentum Ancyranum, an ancient structure; elaborating on its architectural features and historical importance. Current structural condition of the monument, along with the previous investigations and conservation studies will be addressed in detail. Vulnerabilities that leave this structure in need of intervention, objectives of this study and the scope of the research will also be covered.

1.1 Monumentum Ancyranum

Monumentum Ancyranum, also referred to as the Temple of Augustus and Rome, is located in the Ulus district in the city of Ankara. It was constructed between the years 25-20 BC, on the ruins of an earlier temple to the Phrygian god Men, which in turn was built in 2nd century BC (Rose, 2000). The monument was erected following the official formation of Galatia as a Roman province, by the first emperor of Rome, Augustus Caesar; and was meant to facilitate as a display of fidelity of Pylamenes, the King of Galatia, to the Emperor. It was registered as a first order cultural asset in 1972 and was declared as a monument to be preserved by World Monument Fund in 2000.

Upon death of Augustus in 14 AD, his funerary inscription, written down by himself shortly prior to his death, called *Res Gestae Divi Augusti*, the Deeds of Divine Augustus, was read aloud in the Senate and carved unto two bronze pillars in Rome (Dereli, 1949). The text was also sent to be carved upon temples and

monuments all across the Empire. *Res Gestae* Today the bronze pillars are lost, but some of the copies survive; the most important being the copy on the Temple of Augustus in Ankara, which was preserved almost as a full copy, in original Latin and as a translation to Greek, carved upon the walls of the monument. Some parts of text are also found at Antiochia (modern Yalvaç) and Appollonia (today Uluborlu), both located within the province of Isparta, Turkey (Dereli, 1949).

Res Gestae Divi Augusti

Res Gestae is basically an official autobiography of the first emperor of Rome, Augustus Caesar, and it has a first-person narrative (except for the introduction part, which has a third person narrative and was most probably added later). It consists of a short introduction, 35 paragraphs grouped into four parts; his political career, his donations to the public, his military achievements and a political statement regarding the approval of his time on the throne by the people of Rome and his accomplishments. The full title of provides a healthy insight to the contents of the text: "accomplishments of *divus* Augutus, by which he attached the whole world to *imperium* of Roman people, and of expenses he incurred with respect to *res publica* and Roman people (Ehrenberg & Jones, 1955/2003)". In the text, the names of his enemies are never mentioned, but are referred to as "pirate" (referring to Sextus Pompeius), "with whom I fought the war" (referring to Marcus Antonius), and "murderers of my father" (referring to Brutus and Cassisus) (Eck, 2007). The text is, by its nature, propaganda; a justification of the title and position he held as the emperor for a very long time. However still, it is of tremendous importance and unbelievably high value for historians not only because it is a first person account of Augustus' rule, but also because it also reveals his perception of the people of Rome (Dereli, 1949).

Figure 1.1: Res Gestae on the temple exterior

Today the inscription can be found in the original Latin version on the pronaos side of antae and the coroneted gate section. The Ancient Greek translation of the text, on the other hand, was carved onto the exterior of the southwestern wall.

1.1.1 Historical Background

In the year 278 BC, at an invitation of Nicomedes I of Bithynia, who was at the time in a power struggle with his brother for the throne the kingdom, a group of Celts crossed the Bosphorus from eastern Thrace into Asia (A map showing ancient regions of Asia Minor is provided in Figure 1.2 (a)). These Celts, called Galatae by the historians of the time, were a part of a greater Celtic migrating horde led by

Brennus, who invaded Macedon in 281 BC; but they had broken away from the main group in 279 BC and migrated to Thrace under their leaders Leonnorius and Lutarius (Hammond & Walbank, 1972). The Galatae (Galatians), consisted of three separate tribes; Trocmi, Tolistobogii and Tectosages; and numbered about 20,000 men and women.

After successfully establishing his claim to the throne of Bithynia, Nicomedes I employed the Galatians in his war against Seleucid king Antiochus I, where they were heavily defeated in the so called "Elephant Battle" in 275 BC (Rankin, 2002). Antiochus had concealed the 16 elephants he had in his army before the battle, and when they were released at the start of the encounter, Galatians, and their horses pulling the chariots, never having seen an elephant before, broke before swinging a single sword (Fowler & Fowler, 1905).

Even though they were beaten, the existence of Galatians in Asia was far from being over. The three tribes, Trocmi, Tolistobogii and Tectosages, eventually settled at the eastern Phrygia, in the cities of Tavium (near modern city of Yozgat), Pessinus (modern Sivrihisar) and Ancyra (Ankara), respectively. They retained the position of ruling military society and taxed the locals who continued to tend the land. They were often hired to serve as mercenaries by the warring Greek kings, sometimes fighting in both sides in great conflicts. Celtic warlords also continued to carry out frequent and devastating raids in the western Anatolia for long years (Rankin, 2002). This came to an end when they sided with Antiochus Hierax, a rebel Seleucid prince against Attalus of Pergamon. Galatians suffered heavy defeats in this war; their momentum was broken and they were confined to their own land by a formal agreement around the year 232 BC (Rankin, 2002). This land was started to be called as Galatia by the surrounding peoples. The famous sculpture called "the Dying Gaul" depicts the status of Galatians in this period (Figure 1.2. (b)).

(a) (b)

Figure 1.2: Ancient Regions of Anatolian Peninsula (a) Roman Copy of Dying Gaul, 1st or 2nd Century, AD. Musei Capitolini, Rome, Italy (b)

Galatians allied themselves with Seleucid king Antiochus the Great in the early 2nd century BC, in his battle against Rome. However Antiochus was unsuccessful in his campaign and was defeated twice by the Romans in the Battle of Thermopylae in the Greek peninsula and in the Battle of Magnesia in Asia. Having landed on Asia, in 189 BC Romans attacked Galatians and humiliated them in the Battle of Mount Olympus and in the Battle of Ancyra (Bettison 1976). Galatia was dominated by Romans from then on. They supported Rome in the Mithridatic Wars, and became a client state to it by 64 BC when a three leader system (one for each tribe) was imposed on them by Pompey. One of these leaders, Deiotarus, who lived at the time of Julius Caesar and Marcus Antonius, dominated the other two tribe leaders and was recognized as the king of Galatians (Rankin, 2002). Following his death, Galatia was given to Amyntas, the prince of Lycaonia and a former supporter of Marcus Antonius, who had defected to the side of Augustus (Rankin, 2002). It was finally made into a Roman province by Augustus. The temple of Phrygian god Men in Ancyra was rebuilt in the name of Augustus by the heir of Amyntas, called Pylamenes, as a display of loyalty to him. *Res Gestae* was carved on the walls of this temple, where it was preserved until today.

1.1.2 Architectural Characteristics and Structural Features of the Monument

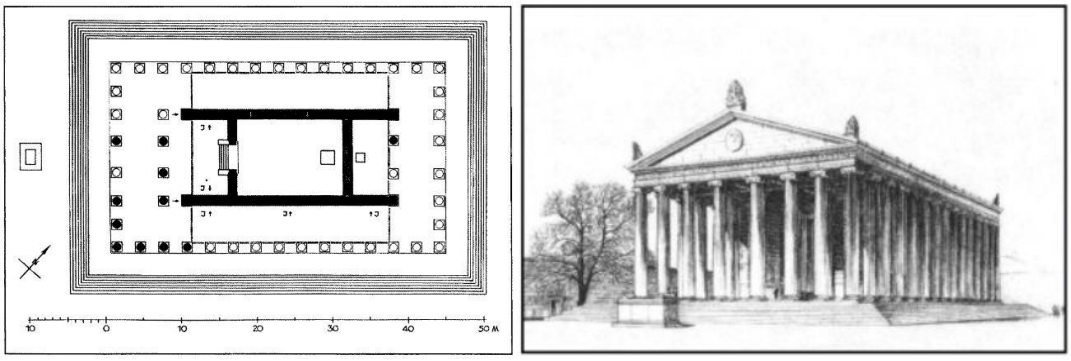

(a) (b)

Figure 1.3: Original Plan of the Temple, where sections of naos can be identified as pronaos, cella and opisthodomos from left to right (a) Imagination of the temple in its intact form. From *Der Tempel in Ankara*, Krencker and Shede, 1936 (b)

The Temple of Augustus and Rome was built in accordance with the Corinthian order, which was the last to be developed of the three main Greek and Roman orders, the other two orders being the Doric order, developed earliest, and the Ionic order, developed next. The marble temple has a pseudodipteral plan (Figure 1.3 (a)), located on an area of 36mx54.82m, elevated on a platform by 2 meters. It sits on the southwest – northeast direction. It was adorned with 8 ionic columns on the short sides and 15 ionic columns on the long sides forming the peristyle. The internal complex (naos) consisted of three sections, "pronaos" (inner area of the portico), "cella" (the central chamber) and "opisthodomos" (rear porch). There used to stand four Corinthian columns in the pronaos and two more in the opisthodomos, located between the extensions of lateral walls, in consistency with the "in antis" style ("The Augustus Temple of Ankara", 2015). Access to the cella was provided through the main gate with ornate lintel, located at the rear end of pronaos. Cella was the sacred chamber of the temple where only the priests were allowed to enter. It also had an elevated floor which was approximately 1 meter above the

surrounding platform, and housed the divine statue of the temple (Perrot & Guillaume, 1872) (Figure 1.4).

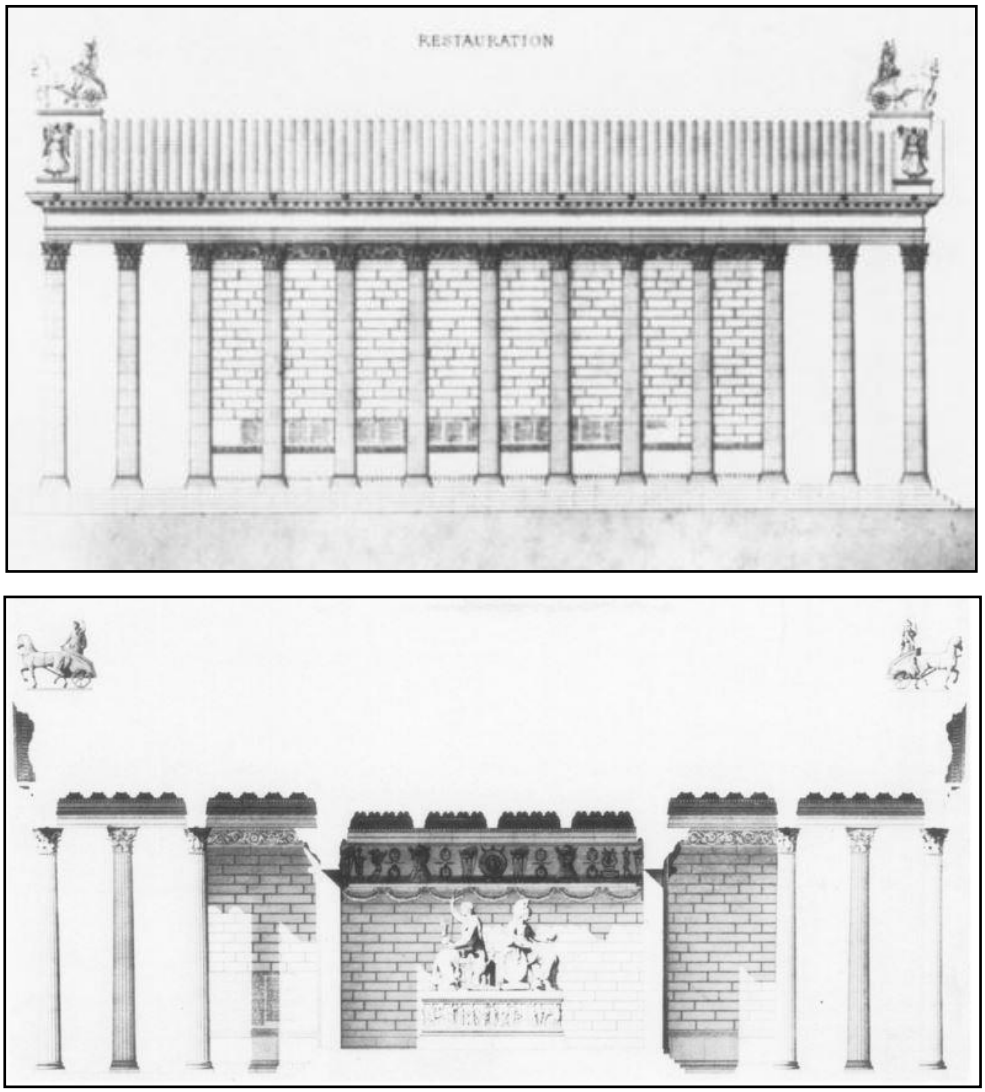

Figure 1.4: Reimagination of the temple, from the southeastern point of view (Top) Cross section view with the statues of Rome and Augustus (Bottom) From *Exploration archeologique de la Galatie et la Bithynie*, G. Perrot and E. Guillaume, 1872.

The monument went through various changes to its architecture in later time periods. In the 6th century, during the Byzantine period, it was converted to a Christian church. Cella, originally an enclosed space designed not to receive any sunlight, was illuminated by the introduction of three large windows on the southwestern wall. Its elevated floor was leveled down to the platform height. Most significantly, the wall between cella and opistodomos was removed, instead of which an apsis wall and a crypt was built ("The Augustus Temple of Ankara", 2015).

In the years 1427-1428, a mosque, Hacı Bayram Camii, was built with a corner intersecting with the western tip of the northwestern wall (Figure 1.5). Basing their ideas on the writings on the various parts of the walls, some scholars consider that the temple building might have been used as a madrasa, a Muslim theological school, for some time (Greenhalgh, 2013).

Middle portion of the northwest cella wall was substantially damaged in 1834 (Greenhalgh, 2013). Today, the temple is missing all of its columns, along with its roof. On the other hand, most parts of the core; the northern portion of the northwestern wall, along with the southeastern wall and the gate section were preserved, with Res Gestae inscription almost intact. In addition to the Res Gestae, on the northern anta of the northwestern wall, a list of emperor cult priests and their achievements; and on the southern anta of the same wall, a short inscription about another priest from a later period, were also preserved.

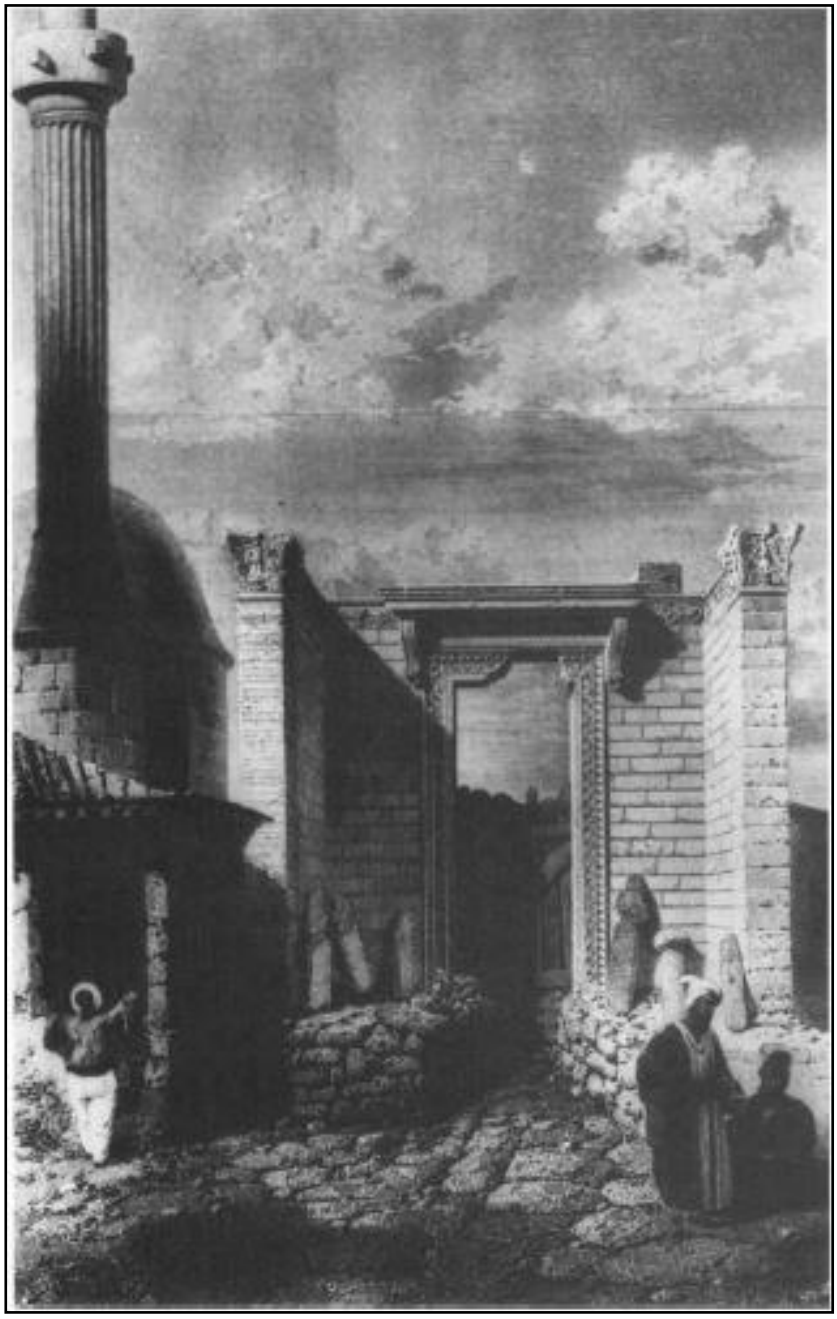

Figure 1.5: A view from the front of the temple along with the minaret of the nearby mosque of Hacı Bayram Camii from 1830's. Some part of Res Gestae carved unto ante is visible. From *Description de L'Asie Mineurel*, C. Texier, 1839

Temple walls exhibit a simple and regular order. With the exception of the gate section, the walls are made up of 23 layers of stone. The ornamented bottom layer has a cross section that resembles a rectangle at the bottom half and trapezoid at the top half. Approximate height of the layer is 45 cm, and the width varies from around 135 cm at rectangular portion to 110 cm at the top of the trapezoidal portion. Next layer is placed as two rows in vertical, except for the extreme ends of the walls (anta). This layer has a height of 120cm, showing slight changes in the order of centimeters on different sections of the wall. Width of the layer is 1 meter. This layer is followed by a layer with ornamented units, with a height of 34 cm and width that is barely over a meter that is mostly due to the ornaments. Similar to the previous layer, it is possible to observe double rows in vertical direction on this layer as well. Following 19 layers are considerably uniform, with each having 45 cm height and approximately 90 cm thickness, on average. The wall thickness displays a subtle taper, where it gets smaller with each layer. Length of the stone units shows a high variety; they range from slightly above 3.5 meters to as low as half a meter, but most of the units have a length around 1.7 meters. The stone laying order resembles ashlar masonry and the units are chamfered. Finally on the topmost layer, which is also ornamented, height is increased to 60 cm and the width back to an average of 1 meter. Regularity of the cross section geometry is lost due to wear, but reverse taper is distinguishable. On this layer, it is also possible to observe the coincident slots on the interior sides of southeastern and northwestern lateral walls, where most probably the wooden beams of the roof used to rest.

Consequently the remains of the temple reach up to an approximate height of 11.20 meters. Length of the original longitudinal walls placed in the southwestern - northeastern direction is roughly 28.20 meters. Center to center distance between these walls is about 11.35 meters; with the total distance changing in accordance with layer thickness.

As mentioned earlier, the wall between cella and opisthodomos was demolished and a new apsis wall was built when the temple was converted into a church.

Location of the old opsithodomos wall is still noticeable on the interiors of lateral walls; however, on the contrary, Byzantine era apsis wall can only be traced by the crypt walls located between the ante of old opisthodomos. This wall section and the crypt were not constructed using the material of the original temple, that is marble, but local stones were employed. With the inclusion of the crypt section, the length of the temple core was increased from around 28 meters to 37.5 meters. This crypt is accessed from inside the temple through a small gate.

Figure 1.6: A general view of the temple from southern vantage point, as seen on a postcard of Museum of Anatolian Civilisations, Ankara

The connection of main gate section between the pronaos and cella to the lateral walls was established by means of T shaped stones on alternating layers in the regular 19 layer portion. On each side of the gate, a column with 8.3 meter height with approximately 0.7m x 0.7m base area. These columns again display a slight

taper. The coroneted door lintel, on the other hand, has a complex structure which had to be specifically discretized for discrete element analysis. A view of the temple it is current from, before the latest interventions, is presented in Figure 1.6.

This remaining core portion of the temple features an ancient stone masonry building technique of Opus Revinctum, which may be translated from Latin as "binding work".

The masonry units of the ancient times, bricks and stones, have substantial compressive strength. They, however; perform poorly under tensile and shear stress. When such stresses develop, they must be transferred to the rest of the structural elements and the integrity of the structure must be preserved. This robust technique used by the ancient masons prevailed under such conditions.

Opus Revinctum

Historically, many important structures were made applying Opus Revinctum, where iron connectors embedded in lead casing were employed to attach blocks of masonry to each other, in order to hold together columns and masonry walls during frequent earthquakes in the Aegean region (Kázmér, Major, Hariyadi, Pramumijoyo & Haryana, 2010). The method was actually recommended by Vitruvius in his 2000 year old work "De Architectura Libri" for those who do not want the structures they build to perish in time.

Traditionally, dowels were used to provide stability in the vertical direction while clamps were employed in the horizontal direction (Figure 1.7). Before the usage of iron; these connectors were made of wood, bronze and lead. However, most frequent material of choice was iron, which is, despite being stronger than other materials, prone to corrosion. Corroded iron expanses, which causes serious damage in the masonry units. In order to prevent iron from corroding, molten lead was poured in the area surrounding the iron connector, in order to serve as a barrier

between the iron connector and the atmosphere (Schueremans, Ignoul, Lembrechts, Vandewalle, Gemert, Balen, 2003).

Covering of the iron connector in lead not only prevents it from corrosion, but also provides ductility in the joint and creates additional energy absorption capacity. Moreover, the relatively low melting point of lead (~380°C) makes in-situ production easier.

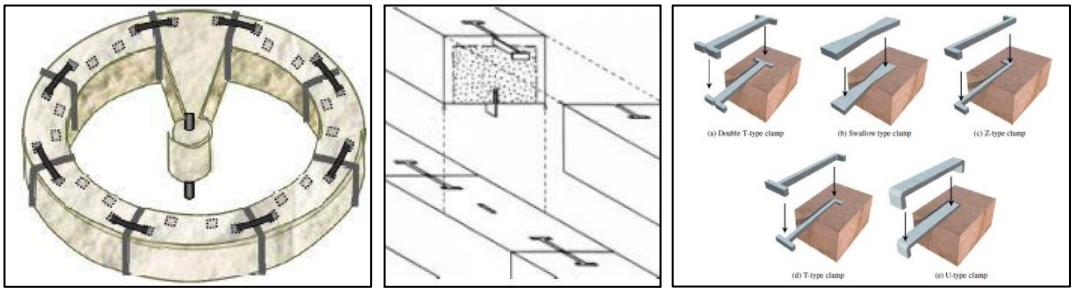

Figure 1.7: Various types of dowels and clamps, used in various types of structures. From *Seismic Performance of Historical and Monumental Structures*, H. Sezen and A. Dogangun, 2012

Unfortunately working with molten lead requires skilled handiwork: The linear expansion coefficient of lead (29.1μm/m°C) is higher than the value of common construction materials (natural stone: 4-12 μm/m°C, cast iron: 10.5μm/m°C, steel: 12-13 μm/m°C); therefore if lead is poured too fast or too much, or simply when it is too hot, it may create thermal stresses that exceed the tensile strength of stone and cause cracks. Moreover, if molten lead comes in contact with water in any way, rapid evaporation of water due to the heat of the lead causes explosive reaction (Sezen and Dogangun, 2012). Moreover, molten lead releases toxic fumes, and will burn the limbs of workers even in the case of a small leak. Presence of such hazards at the work site may have led to dismemberment of workers and poor production of the joints.

In general there were two different methods employed in the execution of joints. In the first one (Figure 1.8, (a)) a canal to cast the molten lead is drilled in the upper stone, the upper stone is laid upon the lower stone with the dowel in between, then the lead is poured from the canal. In the second method (Figure 1.8, (b)), the upper stone is placed upon the lower one after the dowel is placed into the hole with lead encasing, a gap between the two stones and a canal for the air to leave is provided, and then with the help of a funnel, molten lead is poured in between the stones (Schueremans et al, 2003).

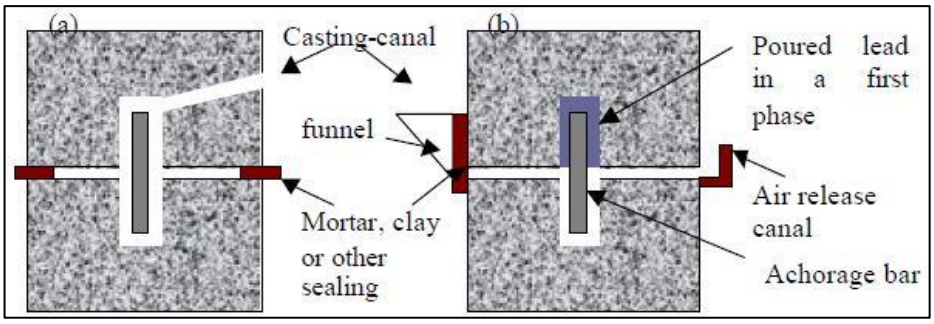

Figure 1.8: Different methods employed in the joint realization. From *Metal anchors in lead, fundamental approach and alternatives*, Schueremans et al, 2003

Lead has good resistance to corrosion in most environments. After hardening, a protective layer of lead sulphate is formed at its surface. Therefore, theoretically, covering iron connectors mechanically in this medium is a very good idea. In reality, however, iron was often found to be corroded. Encountering completely corroded iron braces is not a rare sight (Schueremans et al, 2003). Expansion of corroded iron severely damages the stones. Since corrosion process is started with an electrolyte, humidity must be penetrating into the iron connectors.

The problem is to be found not solely at the materials, but at the execution of the joints, since if the iron was fully covered, corrosion would not occur. Most of the time lead was found not to have fully encapsulated the iron. Extreme ends of the

iron connectors are often in contact with the stone. In vertical connections lead does not fill the void all the way to the top. In horizontal connections most of the time only the end parts of the clamp is covered.

Despite these problems encountered in the production of these type of connections, a proof of the durability and integrity provided by the use of iron clamps can be observed in the number of such historical structures survived to this day, including Parthenon in Athens (447-432 BC), Colosseum in Rome (70-80 BC), Hagia Sophia in Istanbul (573 AD), and many surviving mosques and their minarets from the Ottoman period. Moreover, the frequency of the application of such connectors can be observed in the ruins of Greek and Roman settlements dating back to the period, around the Aegean Sea. The picture given in Figure 1.9 was taken by the author at the Temple of Augustus, showing the marks of Opus Revinctum on the temple blocks at a cracked section.

Figure 1.9: Marks showing the application of Opus Revinctum on the temple

1.1.3 Current Structural Condition of the Monument

As mentioned briefly in the previous section, the southeastern wall, along with the damaged northwestern wall and the gate section between the pronaos and cella are the surviving parts of the monument.

Damage to the northwestern wall basically divided it into two parts: The part in the south that is connected to the rest of the temple and the northern part, which is standing on its own without support. This northern part of the wall is connected to the Byzantine era crypt wall, but being too short in comparison, this wall does not provide enough support, leaving the north part of the northwestern wall a cantilever wall. This cantilever wall part has a varying length due to the shape of the crack, but in average it is around 10 meters. Section between this cantilever wall and the rest of the northwestern wall was later filled in with a disorderly rubble wall. This rubble wall extends halfway beneath the cantilever wall (Figure 1.10), where some stone blocks are missing in the interior (Interior counterparts of double leaf layers are missing, but the exterior counterparts intact). As a result, the cantilever wall displays a tilt of 3 degrees, reaching up to 52 centimeters at the top section, displaying a bending-twisting behavior. Progress of this tilting was measured and it will be discussed in detail in this study. Although the wall shows no tilt at the other end; this unstable behavior may lead to very undesirable consequences, since the wall is unsupported. This section is the most troubled part of the temple, where risk of collapse, especially in the case of an external trigger such as an earthquake, is very high. A plan of the temple's current form is given in Figure 1.11.

Figure 1.10: A pre-intervention system view of the northern isolated wall, showing the extention of the rubble wall beneath it.

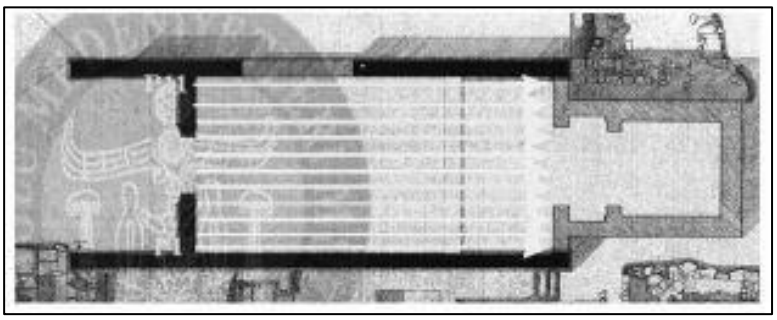

Figure 1.11: The current plan of the temple with the surviving sections (retrieved from http://www.anadolumedeniyetlerimuzesi.gov.tr/TR,77863/plan.html, 2016)

Similar to a degree with the abovementioned cantilever wall, the inner leaf blocks of the double leaf layer of the southeastern wall were also removed; and they were

replaced with a rubble wall similar to what was mentioned above in some parts; and in other parts blocks of local material (andesite) were used to support the structure. Fortunately, the southeastern wall is connected to the gate section and instability is not a visible risk. The ornate lintel of the gate section is also in a deteriorated state, where an earlier attempt to intervene with metal strips, is visible. Its balance is prone to be disturbed by a slight external effect, and this may lead to its loss with a collapse (Figure 1.12).

Figure 1.12: Door lintel in a deteriorated state. Intervener and the date of intervention are unknown.

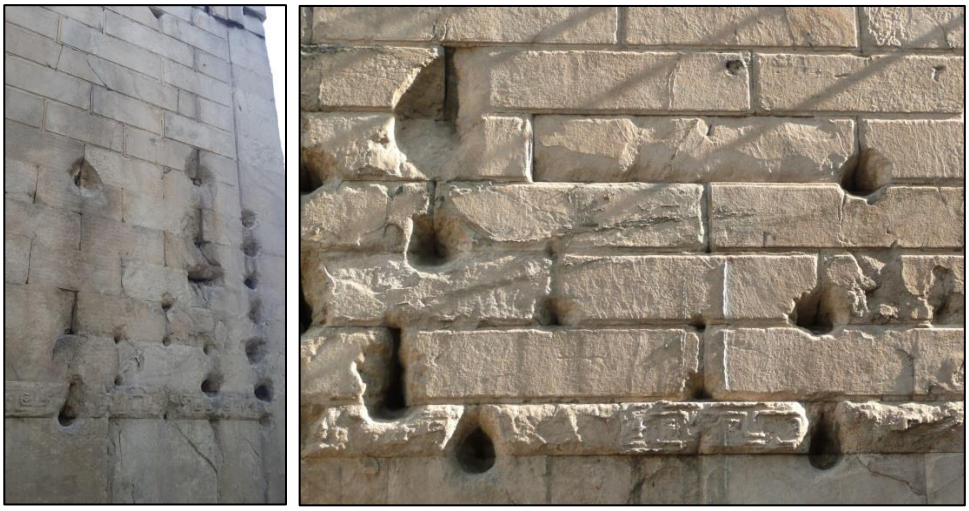

Figure 1.13: Drilled holes on the walls

In addition to the aforementioned local defects, all around the structure there are holes on the walls, especially at the intersections of masonry blocks, caused by uncertain reasons. They may have been drilled by treasure hunters in pursuit of iron clamps or the encapsulating lead. Another cause may be the expansion of iron connectors as a result of corrosion (Figure 1.13). Furthermore, as a result of two thousand years of exposition to adverse effects of the atmosphere, all round material degradation can be observed on the blocks.

A set of pictures are provided in Appendix A showing the most recent form of the temple with the emergency intervention system.

1.2 Previous Structural Identification and Strengthening Studies on the Monument

Even though the *Res Gestae* inscription has sparked the attention of western scholars starting from the 16th century, the temple itself and its condition has been started to be studied only in the recent years, albeit intensely.

Earlier in the 20th century, a study was conducted by M. Schede and D. Krencker on the temple, regarding the temple structure and the inscriptions, compiled in their work *Der Tempel in Ankara* (1936). More recently, following the call of famous Turkish archeologist Ekrem Akurgal to save the memory of Augustus in Ankara, a research program was approved by the University of Trieste, named the Ancyra Project in 1997. This project, led by Paula Botteri and primarily funded by the Italian Ministry of Foreign Affairs, received participation from various departments of the University of Trieste, along with other professionals and individuals from a wide amount of centers and universities internationally (Botteri & Fangi, 2002). The main aim of the study was to examine the epigraphic content of the Greek version of the *Res Gestae Divi Augusti*, along with a metrical and topographical survey of the temple itself. The expected outcome was to come up with a plan to

protect the inscriptions, stop the degeneration of the text, and ensure temple's stability. As a result of a wide range of studies, the whole plan of the site, mineralogical and petrographic analysis results, photogrammetry of the Greek and Latin inscriptions and the tachogrametric and photogrammetric survey of the temple structure were obtained. In generation of the numerical models used in this study, these survey results were employed primarily. Preliminary plans for the stability of the temple were also drafted with this study. Many publications were released as products of this work, with some of the results being wrapped up in The Ancyra Project: The Temple of Augustus and Rome in Ankara, P. Botteri & G. Fangi, 2002.

In 2006, a structural analysis study was carried out by Turer and Eroglu, consisting of the determination of natural vibration frequencies of the temple experimentally, generation of a computer model calibrated with the results of this experiment and the evaluation of seismic risk posed on the structure. As a part of the work, plans and proposals to ensure the stability of the temple, were also provided. In this thesis, experimental results obtained by Turer and Eroglu (2006) are also referred. Their work was released under the title Structural Analysis of Historic Temple of Augustus in Ankara, Turkey, A. Turer & T. Eroglu (2006).

In 2007, an emergency intervention system was installed as a part of an Ankara Metropolitan Municipality project, by ATAK Engineering Company. This current emergency intervention system was initially designed to restrict lateral temple walls (southeastern wall and the isolate north wall) in the out-of-plane direction, the vulnerability of which during seismic activity was also revealed in this study. A further aim of this system was to preserve the visibility of the inscriptions on the temples exterior; therefore the "mass" of the system was placed inside the temple. Basically a truss system, it was intended to be made of easily transportable, light parts that would make its construction at the site easier. The truss system is made up of slender elements with diameters ranging from 6cm to 13.9cm; with the desired strength provided through a frequent employment of these elements. The

foundation blocks were selected as 50cm x 50cm cross-sectioned blocks extending from one lateral wall to the other. A view of the system from different axes is provided in Figure 1.14.

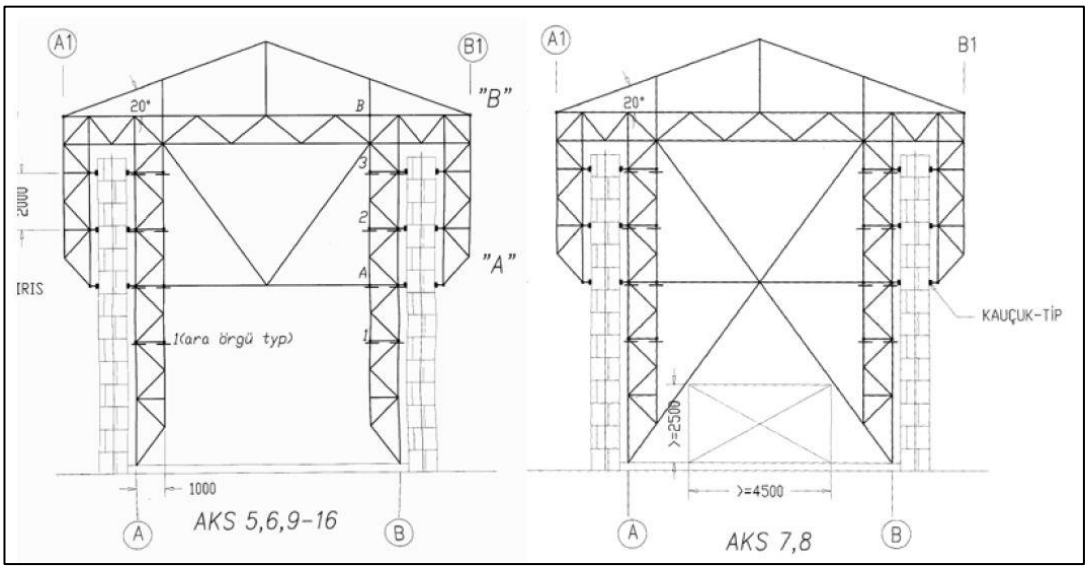

Figure 1.14: Emergency intervention system, viewed from different axes.

This system also features rubber pads at the protruding ends of the truss, originally designed not to get in contact with the walls themselves. Unfortunately, while the design was progressing with academic support from Middle East Technical University, the construction was started without the final consent of the supporting professors, leading to a number of problems uncalled for in the original design. The rubber pads, designed not to be in contact with the walls, were built contacting them, affecting the walls' behavior. Contrary to the academic advice, Portland cement was used in the foundation blocks, which may lead to material degradation of the temple walls surrounding and beneath it. Moreover, the roof of the system seen in the Figure 1.14 was not built, leading the further exposition of the temple and the inscriptions outdoor conditions such as acid rains and snow.

In 2008, an archeometrical investigation was carried out by Kadıoğlu and Akyol, aimed at the determination of the temple blocks' basic physical properties (hardness, density, porosity and moisture capacity) along with other properties using various analytical methods and laboratory tests. The ultimate objective was to identify the layer samples of rocks, blocks, soil samples and iron connectors, in addition to the estimation of the source of rocks constituting the temple. The presence of the iron connectors within the existing sections of the walls were also proven with the help of ground radar analysis conducted as a part of this study (Figure 1.15). Their work was published under the name of Augustus Tapınağı 2008 Yılı Arkeometrik Çalişmalari, Y. K. Kadıoğlu & A. A. Akyol, 2008.

Figure 1.15: Iron connector samples from the Temple of Augustus. From *Augustus Tapınağı 2008 Yılı Arkeometrik Çalişmalari*, Y. K. Kadıoğlu & A.A. Akyol, 2008.

In 2009, a structural health monitoring system consisting of two tiltmeters and two temperature transducers were installed at the site on the northern isolated wall by A. Turer, as prescribed in his previous study Structural Analysis of Historic Temple of Augustus in Ankara, Turkey, (A. Turer & T. Eroglu, 2006). The measurements recorded by these transducers were obtained and post processed in this study.

In addition to the studies listed in this section, there are many others that can be found in the literature focused on the materials constituting the temple, the inscriptions and the architectural and structural system of the temple. The monument, with its central location in the Turkish capital, continues to attract the attention of researchers both domestically and internationally.

1.3 Definition of the Problem

As mentioned in detail in Section 1.1.3, the temple structure encounters many problems. The main problem is its stability concern in the case of a seismic action. The northern isolated wall is missing some of its original blocks in the lowest layers in the interior, it is tilting and thus it is in a critical state against collapse. Some of the blocks protruding from its southern end at the topmost layers pose a danger of falling. The southern end of the southeastern lateral wall has cracks and may pose a danger of collapse. The complex of blocks forming the ornamented gate lintel are cracked and damaged, facing a danger of disintegration and instability. The portland cement based footing of the emergency support system poses a chemical attack hazard for the original blocks surrounding and beneath it. There are holes in the walls and the iron connectors between the blocks are possibly rusted, losing their effectiveness in supporting the structure. There is overall material degradation and along with a structural hazard, this poses a danger for the invaluable inscriptions on the temple walls. Therefore, the structure is in the need of a permanent strengthening system that will address these problems.

1.4 Objectives

A substantial portion of the Temple of Augustus and Rome survived for more than two thousand years until today, and the preservation and conservation of this invaluable historical relic for many years and many generations is of tremendous importance. The aim of this study is to identify and analyze the current performance

of the temple against the foremost hazard of earthquakes, followed by propositions and evaluations of various strengthening systems to make sure that this monument that is a unique piece of local and global heritage and a legacy of earlier peoples and this land can be transferred to the future, safely.

In order to achieve this aim, the first target of this thesis was determined as the structural identification of the monument through dynamic ambient vibration measurements and long term structural health monitoring. Successful execution of these tasks would also increase the accuracy of other tasks since the outputs of this target are employed as inputs in the next steps.

Next goal is to investigate the best modelling method for realistic seismic simulation of the monument. In order to achieve this goal, two main simulation methods, linear elastic finite element modelling method and nonlinear discrete element modelling method, with one being a considerably heavier work than the other, are employed. Their results are compared to each other with accuracy and realism in consideration.

Finally, a system to increase the overall structural stability and seismic strength is considered and designed with the least possible intervention principle in mind, as mentioned in the ICOMOS Charter of Principles for the Analysis, Conservation and Structural Restoration of Architectural Heritage (2003). While strengthening the structure, preserving the beauty and uniqueness of the monument was one of the concerns. Therefore, a strengthening system was sought that does not completely invade the structure but integrates with its authenticity and utilizes the monuments own capability with minimum and reversible intervention.

1.5 Scope (Research Methodology)

This study was carried out in several steps, compatible with ICOMOS Charter (2003) approach of "anamnesis, diagnosis, therapy and controls", including site investigations, collection and evaluation of long term monitoring data along with the construction of numerical models to evaluate structural behavior and capacity in the case of seismic activity, both for current status of and the strengthening proposals for the temple.

Site surveys

First site visit was conducted at start of the study, in March 2013 with the main objectives of getting to know the structure and familiarize with its geometry and main features, along with the collection of long-time monitoring data.

The construction technique and the architectural form, along with the visually evident structural problems were identified. Present condition of the *Res Gestae* inscriptions and occasional ornaments were examined. An extensive photographic database of the structural form and the visible problems were formed in order to be used for reference in the future studies.

A set of long-term measurement data being recorded by the temperature and tilting measurement gages installed earlier on the northern isolated, tilted portion of the northwestern wall were also collected in this visit.

This site visit also marked the initiation of the construction of numerical models and the post processing of the collected data.

In July 2015 a second site visit was carried out with a broader scope, targeted at conducting a series of non-destructive tests and investigating in detail some complicated portions of the temple for the discrete element model.

Non-destructive tests were aimed to obtain an estimate for the mechanical properties such as modulus of elasticity and strength of the materials constituting the main parts of the structure, and also to have an idea about the extents of material degradation. Schmidt hammer tests and ultrasonic pulse velocity tests were performed. Another set of data was also collected from the long-term temperature and tilt measurement gages.

In addition to abovementioned tests, dynamic characteristics of the northern isolated tilting wall and the southeastern lateral wall were determined by means of ambient vibration testing. The natural modal vibration periods of the northern wall section was captured in three different locations at three different measurement sessions. Dynamic characteristics of the southeastern longitudinal wall were also attempted to be captured with another measurement. These tests were carried out under artificial and wind excitations, with the employment of highly sensitive accelerometers with 0.000004g resolution.

Data collected in Schmidt hammer, ultrasonic pulse velocity, long-term monitoring gages and most importantly ambient vibration tests were handled and processed later, the details of which are provided in Chapter 2.

Furthermore, as another objective of this site visit, some specific parts of the temple were visually inspected with their dimensions, orientations, locations and connections with each other were recorded by hand drawings and pictures by the author, from different points of view when possible (Figure 1.16). These parts include the lintel of the gate section, bottom layer of the northern wall where missing blocks were replaced with a rubble wall, the similar spot for the southeastern wall and also the Byzantine era crypt and its contact with the original

temple walls. Even though in the process of modelling, macro dimensions of the main temple elements and micro dimensions such as the length and height of each wall were taken from outputs of the identification studies by Botteri and Fangi (2002) and other studies found in the literature, these inspections were necessary to for the better and more accurate discretization of the temple elements, which was very critical for the discrete element analysis model created in ABAQUS software.

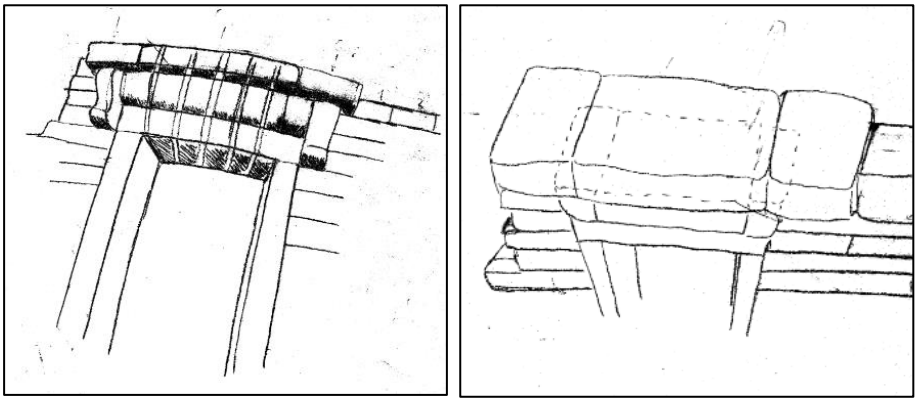

Figure 1.16: Discretization of the ornamented gate lintel

Structural Health Monitoring

Long term health monitoring data collected in these site surveys were later processed to see the effect of daily and yearly temperature cycles on the tilting of the wall, along with degree of the progression of the tilt over the years.

Seismic Hazard & Ground Motion Selection

In order to be able to analyze the performance of temple in its current status and also in the proposed strengthened conditions, a set of ground motion data was obtained using the seismic hazard data of Ankara obtained from European Facilities for Earthquake Hazard & Risk (EFEHR) website, and then scaling and comparing ground motions from a vast database of earthquakes that took place around the

world with the obtained local conditions. Ground motions selections were conducted for 475 years and 2475 years return periods. This procedure and the selected ground motion data are presented in detail in Chapter 3.

Computer Models

Constituting the major part of this study, two sets of computer models were produced, making use of the geometry and dimensional data provided by the works of Botteri and Fangi (2002) and site visits conducted.

The first set of models consists of linear elastic finite element models created in SAP2000 software, within the context of macro modelling. Firstly the current structural form of the model was created, calibrated in accordance with the results of the ambient dynamic measurement surveys conducted at the site, and its performance was investigated under time history data generated, as mentioned above, along with a response spectrum analysis. Then another model was produced reflecting the primary strengthening proposition and it was tested under the same conditions with the model reflecting the current structural form of the temple. Next, an alternative set of models were created in the ABAQUS software. In this software, discrete element models were created, aimed to fully represent the temple and its status. Each single stone block was generated with its unique dimensions, and was placed in its respective location on the actual structure to complete the model. Initially, a model reflecting the current status was created to fulfill a similar purpose with the first SAP2000 model. It was calibrated with the same data as the SAP2000 model. Using this model, seismic capacity of the temple was put to test using the aforementioned time history data, and the collapse mechanisms were investigated. As the next part of the study, four more models were produced reflecting the main primary and secondary strengthening proposals. Their capabilities and behavior were also analyzed in a similar manner.

Ultimately, more than 50 result oriented analyses and a number of auxiliary analyses were performed. Details of the production of the models, conducted analyses and the strengthening proposals are discussed in detail in their respective chapters.

CHAPTER 2

STRUCTURAL HEALTH MONITORING AND IN-SITU TESTING OF THE MONUMENT

Two site visits were conducted during the course of this study, in March 2013 and again in July 2015. During these visits, structural health monitoring data were collected, ambient vibration measurements were carried out and non-destructive tests were conducted.

2.1 Long Term Monitoring of Tilt and Temperature

The northern isolated wall section was being monitored with a long term health monitoring system consisting two tiltmeters with a temperature gage each. The measurements were collected and recorded by a data acquisition system, located at the site. The entire system was supplied with solar power. The system's installation was advised in a previous study conducted by, Turer and Eroglu (2006). Correspondingly, abovementioned system was installed and the measurements were started to be recorded in summer 2010.

Monitoring data between the dates July 29th, 2010 – August 10th, 2010; September 5th, 2010 – April 15th, 2011; October 16th 2012; – March 1st 2013 and June 6th, 2014 – July 7th, 2015, are available. For each gage, data was collected in ten-minute intervals. This data was studied in date order, and correlatively compared. Locations of these gages on the northern isolated wall are given in Figure 2.1. In this section, the data obtained from tiltmeter 1 is shown in blue color in graphs whereas red color was used for tiltmeter 2. As a result of these tiltmeters facing

opposite directions, tilting curves on all the graphs are obtained to be in opposite directions. Actually tiltmeter 2 needs to be multiplied by one, as the positive tilting direction is towards North. The North wall tilts towards South during winter and vice versa most likely due to the expected behavior of the temporary support system. Although the existing support system was initially proposed not to touch the walls but remain about 1cm distance to hold it in case the wall would dangerously tilt towards collapse, the implementation had the supports fully touch the walls. During winter and summer the steel truss expands and contracts, pushing and pulling the North and South walls towards each other.

The expected thermal movement is about 10 m * 50 ^{o}C degrees * 12 me/^{o}C = 6mm. The average height considered to be 5m from the ground level, this movement would cause about 3mm/5000mm to 6mm/5000mm, in the order of 0.05 degrees to in the order of 0.1 degrees in total. The measurements reveal the same order of magnitude indicating that wall tilts are due to temporary steel supports.

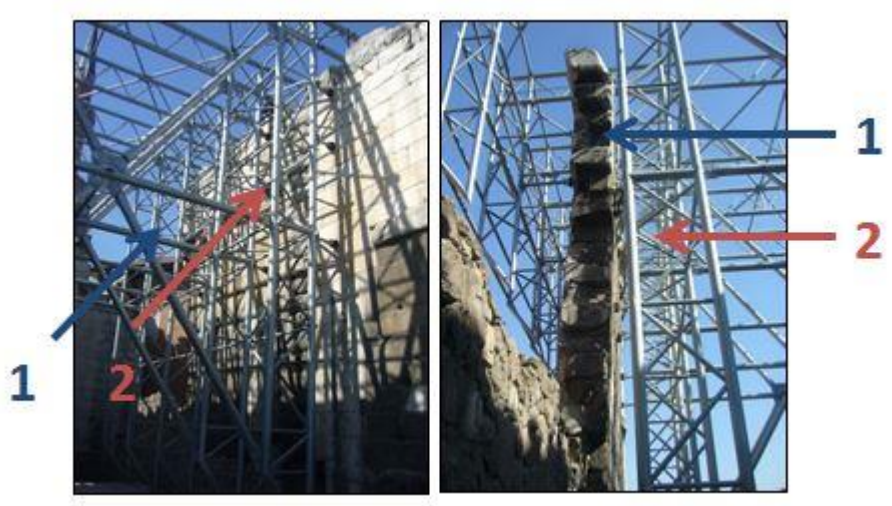

Figure 2.1: Tiltmeter locations

The data obtained in the short time period between July 29th, 2010 and August 10th, 2010 mainly demonstrates the daily tilting cycles of the wall in the summer depending on daily temperature change. Measurements were collected for 12 days.

Graphs of tilt and temperature with respect to time are presented in Figure 2.2 and 2.3. They clearly show the direct relation between the daily tilting cycles and the daily temperature changes.

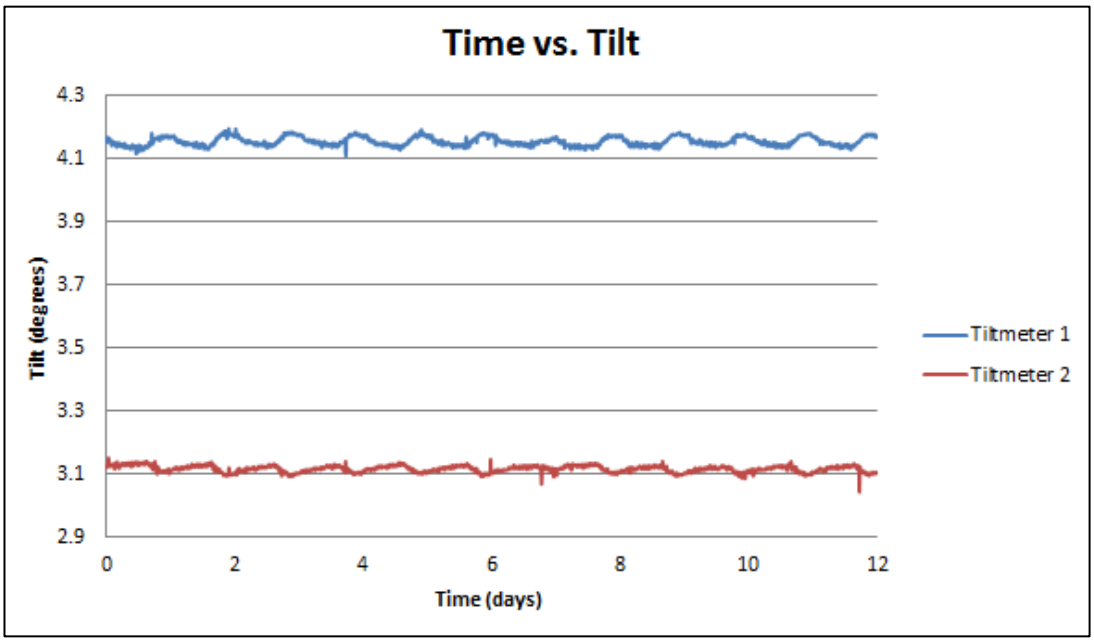

Figure 2.2: Time vs. Tilt graph between 29.07.2010 - 10.08.2010

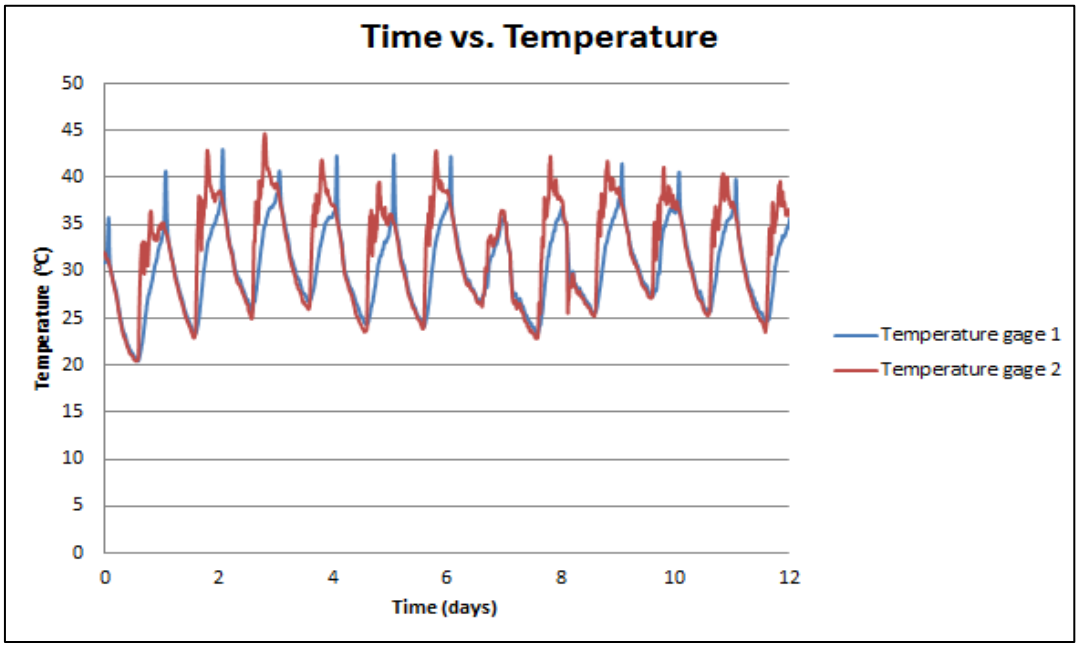

Figure 2.3: Time vs. Temperature graph between 29.07.2010 - 10.08.2010

Graphs of tilt and temperature with respect to time for the data obtained between dates September 5th, 2010 and April 15th, 2011 are presented in Figure 2.4 and 2.5.

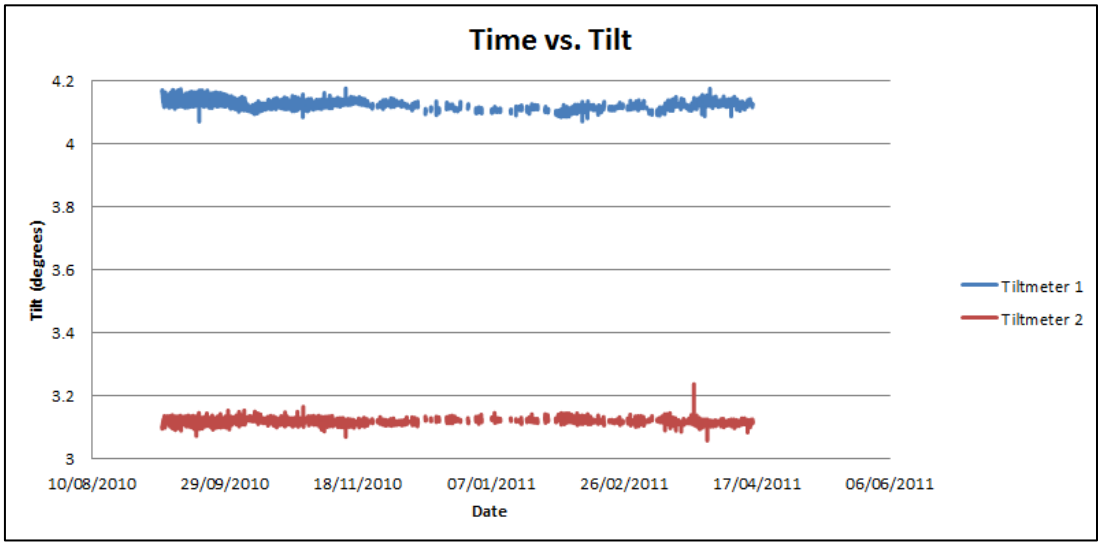

Figure 2.4: Time vs. Tilt graph between 05.09.2010 - 15.04.2011

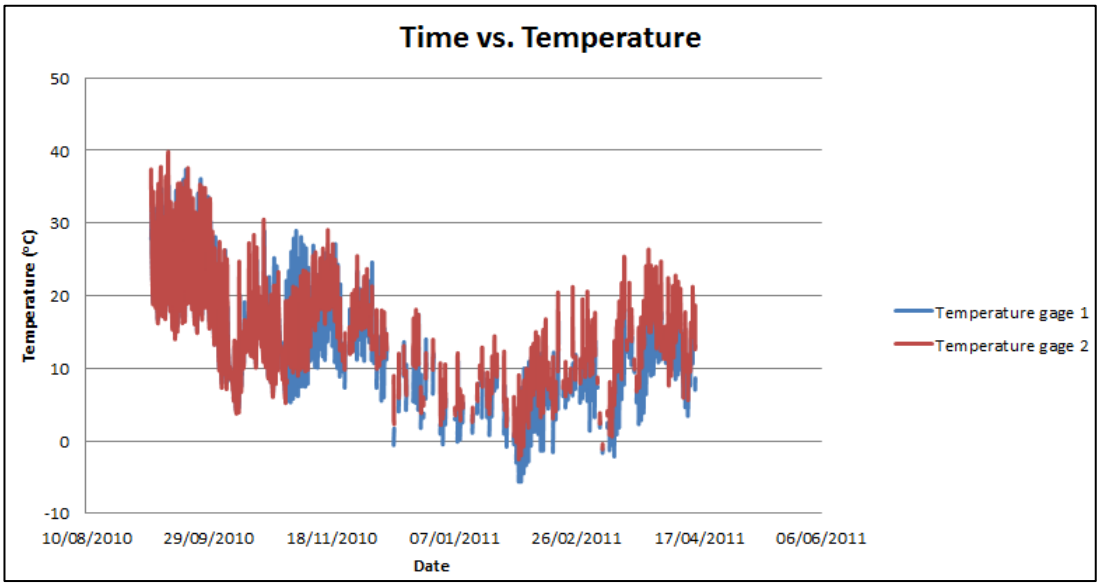

Figure 2.5: Time vs. Temperature graph between 05.09.2010 - 15.04.2011

Originally, in this data set, both of the inclinometers displayed excessive and unstable tilting, lasting for about two months' time. Further inspection into data revealed that battery voltage had been low during this interval. This has most probably been caused by lack of power in this solar powered system during snowy or very cloudy days. In the graph the erroneous data corresponding to low voltage values have been cleared out, and thus some days have no tilting data.

Data set for the days between October 16th, 2012 and March 1st, 2013 spans through a period of 4.5 months with data acquired at ten minute intervals. They are presented in Figures 2.6 and 2.7.

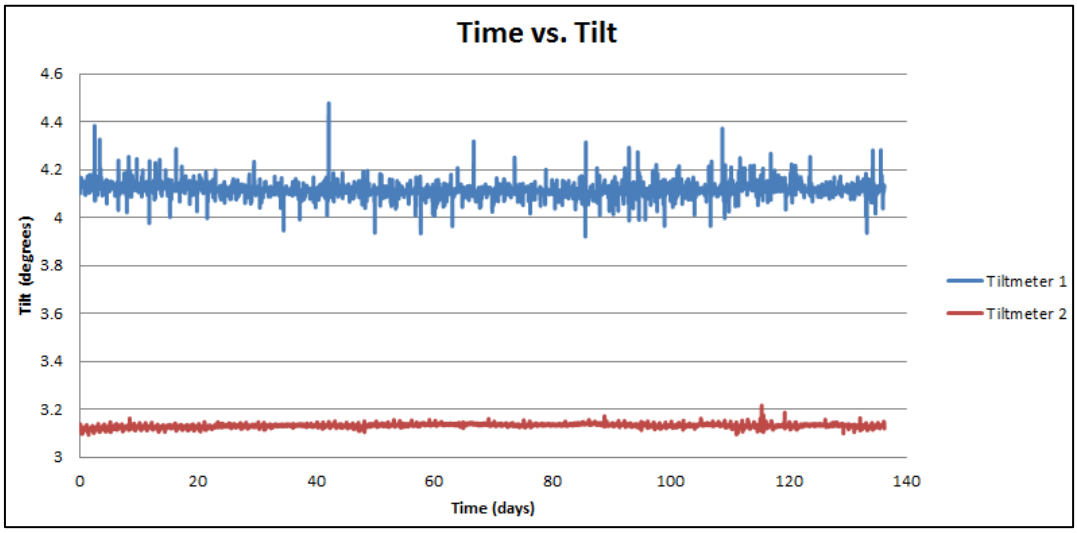

Figure 2.6: Time vs. Tilt graph between 16.10.2012 - 01.03.2012

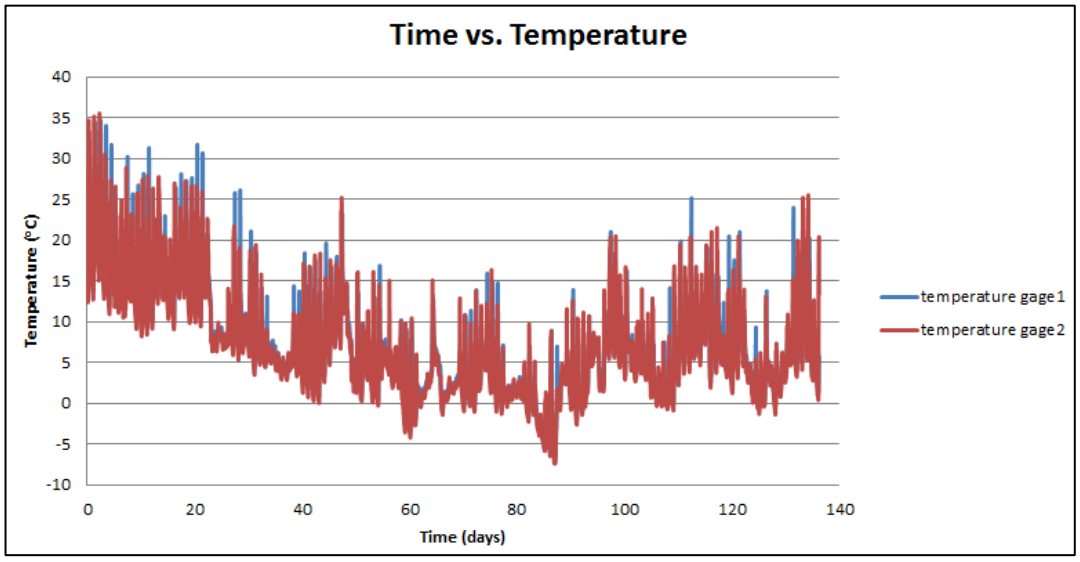

Figure 2.7: Time vs. Temperature graph between 16.10.2012 - 01.03.2013

The data obtained by tiltmeter 1 displays behavior too unstable to be real. This may have been caused by the strong winds in the area, or birds nested nearby touching the tiltmeter. On the other hand, this is the most stable long time measurement, making the observation of seasonal cycles possible (Figures 2.8, 2.9, 2.10).

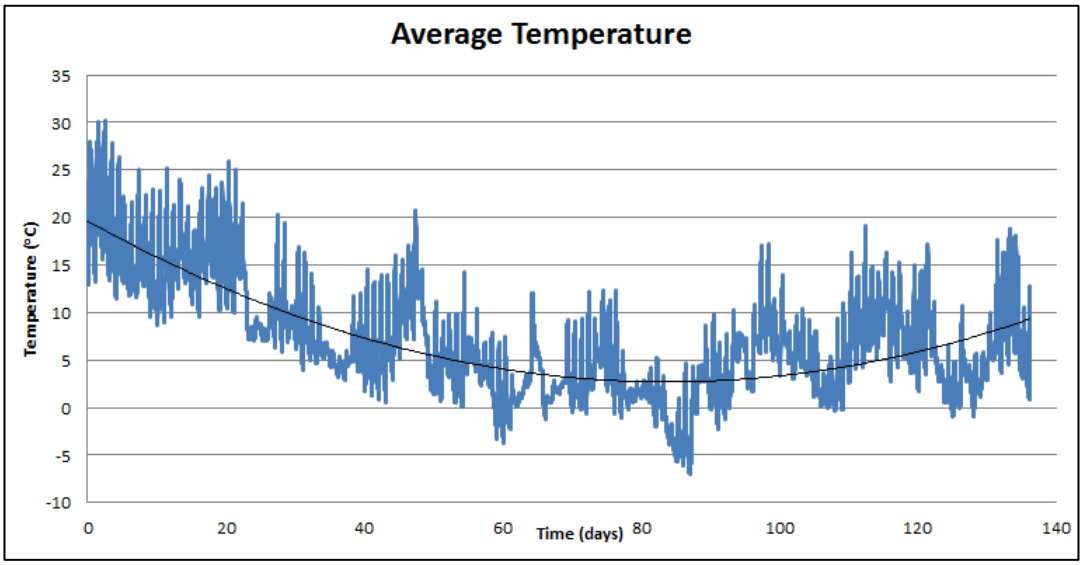

Figure 2.8: Average temperature with a polynomial trend line in this time interval

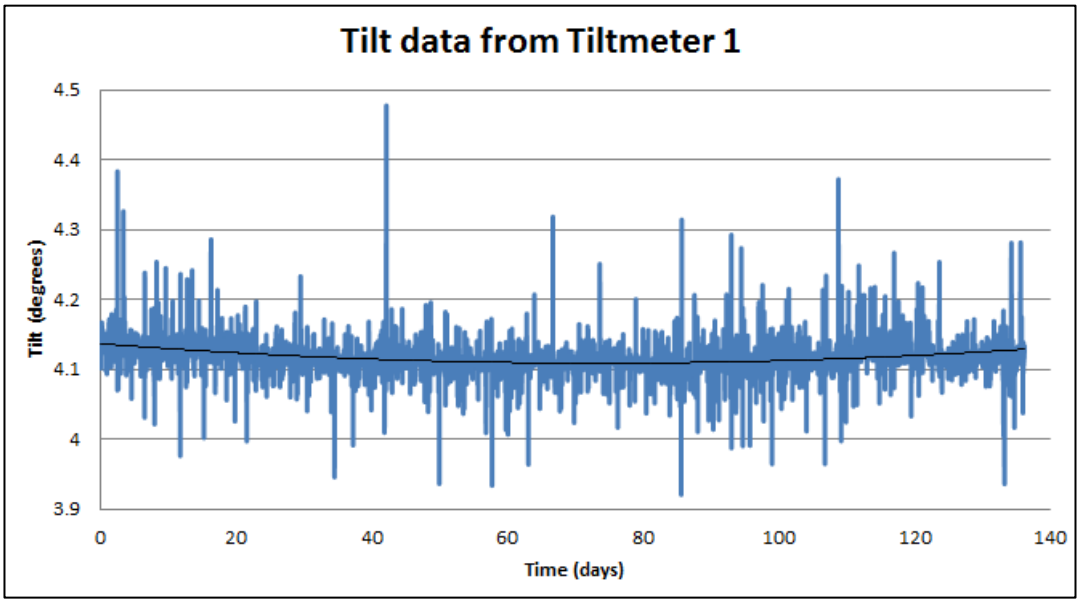

Figure 2.9: Tilt data with a trend line, obtained from tilt meter 2 between dates 16.10.2012 - 01.03.2013

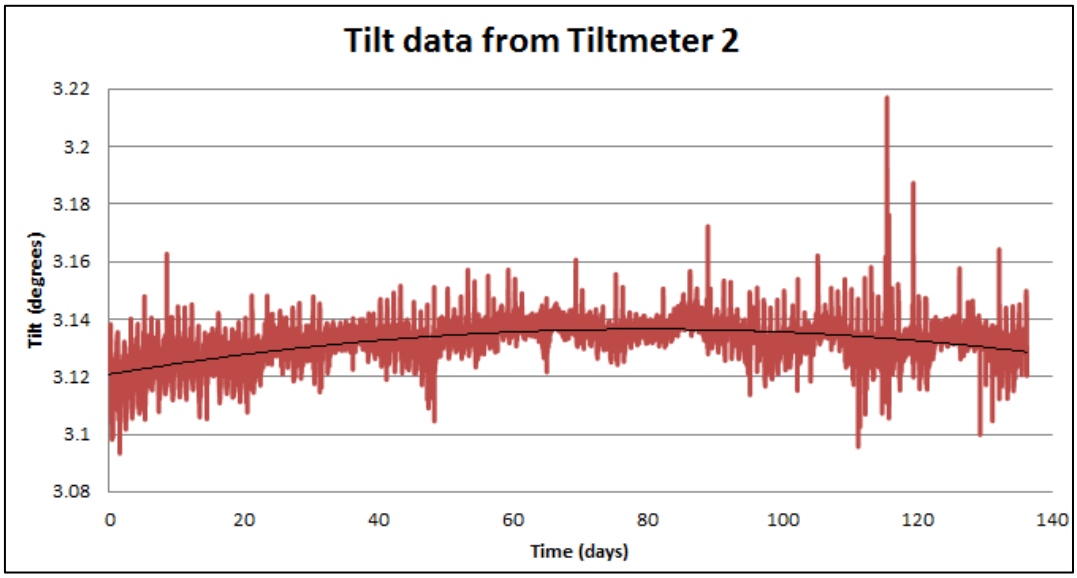

Figure 2.10: Tilt data with a trend line, obtained from tilt meter 1 between dates 16.10.2012 - 01.03.2013

Most recent data was collected during the second site visit, July 7th, 2015. Obtained data covers between the dates June 6th, 2014 – July 7th, 2015. Even though these dates constitutes the longest period of measurement, unfortunately, some parts of the obtained data display noisy data. Since the battery was damaged and as the daylight is lost towards evening and night hours, the datalogger seems to have made erroneous measurements. The data that was obtained to be extremely out of bounds were removed to clean the data from erroneous readings. The original temperature data and cleaned tilt data are presented in Figures 2.11, 2.12, and 2.13.

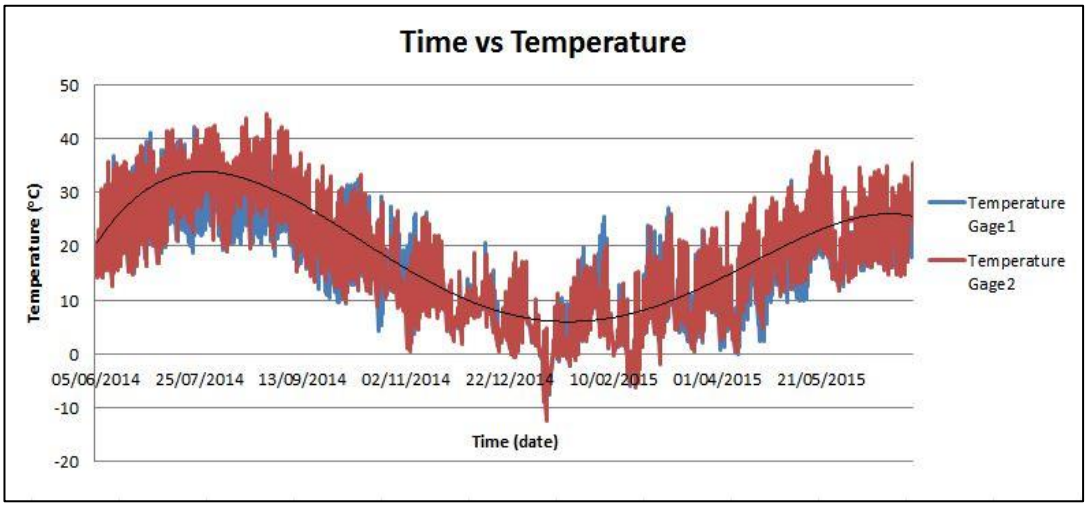

Figure 2.11: Time vs Temperature for the time period between June 6th, 2014 – July 7th, 2015, making a full yearly cycle.

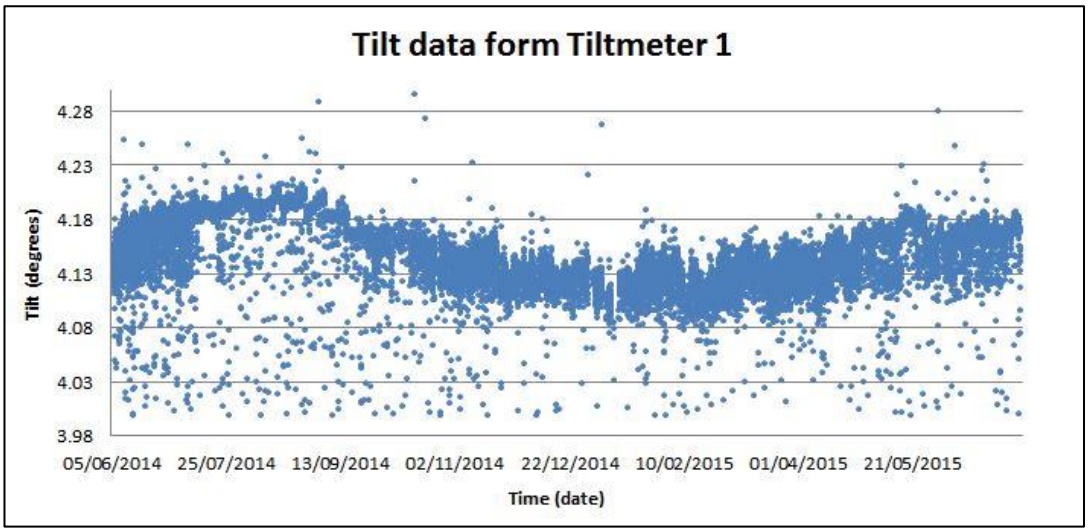

Figure 2.12: Tilt data obtained from tilt meter 1 between dates June 6th, 2014 – July 7th, 2015

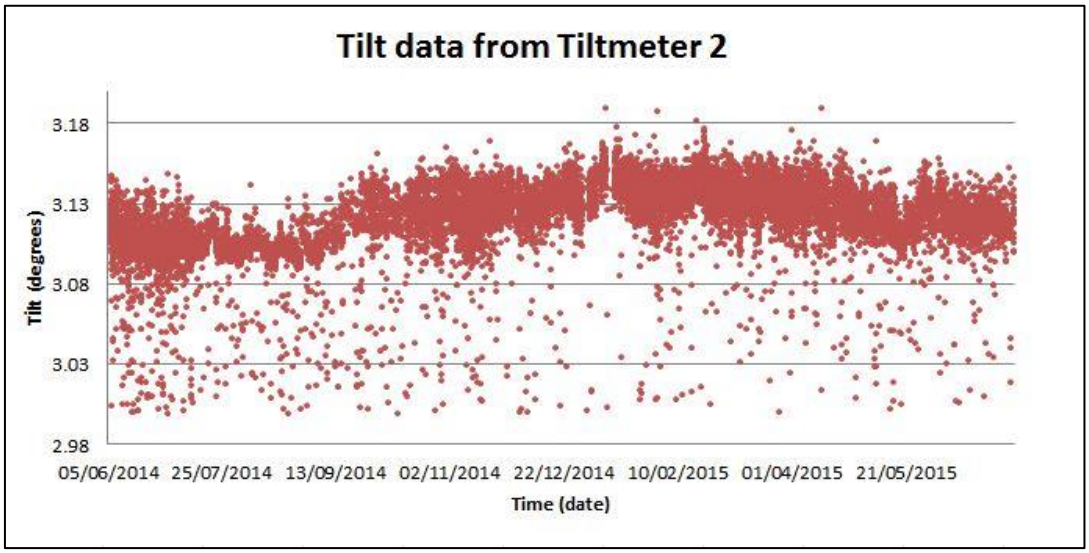

Figure 2.13: Tilt data obtained from tilt meter 2 between dates June 6th, 2014 – July 7th, 2015

Nevertheless, along with the addition of this most recent data, a data set spanning across almost five years was acquired. Even though there are large periods of time devoid of tilting data, when the data were added together a certain recurring trend in the tilting was observed. In order to make out the progress of the tilting, sinusoidal curves were fitted. These are provided in Figure 2.14 for tiltmeter 1 and Figure 2.15 for tiltmeter 2.

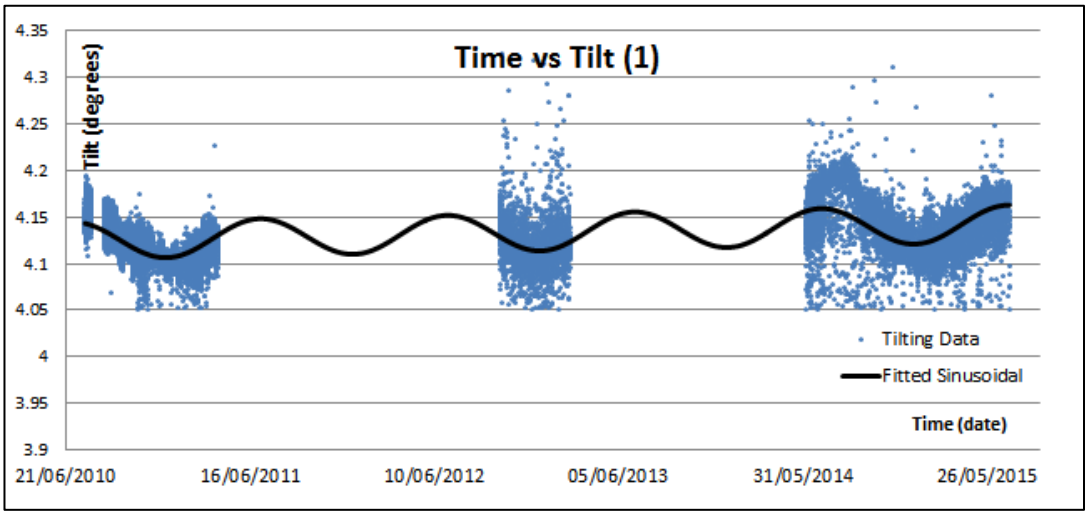

Figure 2.14: All tilting data collected from tiltmeter 1 with a fitted sinus curve. Curve's equation is $y=10*(10^{-6})*(t)+4.125+0.02*\sin(2*\pi/365*((t)-250))$ where t stands for elapsed number of days

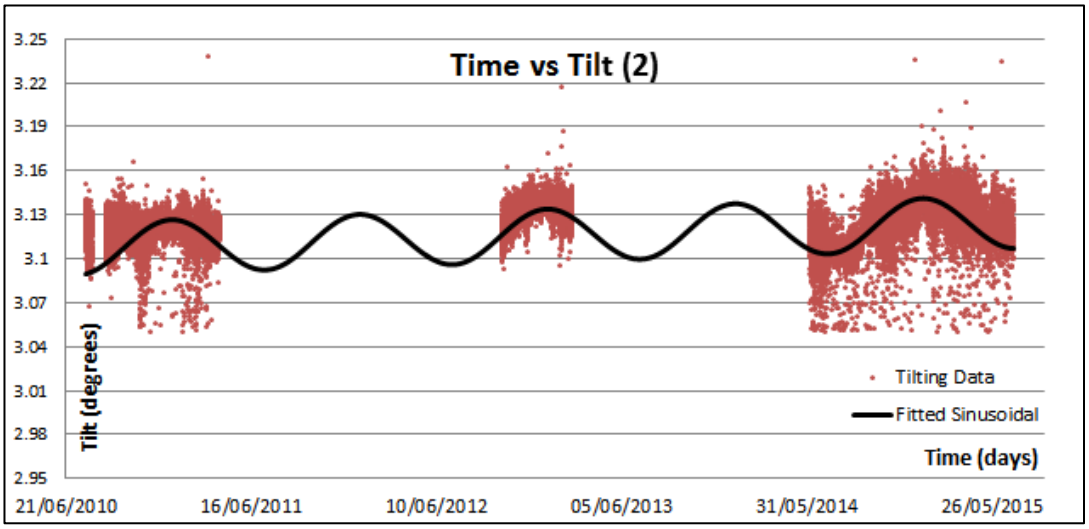

Figure 2.15: All tilting data collected from tiltmeter 2 with a fitted sinus curve. Curve's equation is $y=10*(10^{-6})*(t)+3.1069+0.018*\sin(2*\pi/365*((t)-75))$ where t denotes the number of days.

Both curves indicate a small increasing trend for the wall's inclination. Of the parts of the wall, section where the tiltmeter 2 is located apparently tilts at around twice the rate of tiltmeter 1's section.

As a part of the review on the tiltmeter measurement records, the correlation of tilting with the daily temperature cycles were investigated. In order to negate the effect of daily cycles, daily means were taken both for temperature and tilting data. Data obtained between dates October 16th, 2012 and March 1st, 2013 were employed. Figure 2.16 shows the average temperature while Figures 2.17 (a) and (b) display the daily tilting averages.

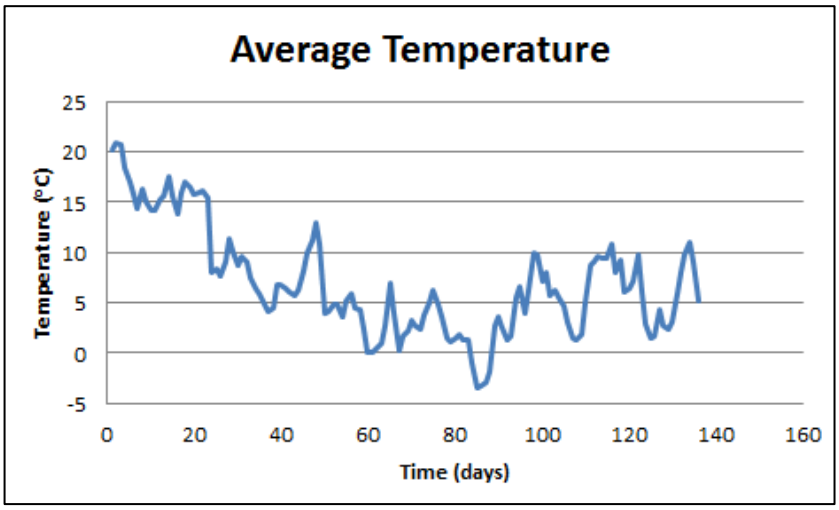

Figure 2.16: Average values for temperature

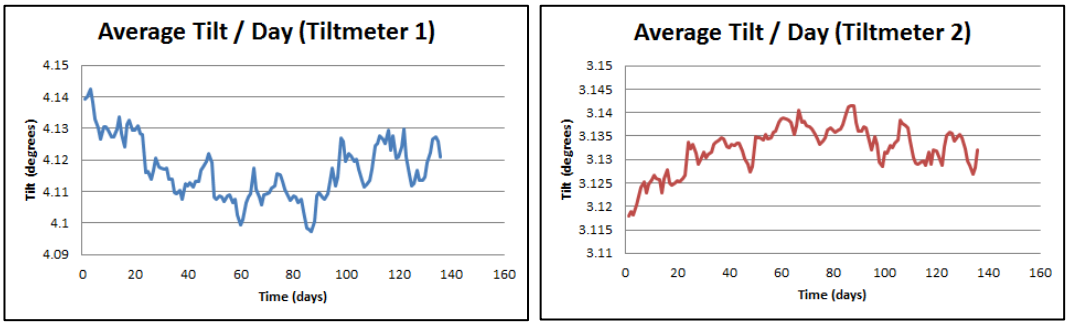

(a) (b)

Figure 2.17: Average tilting values recorded by each tiltmeter

With Figures 2.16 and 2.17, the scale increases from daily changes to day to day changes. Figures 2.18 and 2.19 represent the correlation between temperature changes and tilt changes through the days.

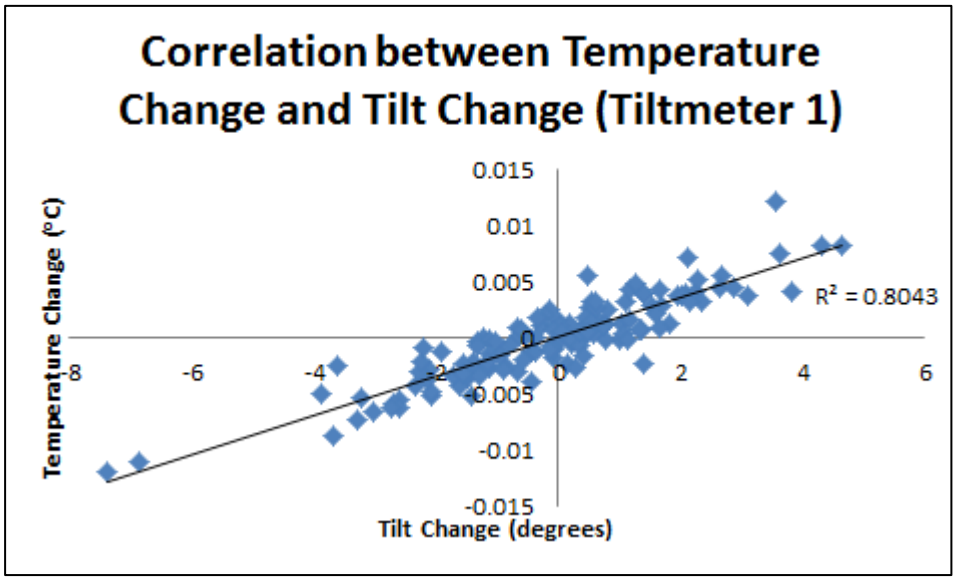

Figure 2.18: Correlation between temperature and tilt changes (tiltmeter 1)

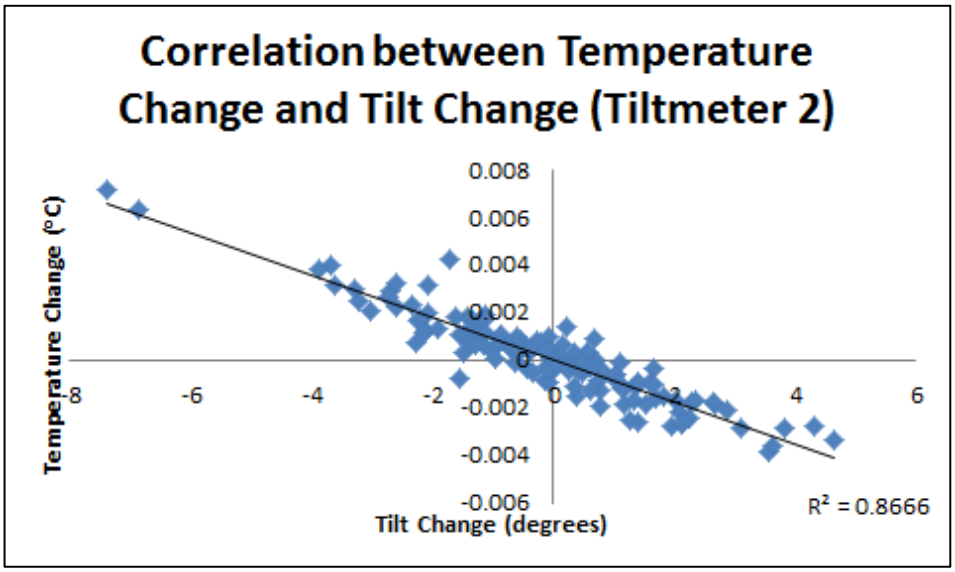

Figure 2.19: Correlation between temperature changes and tilt changes

This relation of the tilting to the temperature change may be attributed to the differential heating of the both sides of the wall. However, it is more likely that tilting takes place as a result of the thermal expansion of the emergency intervention system, being in contact with the wall.

2.2 Ambient Vibration Measurements and Determination of Natural Frequencies

During the second visit to the site in July 2015, ambient vibration testing was conducted on the temple, focused on the northern isolated wall and northern part of the southeastern wall. On the northern isolated wall, three sets of dynamic measurements were taken. Of these three sets, two consisted of two accelerometers placed simultaneously while the other set has only one reading. The first two sets of measurements were taken with accelerometers placed at the top layer of the northern isolated wall, at around mid-length. Other measurement was taken at around mid-height, mid- length, with the accelerometer placed in one of the holes

in the interior side of the wall. The exact placement is visualized in Figure 2.20 (a). On the southeastern wall, one measurement was taken with a single accelerometer, at around 1/3 length from the northern end and 1/3 height (Figure 2.20 (b)).

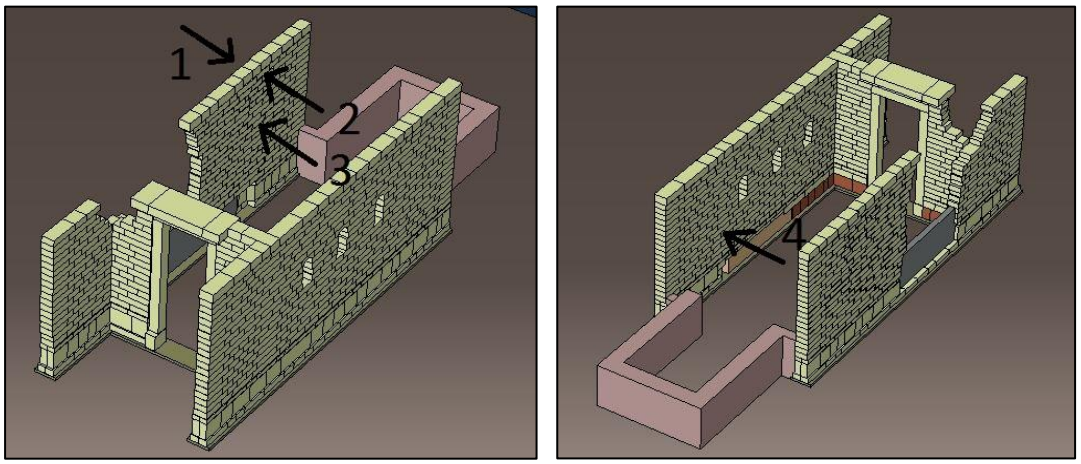

(a) (b)

Figure 2.20: Visualisation of accelerometer locations. 2 reading sets were taken at locations 1&2, another at location 3 and finally at 4.

For all measurements, the excitation was provided by the wind blow. Longest measurement was one of the simultaneous two accelerometer sets, collected from the top of the wall, lasting approximately 3.5 minutes. Raw data obtained from this measurement is provided in Figure 2.21.

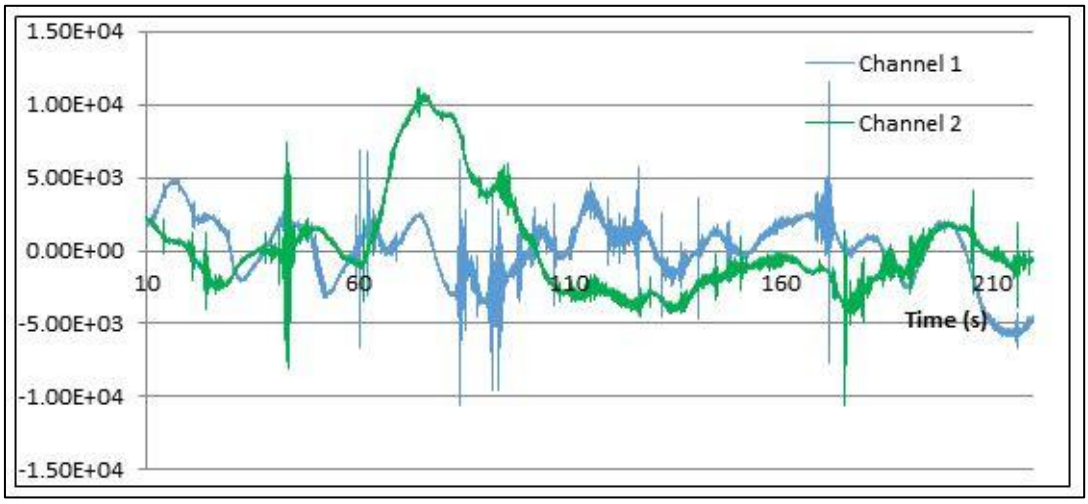

Figure 2.21: 3.5 minute measurement taken at the top of the wall with two accelerometers. It contains more than 550000 data points.

Another measurement was taken at the top of the wall with more favorable conditions for this type of test, where silence and the stillness of accelerometers were tried to be maintained as much as possible. Obtained raw data is provided in Figure 2.22.

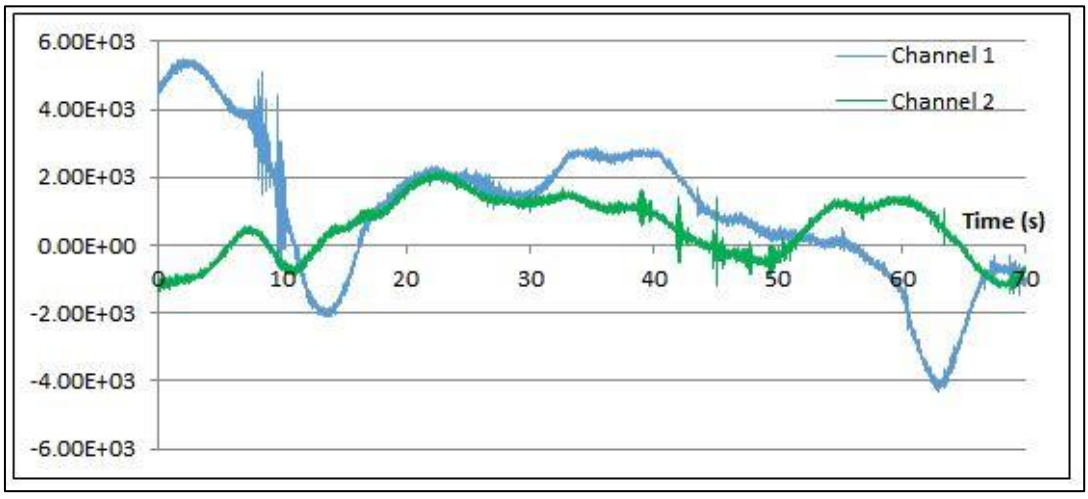

Figure 2.22: Second ambient vibration measurement recorded at the top of the Northern isolated wall.

Effect of relative silence and stillness can be observed in the amplitudes of the record. Final measurement for the northern wall was collected at the mid-height as mentioned before. Its raw record is given in Figure 2.23 (top). Measurement record taken from the southeastern wall is also provided in Figure 2.23 (bottom).

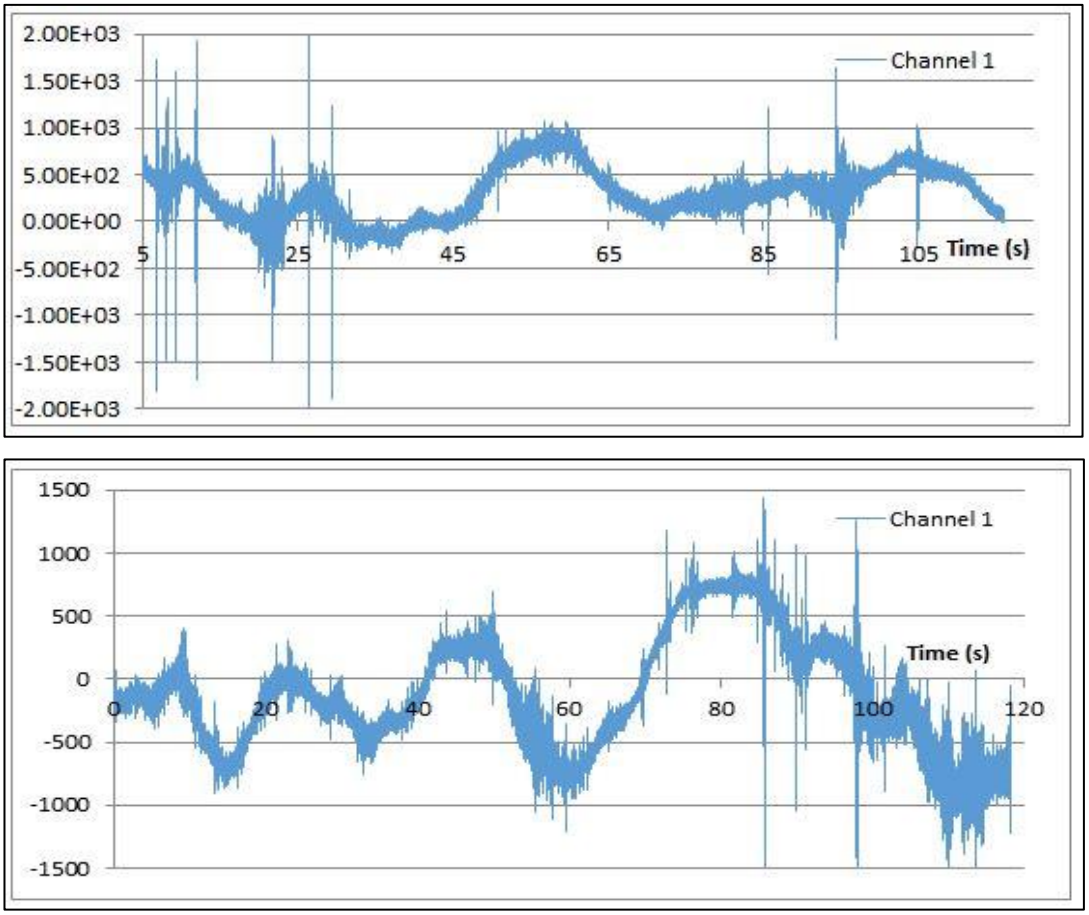

Figure 2.23: Measurement taken from the northern wall mid-height (top). Measurement record of the southeastern wall (bottom)

This raw data was converted from time domain to frequency domain by means of Fast Fourier Transformation (FFT) using a simple code in written in MATLAB in order to be able to view modal frequencies more clearly. Following the transformation, data belonging to the northern isolated wall (a total of 5

measurements) were superimposed by being plotted on the same chart (Figure 2.24). This provided a better way to distinguish peaks that belong to the modal frequencies. Separately, FFT results of the measurements for the southeastern wall is provided in Figure 2.25.

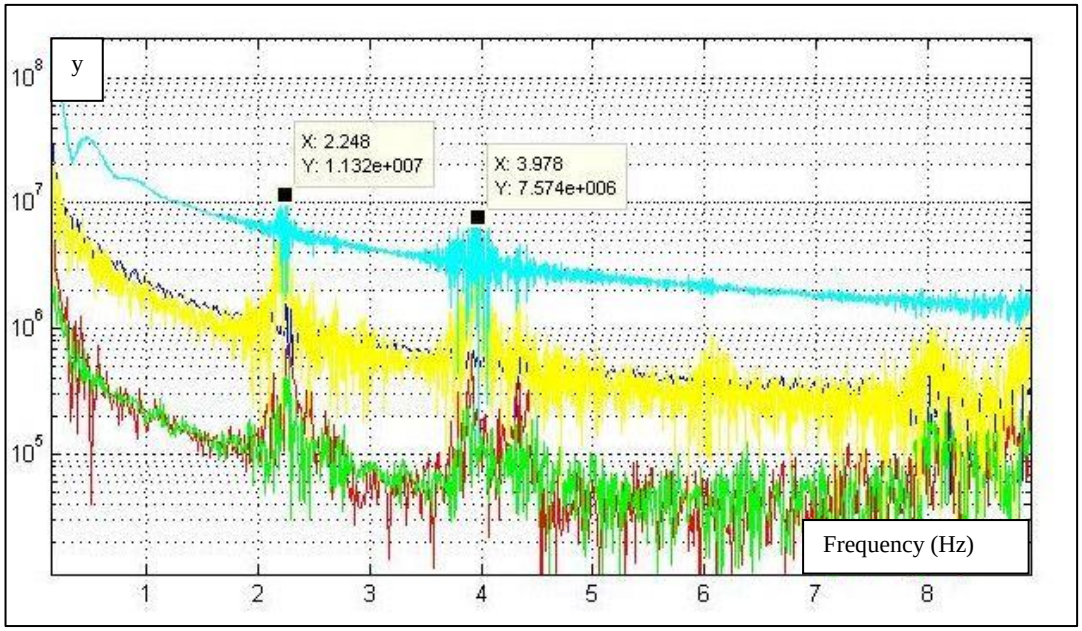

Figure 2.24: FFT results for the measurements from the northern isolated wall.

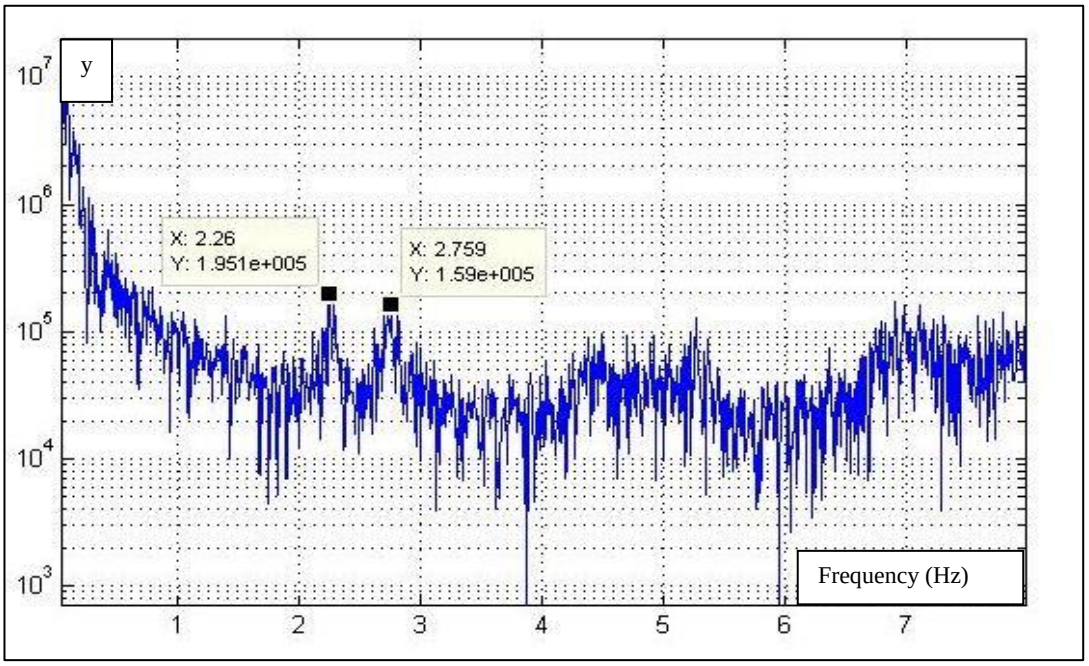

Figure 2.25: Southeastern wall measurement data converted with FFT to frequency domain.

First and second natural frequency and corresponding period values obtained after Fast Fourier Transformation are provided in Table 2.1 for both the northern isolated wall and the southern wall.

Table 2.1: The first two measured natural vibration frequencies and periods of the both walls tested.

	Northern Isolated Wall		**Southeastern Wall**	
	Frequency (Hz)	Period (s)	Frequency (Hz)	Period (s)
First Mode	2.248	0.445	2.260	0.442
Second Mode	3.978	0.251	2.759	0.362

The values obtained in this study were compared to the results of a similar test carried out on the same wall sections of the structure by Turer and Eroglu (2006). The result of their test is provided in Table 2.2.

Table 2.2: The first two measured natural vibration frequencies and periods of the both walls as obtained by Turer and Eroglu (2006)

	Northern Isolated Wall	**Southeastern Wall**
	Period (s)	Period (s)
First Mode	0.758	0.455
Second Mode	0.290	0.245

Comparing the results, it was possible to see that the first and second period values of the northern isolated wall are reduced by 41.3% and 13.4%, respectively. For the southeastern wall, the first period values were found out to be similar; however an increase of 47.7% was noted in the second period values.

At the time of the study conducted by Turer and Eroglu (2006), the current structural emergency intervention system was not in place; while at the time of this study, it was. The intervention system is likely the main reason for the reduction observed in northern isolated wall's first and second natural vibration periods. A possible contact between the wall and the emergency intervention system's rubber pads would initiate a constraint, diminishing the wall's natural vibration period. Indeed, when these ambient vibration tests were being conducted on the northern isolated wall, rubber pads were spotted in contact with the wall surface (Figure 2.26)

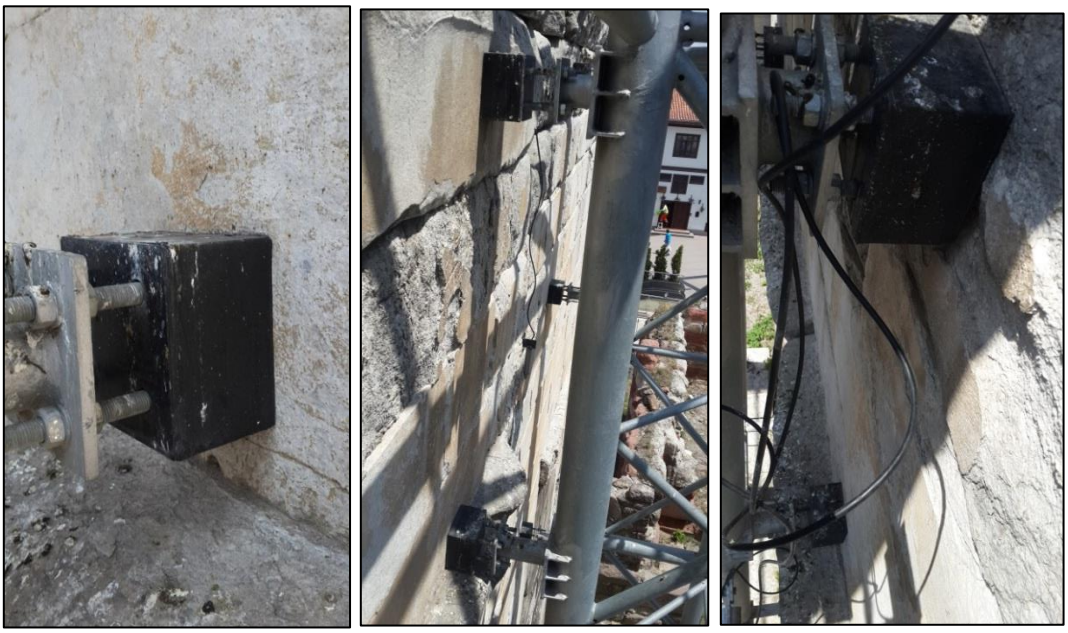

Figure 2.26: Rubber pads in contact with wall surface

A number of reasons may have caused the observed increase in the southeastern wall's second mode period. This could have been a result of further degradation of material, leading to higher flexibility. However this case is unlikely, considering that the amount of time between two tests is quite small compared to the structures life, and that the area around the structure is fenced, protecting it from intentional harm. If contact was initiated between the wall and the emergency intervention system, some of the mass may be transferring from the northern isolated wall to the southeastern wall and being carried by it, leading to an increase in its period value.

The difference between the measured period values in this study and those measured by Turer and Eroglu (2006) suggested that the emergency intervention system affects the natural vibration periods of the structure in one way or the other. As a result, considering that the calibration studies (explained in detail in Chapter 3) would be conducted on the analytical models of the structure that do not take into consideration the presence of emergency intervention system, period values

determined by Turer and Eroglu (2006), when there was no intervention system installed on the building, were taken as a basis.

2.3 Non-Destructive Material Tests

Schmidt Hammer and Ultrasonic Pulse Velocity tests were carried out at the site on the second site visit, aimed at obtaining an approximate value for the strength and elasticity modulus parameters, respectively. Obtaining an estimate for strength was expected to give an idea about the material degradation and be useful during the evaluations of analytical analyses. Having an approximate value for the modulus of elasticity obtained at the site would also be convenient for validating the material properties obtained by the model calibration studies.

Schmidt Hammer tests

The Schmidt hammer, also referred to as the rebound hammer, measures the rebound of the mass, loaded by a spring, after its impact on the target surface. The energy with which the hammer hits the surface is known, thus, from the robund, the hardness of the sample surface may be designated (Rubene & Vilnitis, 2014)

On the field, measurements taken were focused on the blocks constituting the original temple. From different blocks, strength values ranging between 18 to 40 MPa were obtained.

This difference may be attributed to the test mechanism where the material conditions on the surface play a determining role on the result. On the weathered surfaces, the test gives lower results and on the more intact surfaces it gives higher results, regardless of the material condition behind the surface. It is likely that higher strength values can be obtained from the material behind the surface.

Ultrasonic Pulse Velocity tests

Ultrasonic Pulse Velocity tests works with the employment of the principle where the ultrasonic waves travels through materials at a known velocity; which is reliant on the material characteristics. With this method, cracking and the material deterioration can be estimated. This method is also critical as it allows making an approximation for the modulus of elasticity.

Unfortunately, at the site, measurements where a variety of distances were used all yielded the same travel time, leading up to 100% error in the test results. Thus, the results obtained from this test were not taken into consideration.

CHAPTER 3

MODELLING OF MONUMENTUM ANCYRANUM AND STRUCTURAL EVALUATION

Determination of the structural characteristics and the collapse mechanisms of the monument constitute one of the major parts of this study. In this chapter, finite element analyses carried out in SAP2000 software and discrete element analyses made in ABAQUS software with the aforementioned objective are presented in detail.

In order to capture a logical narrative sequence, firstly a review is made about the employment of these two analysis methods for historical structures, followed by a section regarding the determination of parameters that constitute the inputs for both model types. Under specific titles for both model types, specific features of each model, along with their verification through calibration in accordance with dynamic ambient vibration measurement results and the results of the analyses are given. Ultimately a comparison of results is presented regarding the two model types and their accuracy in the representation of the case.

3.1 A Review on the Numerical Modelling of Historical Masonry Structures Using Finite Element and Discrete Element Modelling

In contrast to today's structures, historical masonry structures lacked standardized and calculated design approach. Moreover, each case possesses a uniqueness and uncertainties to itself, both in the design, and in the materials and the construction style. A combination of these concerns lead to difficulties in the prediction of their

behavior, both in mathematical and also in numerical approaches. In this sense, computer models introduced an ease to this task. However; for these digital models, the consideration of complex relationship between the elements that constitute a masonry structure, and also the representation of the masonry units themselves became a concern in obtaining an accurate result. Initially, representation of the main parts that constitute a masonry structure (piers, walls and spandrels) as equivalent frame elements to simulate the behavior was employed as method. Unfortunately, this method proved problematic for structures where shear deformation were preeminent. Consequently, solid and shell planar elements were started to be used for this purpose.

In this study, both macro finite element modelling, where brick units and mortar, or other binders are represented as a smeared entity, and also discrete element modelling, where each unit is represented individually with an interface property were employed. The former method brings about ease of modelling and low computational cost, resulting from an arbitrary meshing regardless of the locations of actual units and a low degree of freedom, but it suffers from the neglection of existing cracks and discontinuities, leading to improper and inadequate representation of the structure and results that are not very reliable. In the latter method, DEM, since the solution is nonlinear, and iterations are necessary, long amounts of time may be required for the computation. Moreover, generation of the model may take too much time and effort, considering the size of each element has to be determined and re-created in the virtual environment. But the difficulties associated with this type of modelling are made up for in the results where almost every different failure mechanism can be examined (Roca, Cervera, Gariup & Pela, 2010). A problem with DEM is that with this type of modelling, the number of unknown parameters increase, resulting in another error margin with each assumption and approximation. Finally, this type of modelling may only be effectively employed in the cases of dry masonry structures, or with the structures that possess iron connectors, ignoring them.

In this study, both methods were employed in the initial stage and also in the last step, bringing about the possibility to compare their results. However, DEM was selected as the suitable method of analysis for the case of the Temple of Augustus and more detailed analyses were carried out with this method.

3.2 Determination of the Model Inputs

In order to obtain reliable results from the computer analyses that constitute a main part of this study, reflection of real conditions into the generated analytical model was of vital importance. Accordingly, in this section, formation of model geometries and derived seismic hazard conditions are presented. For both types of analytical models, due to a lack of related information and impossibility in conducting material tests to obtain material properties, they were estimated by comparison and calibration of modal frequencies with those obtained from the real structure. Any other necessary input parameters had to be taken from the literature.

3.2.1 Generation of Model Geometry

Geometry information required in the model creation was largely obtained from the studies of Botteri & Fangi, 2002. Based on this information, SAP2000 models were formed as a uniform mesh of 2D shell elements with thickness values approximated and averaged for large sections.

Discrete element model geometry generated in ABAQUS has a different composition altogether. Here the model is made up of mostly 8 corner stone block elements, a reflection of the actual structure, representing door lintels, ornamented layers, gate columns, and ordinary stone block elements. Every single one of these elements were created in accordance with their original dimensions (in the order of millimeters where available) for the sake of being able to capture the structural

behavior and probable collapse mechanism as realistically as possible. Moreover, utilizing these discrete elements allowed performance of nonlinear analyses where, at every joint, moment and tensional force transfers were removed, differently from the SAP2000 model.

In both model types, of the elements constituting the temple in its current form, the main emphasis was put on the most approximate reflection of the original temple, i.e. southeastern wall, gate section and the both parts of the northwestern wall. One important note is that considering the difficulty in the execution of metal connectors in lead technique ("Opus Revinctum" method mentioned in Chapter 1) that leads to frequent sightings where connectors were entirely corroded (Schueremans et al, 2003) and the age of the temple adding up to the possibility of connectors being in a deteriorated condition, this feature of the temple was omitted (not represented). Another reason for this omission is the huge amount of time it would take to model these connectors at each joint and the tedious nature of such work. Also the exact layout of connectors (number and position of dowels and clamps) were not revealed at the time of this study, thus an arbitrary modelling could have caused incorrect simulation of behavior. Ultimately, complete omission of these connectors in the model makes the analysis results conservative since the positive effect resulting from their existence is not taken into account.

3.2.2 Seismic Hazard and Ground Motion Selection

In the investigation of seismic capability and the collapse risk of the temple in its current form, along with the performance checks of the strengthening proposals in investigated in the next chapter, developing earthquake data that reflects the local seismic hazard conditions is critical. In order to be able to conduct nonlinear time history analyses featuring discrete elements in ABAQUS, a series of ground motion data were selected and scaled, from the The Pacific Earthquake Engineering Research Center's (PEER) NGA WEST 2 database containing 21540 different

records (flatfile) of earthquakes that occurred around the world. Selected ground motions were also used in the time history analyses conducted in SAP2000, along with the response spectrum analysis.

Selection and scaling study were conducted in accordance with related methodology explained in *Selecting and Scaling Earthquake Ground Motions for Performing Response-History Analyses* guide by U.S. National Institute of Standarts and Technology. Firstly from the European Facilities for Earthquake Hazard & Risk (EFEHR) project website, two uniform hazard spectrum curves were generated from hazard curves provided for peak ground acceleration (PGA) and other spectral accelerations. As an example, PGA hazard curve generated for Ankara is provided in Figure 3.1.

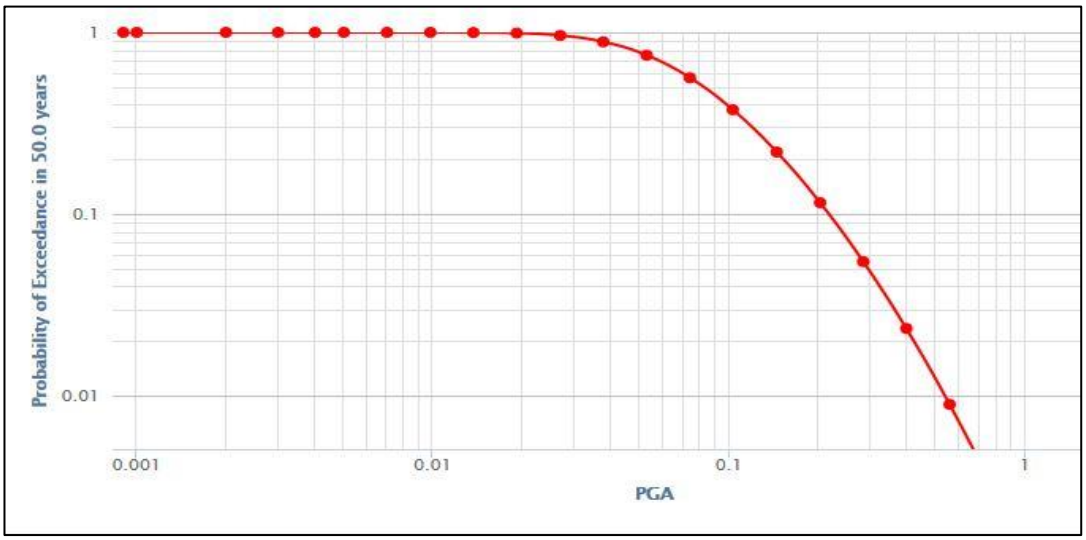

Figure 3.1: PGA Hazard Curve for Ulus area in Ankara (obtained from EFEHR Website http://www.efehr.org:8080/jetspeed/portal)

Two uniform hazard spectra were formed for 475 and 2475 years return period earthquakes using the hazard curves for PGA and other spectral accelerations (Figure 3.2). These spectra curves formed the basis for record selection and

matching from the database of NGA WEST 2. In order to achieve better matching, a piece of code developed in MATLAB was used to scale the records in the database between 0 and 1.5. The code compared the records' spectral acceleration values and the UHS at each defined period and selected the closest match. The scaling coefficients were intentionally selected to be low, in order to avoid abnormalities that may arise from using large coefficients.

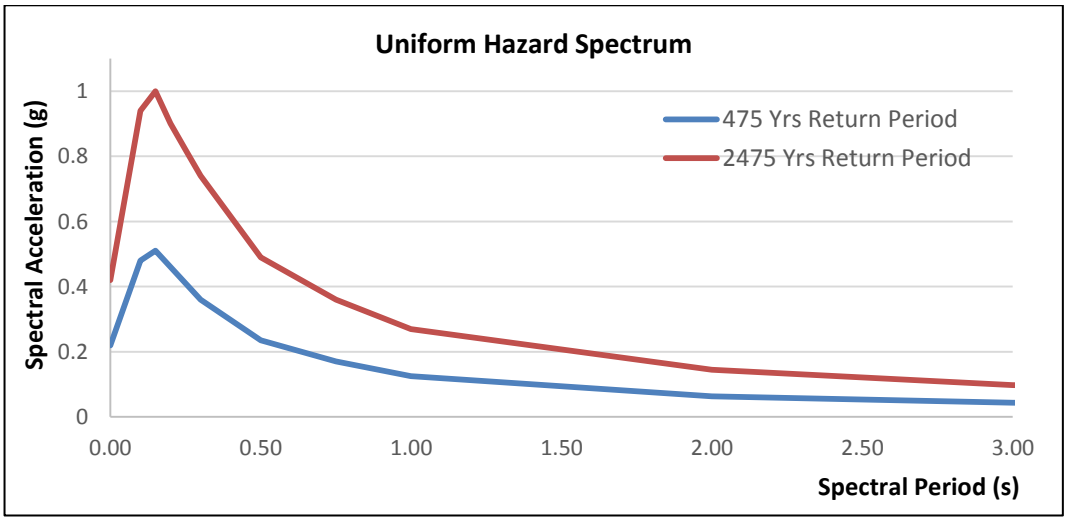

Figure 3.2: Uniform Hazard Spectra for 475 and 2475 return periods

The code was used to select 30 records automatically; both for 475 and 2475 year return period cases, separately. Selected records were then visually inspected and those that displayed sharp divergence from the uniform hazard spectra, which could not be eliminated by the selection algorithm, were eliminated. Finally three records were selected for 475 years return period and one for 2475 years return period cases. Matching results are presented in Figures 3.3 and 3.4, respectively.

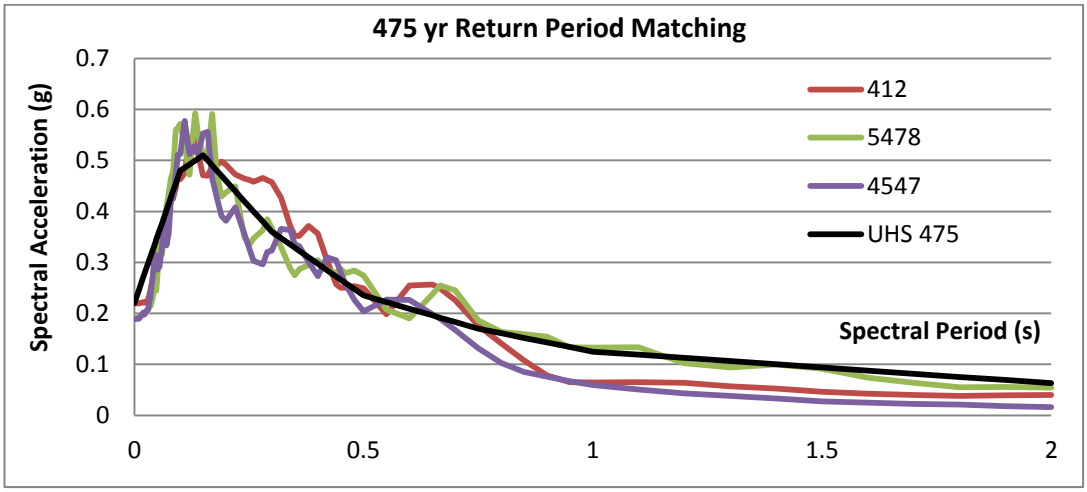

Figure 3.3: Matching results for 475 years return period spectrum and the selected ground motions

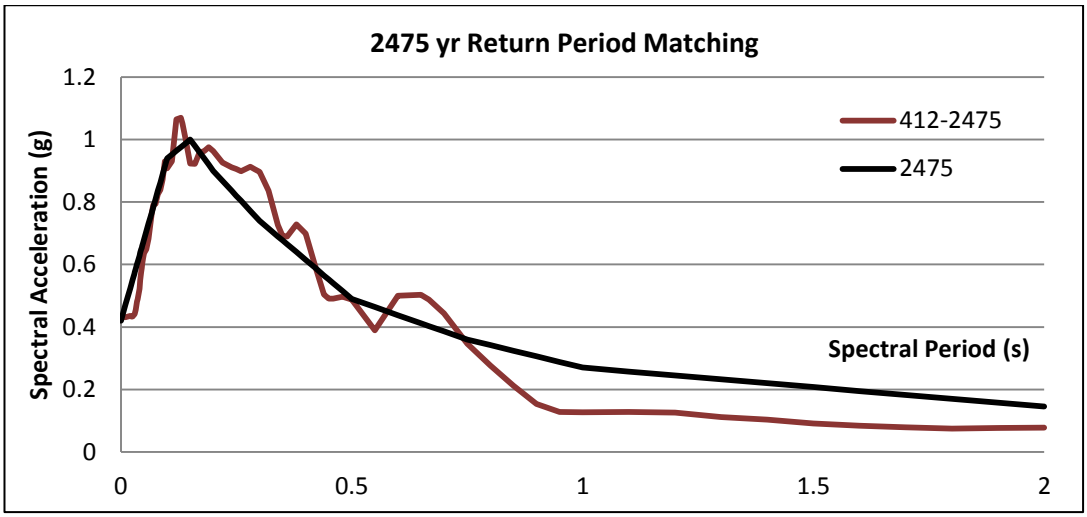

Figure 3.4: Matching results for 2475 years return period spectrum and the selected ground motions

Intentionally those earthquake records that demonstrate different vibration characteristics were selected between the matched options. Moreover, interestingly, the record that demonstrated the best match with 2475 year return period uniform

hazard spectrum was the same earthquake that showed one of the best matches with 475 years return period case, but with a multiplier of approximately 2. Another concern during the ground motion selection process was the record length. Considering the huge amounts of time a discrete element analysis takes to complete in ABAQUS, records that were relatively short (around 20s) were preferred. These selected records are presented in Figure 3.5 (a) 412, (b) 4547, (c) 5478 and (d) 412-2475, below.

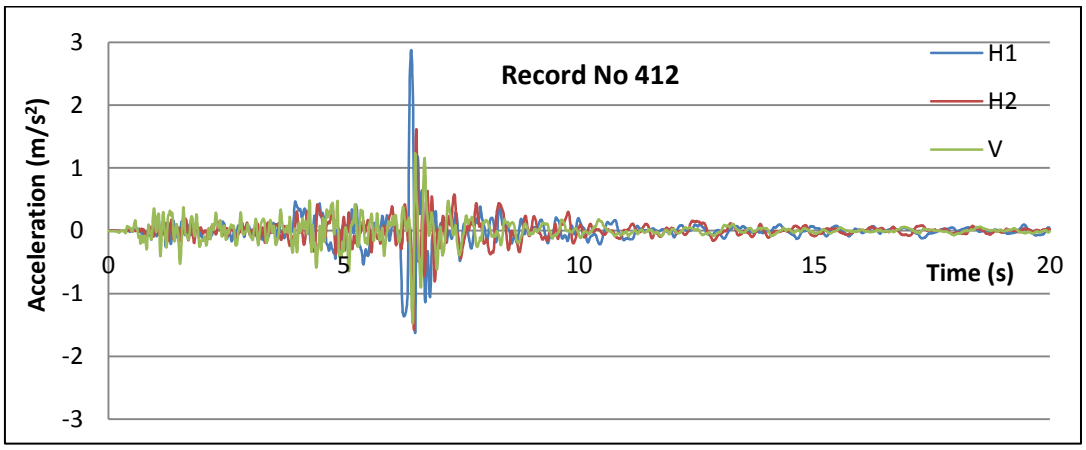

(a)

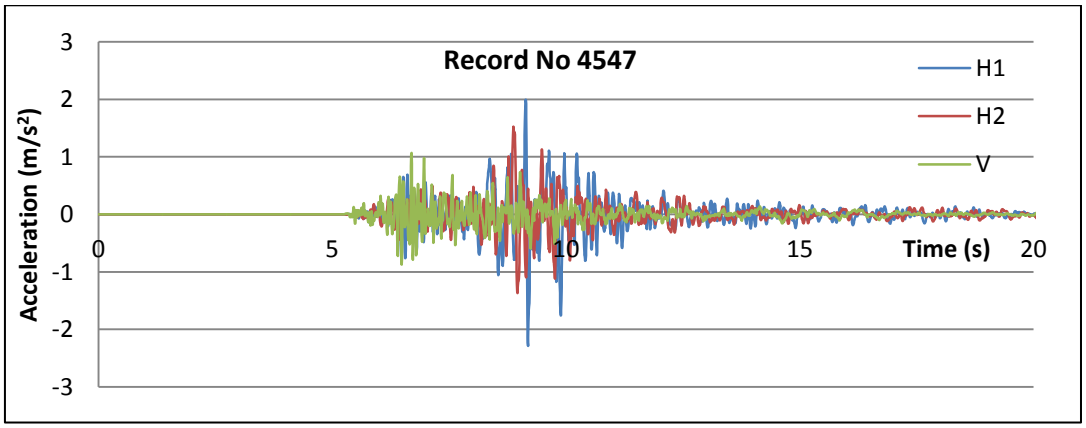

(b)

Figure 3.5: Graphs of selected records, for 475 years return period 412 (a), record no 4547 (b), record no 5478 (c) and for 2475 years return period, earthquake no 412-2475 (d)

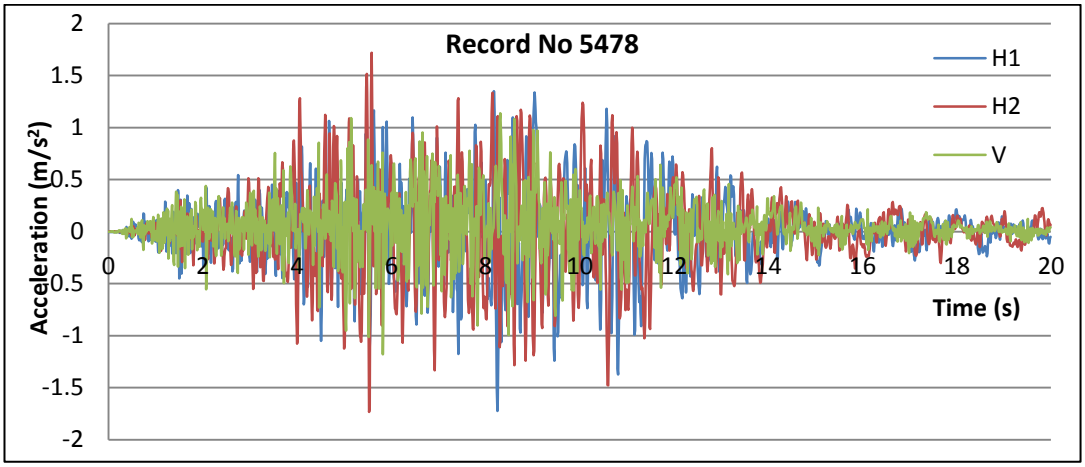

(c)

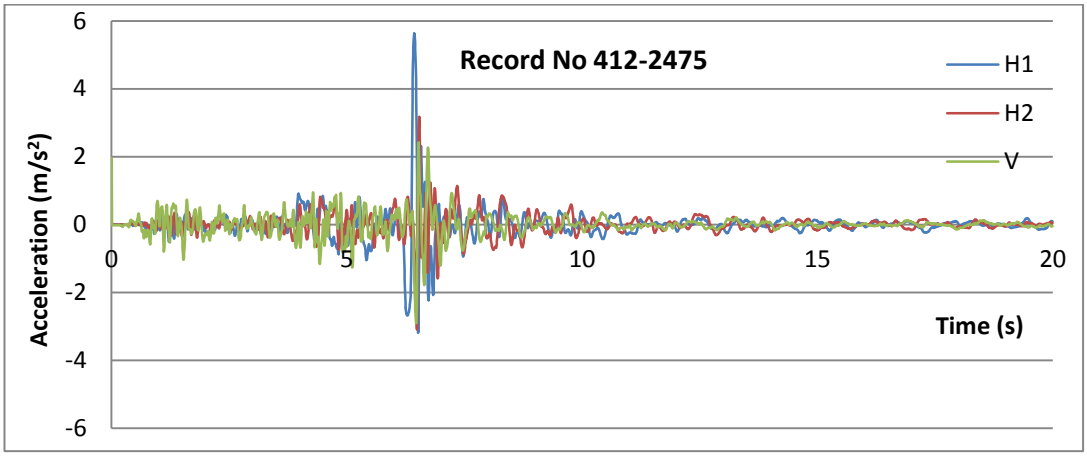

(d)

Figure 3.6 (continued)

Of the selected records, record no 412 has a pulsative nature, belonging to "Coalinga-05" earthquake that took place in 1983 in California, U.S. and recorded at a station named "Pleasant Valley P.P. – FF". Record no 5478 has a harmonic nature; it belongs to Iwate earthquake of 2008 that took place in Japan, recorded at "AKT023" station. The record numbered 4547 has both pulsative and harmonic characteristics. It is a record of L'Aquila earthquake took place in Italy in 2009 and was captured at "L'Aquila - V. Aterno - Centro Valle" station.

In addition to the selected records, a high intensity ground motion was used to be able to properly investigate the collapse mechanism in the discrete element model generated in ABAQUS. For that purpose a record of 1999 Izmit earthquake was utilized. The employed record of the considered earthquake, captured at "Duzce Merkez Meteoroloji Istasyon Mudurlugu" station is provided in Figure 3.6. In addition to serving the purpose of triggering collapse mechanisms both for the temple's current form model and for the models representing the strengthening proposals, results of these analyses carried out with Izmit 1999 record were also useful as a further, more stringent performance evaluation.

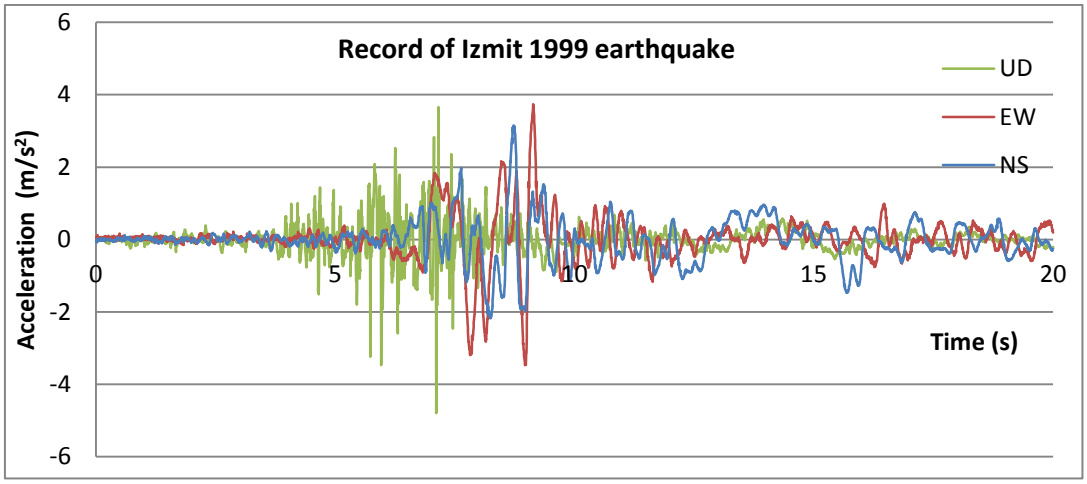

Figure 3.7: Record of 1999 Izmit earthquake employed in the analyses

3.3 Finite Element Modelling of the Monument

As it was stated previously, a linear elastic finite element model of the current state of the temple was formed using SAP2000 software. After the formation of geometry, modal analysis was conducted and their results were compared with the natural vibration periods obtained from the real structure. The generated model was then calibrated until a satisfactory convergence criterion was satisfied. Then, time history analyses with the preselected ground motions along with a response spectrum analysis were conducted to determine the overall stress distributions on the structure. This information was used to evaluate locations of stress concentrations where a failure could take place.

The generated 2D shell finite element model reflects the geometry of the structure on a macro level. Along with the original marble sections, the rubble wall that extends from the northern end of the northwestern wall to halfway beneath the northern isolated wall was added. The Byzantine era crypt at the rear end of the temple was also modelled.

The model was calibrated changing the density and modulus of elasticity of three different materials that make up the model, namely marble (the main material of the temple) rubble (representing the rubble walls) and also the brick (material of Byzantine era crypt). Iterations continued until the natural frequencies of first two mode were in 95% convergence with the natural vibration periods belonging to the real structure. The first six mode shapes are presented in Figure 3.7.

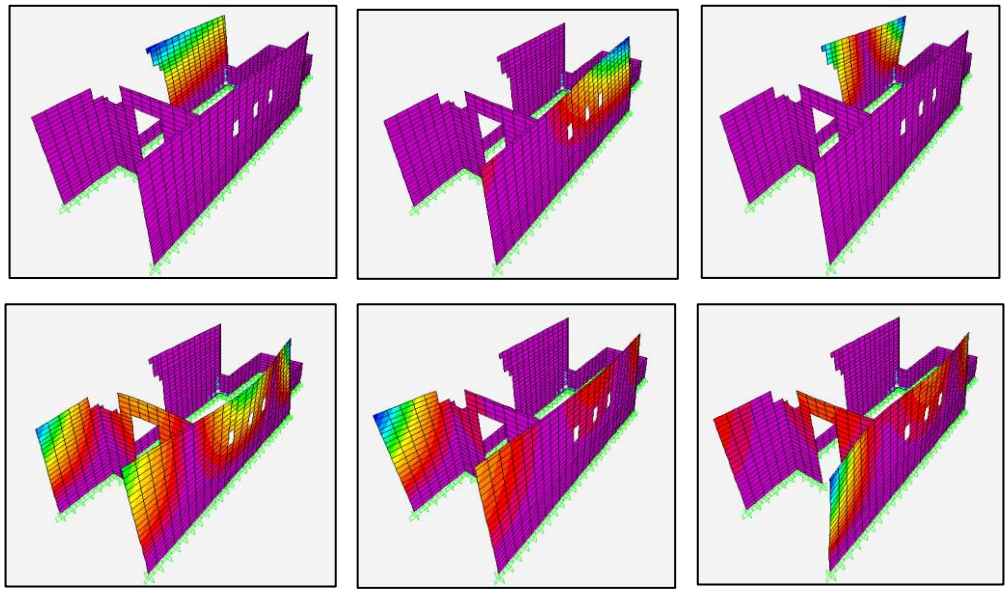

Figure 3.8: Shapes of the first modes of the model, with the first mode being shown in the first row, first column and the fourth mode shown in the second row, first column and so on.

The comparison of the first four mode periods with the experimentally obtained ones is provided in Table 3.1. The material properties determined as a result of the calibration process are given in Table 3.2.

Table 3.1: Comparison of modal periods after calibration

	Model Periods (s)	**Experimental Values (s)**	**Error**
First Mode	0.754	0.758	%0.05
Second Mode	0.455	0.455	%0
Third Mode	0.279	0.290	%3.8
Fourth Mode	0.231	0.245	%5.7

Table 4.2: Material properties obtained as a result of calibration

	Density (kg/m^3)	**Modulus of Elasticity (MPa)**
Marble Blocks	2550	5600
North Wall Rubble	2000	920
Byzantine Era Crypt Blocks	2200	800

Following the calibration of the model, response spectrum and time-history analyses were conducted on the model. Time-history analyses were conducted with the selected ground motions. For the response spectrum analysis, spectrum curve obtained from TEC 2007 was employed with Z3 site characteristics, and in the determination of the coefficient, Ulus was considered as a third degree earthquake zone. Results of these analyses are provided in S11 and S22 directions for earthquake record no 5478, which resulted in highest stress values between all other earthquakes selected for 475 years return period, in Figure 3.8. Similarly, in Figure 3.9, results of time-history analysis conducted with record no 412, scaled for 2475 years return period are given. Response spectrum analysis results are given for application from either direction, in Figure 3.10.

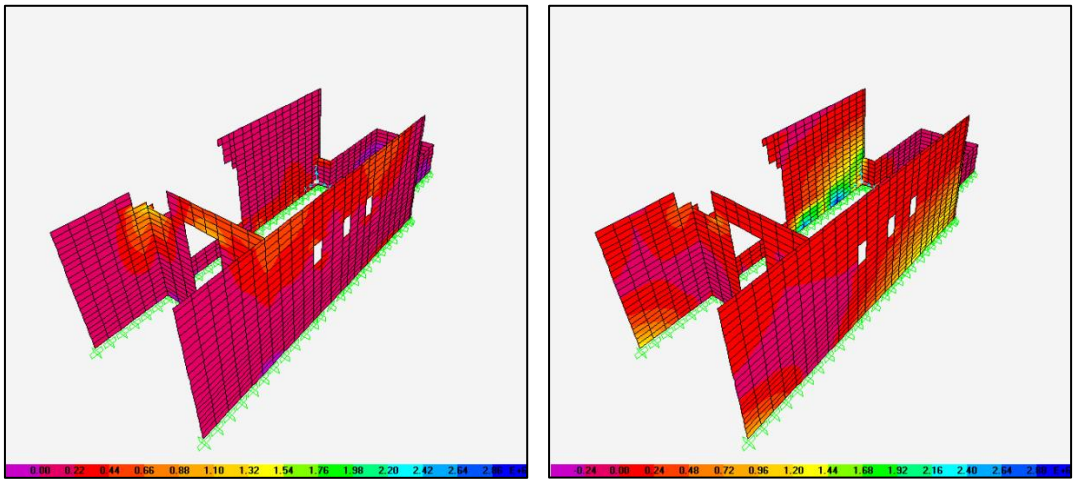

(a) (b)

Figure 3.9: S11 (a) and S(22) results for time-history analysis with record no 5478. Units are in Pa.

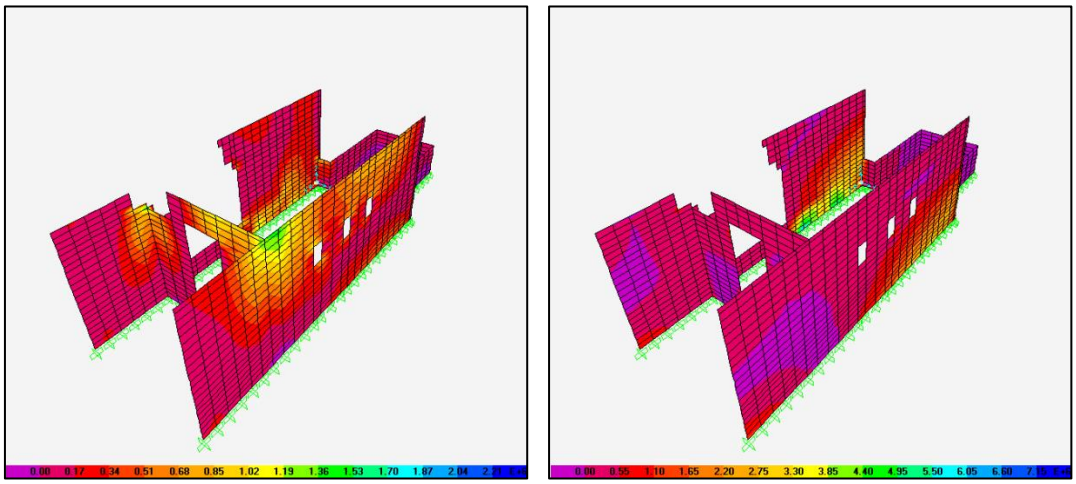

(a) (b)

Figure 3.10: S11 (a) and S(22) results for time-history analysis with record no 412-2475. Units are in Pa.

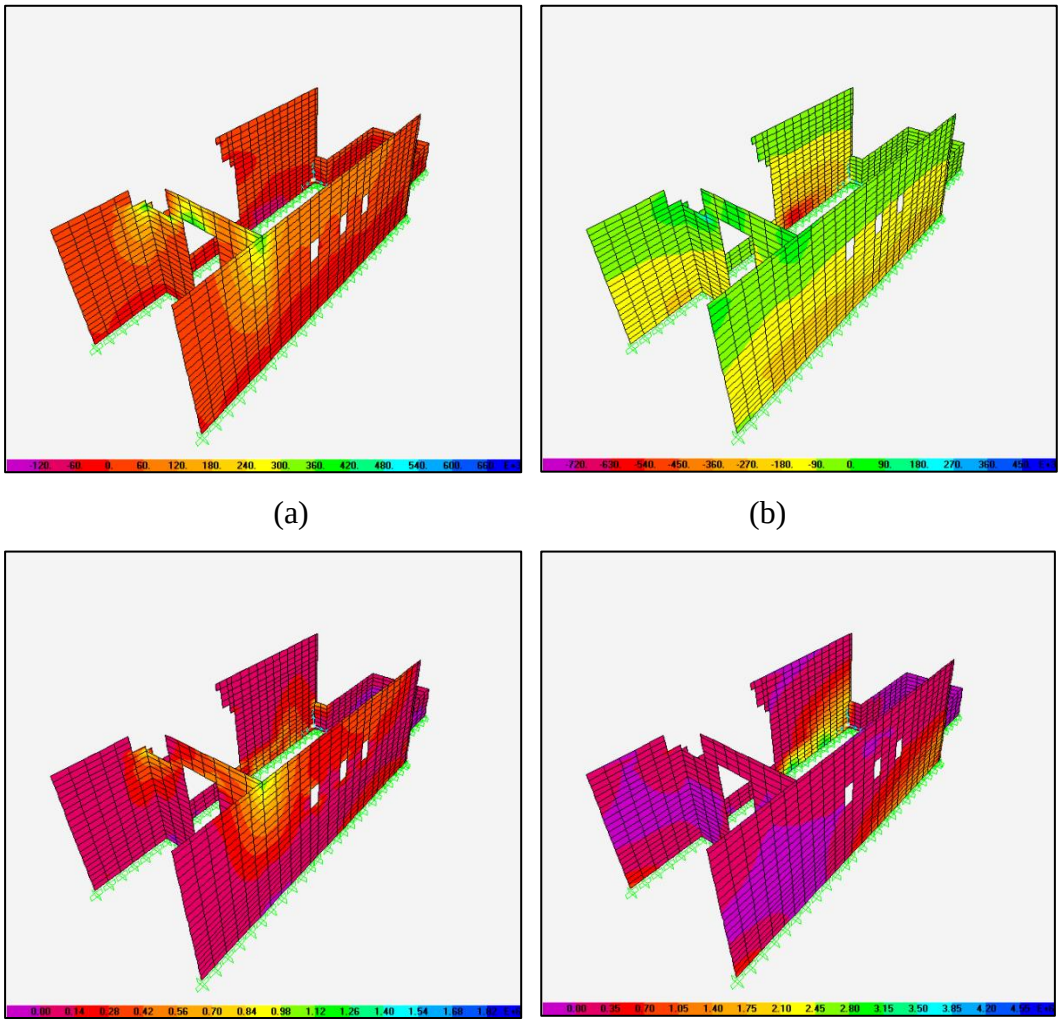

Figure 3.11: Response spectrum analysis results, with longitudinal direction application results on the first row and transverse application results are in the second row. S11 (a), S22 (b), S11 (c) and S22 (d) Units are in Pa.

All results indicated stress concentrations at the lateral wall-gate section connection area, and the bottom layers of the lateral walls, with the northern isolated wall being subjected to greater stresses in each case. At the lateral wall-gate section connection tensile stresses in the range of 1MPa to 450kPa was observed. Beneath the northern isolated wall, for response spectrum analysis and 475 year return period record time

history analyses, tensile stress values around 2.7MPa were obtained. This value was increased to around 5MPa for the analysis conducted with 2475 year return period earthquake record. While it is obvious that the rubble wall part beneath the isolated wall section cannot withstand such amounts of tensile stress in its current weak state, the fate of the lateral wall-gate section connection part and the ornamented gate lintel cannot be determined clearly from this analysis. Presence of the iron connectors, and also the material state at the aforementioned locations may show resistance to collapse. Consequently, the analyses conducted in SAP2000 were unable to fulfill the need for realistic structural behavior modelling demanded in this case. With a continuous linear elastic finite element model, cracking and collapsing simulations cannot be realized, thus the vulnerabilities of the structure and its parts that need intervention cannot be fully and truly identified. As a result, this need for realistic modelling was tried to be satisfied with the discrete element modelling and consequent analysis in ABAQUS software.

3.4 Discrete Element Model of the Monument

Even though the analyses to be carried out in ABAQUS software were aimed to obtain more advanced results, a similar approach employed with the linear elastic SAP2000 FEM models was also applied in the generation of the discrete element model. After the formation of the geometric model representing the temple's current state, modal analysis was conducted and the results were compared with those from the real structure for calibration of the material properties (again density and modulus of elasticity) of different materials making up various parts of the temple. This was followed by time history analyses with the preselected ground motions. These analyses enabled the determination of collapse mechanism of the structure, and revealed the weak zones that require intervention, which is the main topic of the next chapter.

3.4.1 Modelling Criteria

The discrete element model created in ABAQUS is almost an exact representation of the actual structure, where not only the regular shape but also the irregularities and discontinuities in geometry were also modeled. Only the slight taper observed on the lateral wall thickness was not reflected, since it would lead to extra work that would not worth the extra time and effort spent on it in this and the next steps, such as the formation of T shaped stones in the intersections of lateral walls and the gate section on this step, and the generation of proposed strengthening models in the next step. Rubble wall sections on the interiors of each lateral wall and the sections made up of local andesite material were represented. The inclusion of the Byzantine era crypt was decided after the initial set of analyses.

Apart from the material properties, the friction between the elements is another critical parameter unique to discrete element analysis. For the analyses carried out in ABAQUS software, the default Coulomb friction model: where relative motion between two elements may only take place if the critical stress, which is product of μ, coefficient of friction and ρ, surface pressure,

$$\tau_{crit=}\mu*\rho \qquad (3.1)$$

is defeated by "equivalent shear stress", is employed. Since a laboratory test regarding the determination of this parameter was out of the scope of this study, an approximate conservative value was used, taken from the study of Marino, Neri, De Maria and Borri (2014) conducted on friction coefficients for various masonry types.

Before commencing the actual analyses on ABAQUS software, a few trial runs that constituted the "sanity checks" were carried out. There it was observed that an instant application of gravitational acceleration on the model, along with the time

history load would lead to erroneous results. In order to cope with this, an approach employed by Gjorven and Nguyen (2012) was also used here where the gravity load is applied and increased with a smooth amplitude curve for ten seconds until it reaches the actual value, and then it is left unchanged for ten further seconds to decrease oscillations (Figure 3.11). This also enables the attainment of an initial steady stress state.

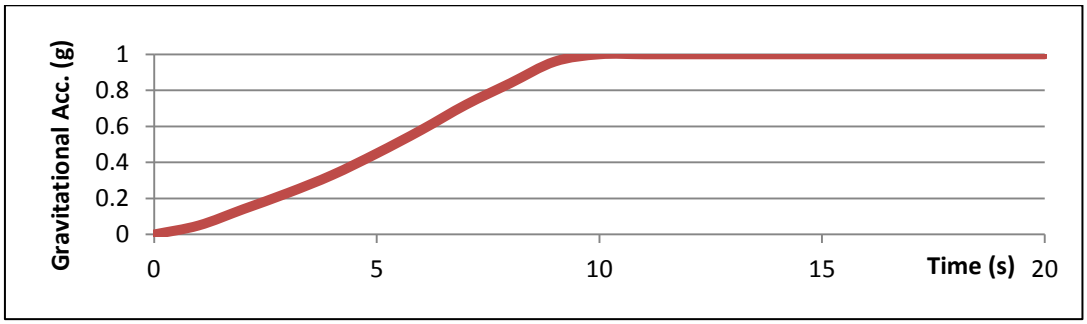

Figure 3.12: Time (s) vs Gravitation Acceleration (g) curve applied to the models at the first step

This constituted the initial step of all nonlinear time history analyses conducted in ABAQUS software.

Mesh convergence analysis

Another important concern for the discrete element analyses was the mesh density. As a rule of thumb, in finite element analysis, finer mesh results in higher convergence, but it is costly in terms of computational work and time. Coarse mesh may produce faster results, but it may not be very reliable. A logical approach to mesh convergence is to increase the mesh density until a convergence of results is achieved. Therefore, as a part of this study, a mesh convergence analysis was conducted based on eigenmodes of a regular wall section. The wall section was made up of blocks resembling the regular blocks of the Temple of Augustus with

two aspect ratios, one with 1.5m length, 0.5m height and 0.9m depth and other with half the length. It is basically a monotonous section featuring 9 layers and 3 rows.

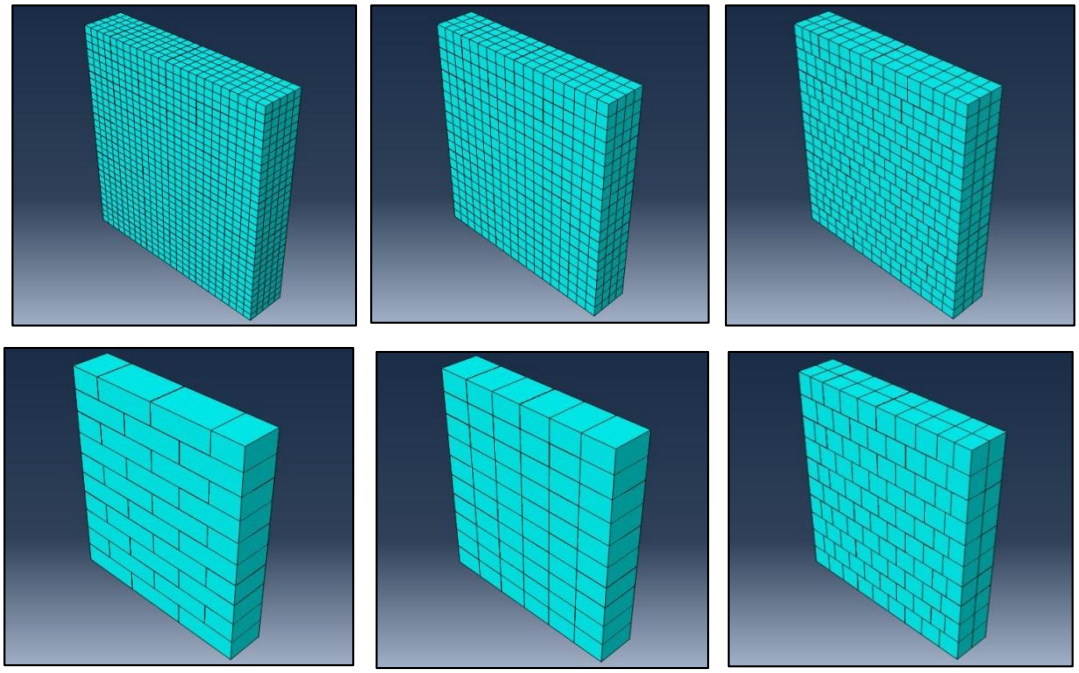

Figure 3.13: Various mesh densities applied on the wall, specimens with 0.2m, 0.25m 0.3m, 0.5m, 0.75m and 1.5m densities are displayed here in clockwise direction sequence

Analyses were carried out with mesh densities that are multipliers of dimensions. Starting out from the coarsest mesh where one block is represented only with a single 8 node element (that is 1.5m density), the density was increased up to 0.1m and modal periods up to third mode were compared. Most coarse 6 of these models are presented in Figure 3.12.

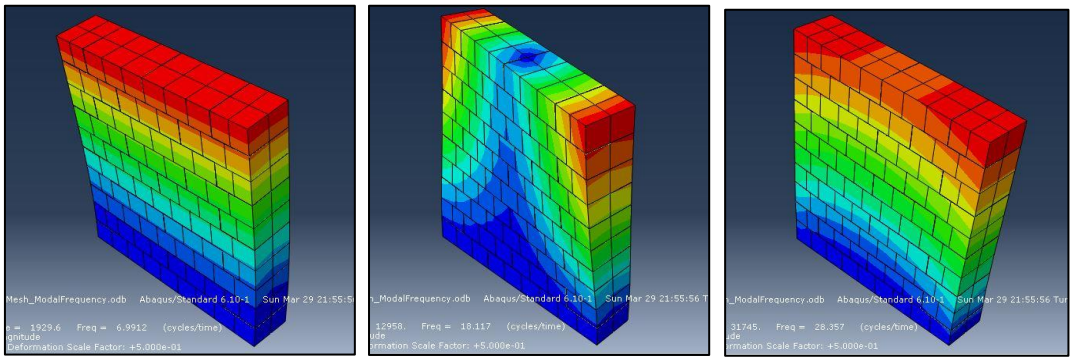

Figure 3.14: The first three modes of the wall section for 0.5m mesh density. Period values are 0.143s (first bending), 0.055s (torsional), and 0.033s (second bending), respectively

Even though mode shapes were similar for all cases (as given in Figure 3.13), analysis results, as presented in Figure 3.14 showed that there is a sharp drop in the period values obtained from the software between the densities of 0.75m and 0.5m. This may be attributed to the mesh line forming in the mid-depth for densities 0.5m and higher. When density increased beyond 0.5m, convergence is increased slightly at 0.3m and then it is stable. Therefore, while it is safe to state that an analysis carried out with a mesh density higher than 0.5m will yield erroneous results, whether investing in further convergence that take place for densities smaller than 0.5m would worth the computational cost is questionable.

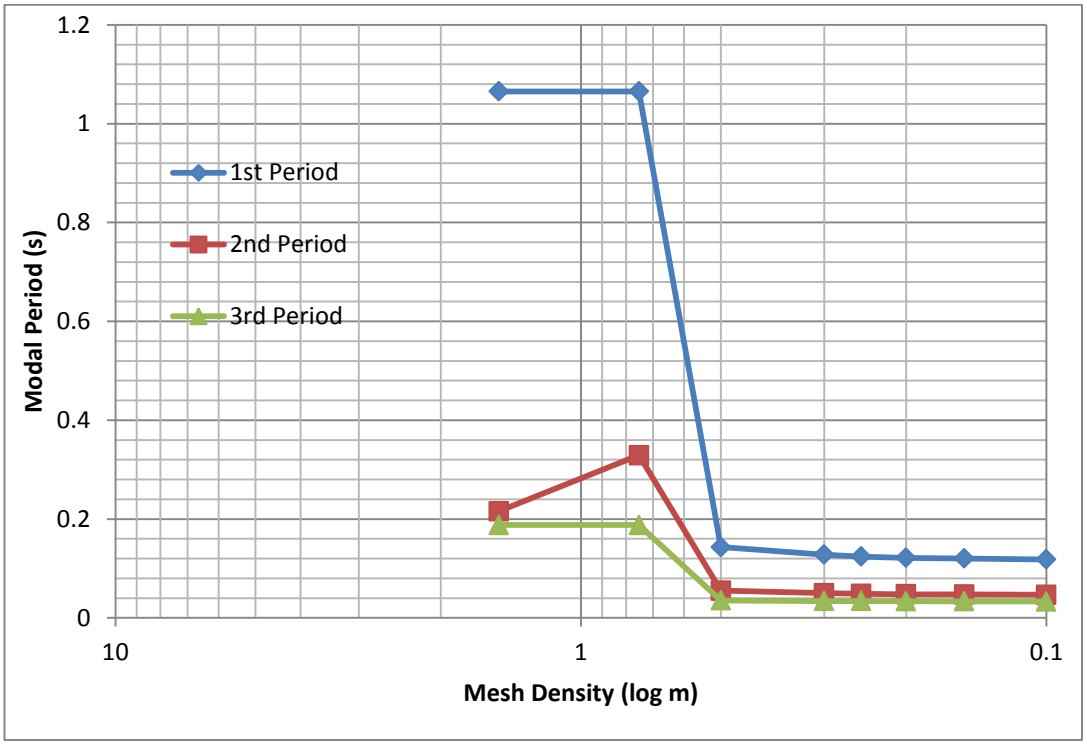

Figure 3.15 : Results of modal convergence analysis. Convergence start can be observed at 0.5m mesh density.

Eventually, considering the heavy computation load in carrying out discrete element time-history analyses in ABAQUS (in this case, with models constituting more than a thousand entities), at this step some small amount of accuracy had to be sacrificed in favor of analysis speed, and 0.5m or a similar mesh density where a mesh line would form at the mid-depth of layers were accepted as the final density. For the main analyses, this observation and resultant parameter was employed.

3.4.2 Modal Analyses and Calibration of the Model

As stated earlier, similarly with SAP2000 model, modal analyses were conducted on the geometrically-completed model and iterations were carried out to converge the modal frequencies of this model with that of the real structure. The first four

modes were taken into primary consideration in the calibration of the model, and they ultimately showed a nice comparison with the experimentally obtained values, as given in the Table 3.3.

Table 3.3: Comparison of analytical modal periods with experimentally obtained period values

	Model Periods (s)	**Experimental Values (s)**	**Error**
First Mode	0.737	0.758	%2.77
Second Mode	0.473	0.455	%3.96
Third Mode	0.280	0.290	%3.44
Fourth Mode	0.236	0.245	%3.67

Calibrated model's first six modes are given in Figure 3.15. They represent first bending of northern isolated wall and southeastern wall, torsional mode of the northern isolated wall and other torsional modes of the temple.

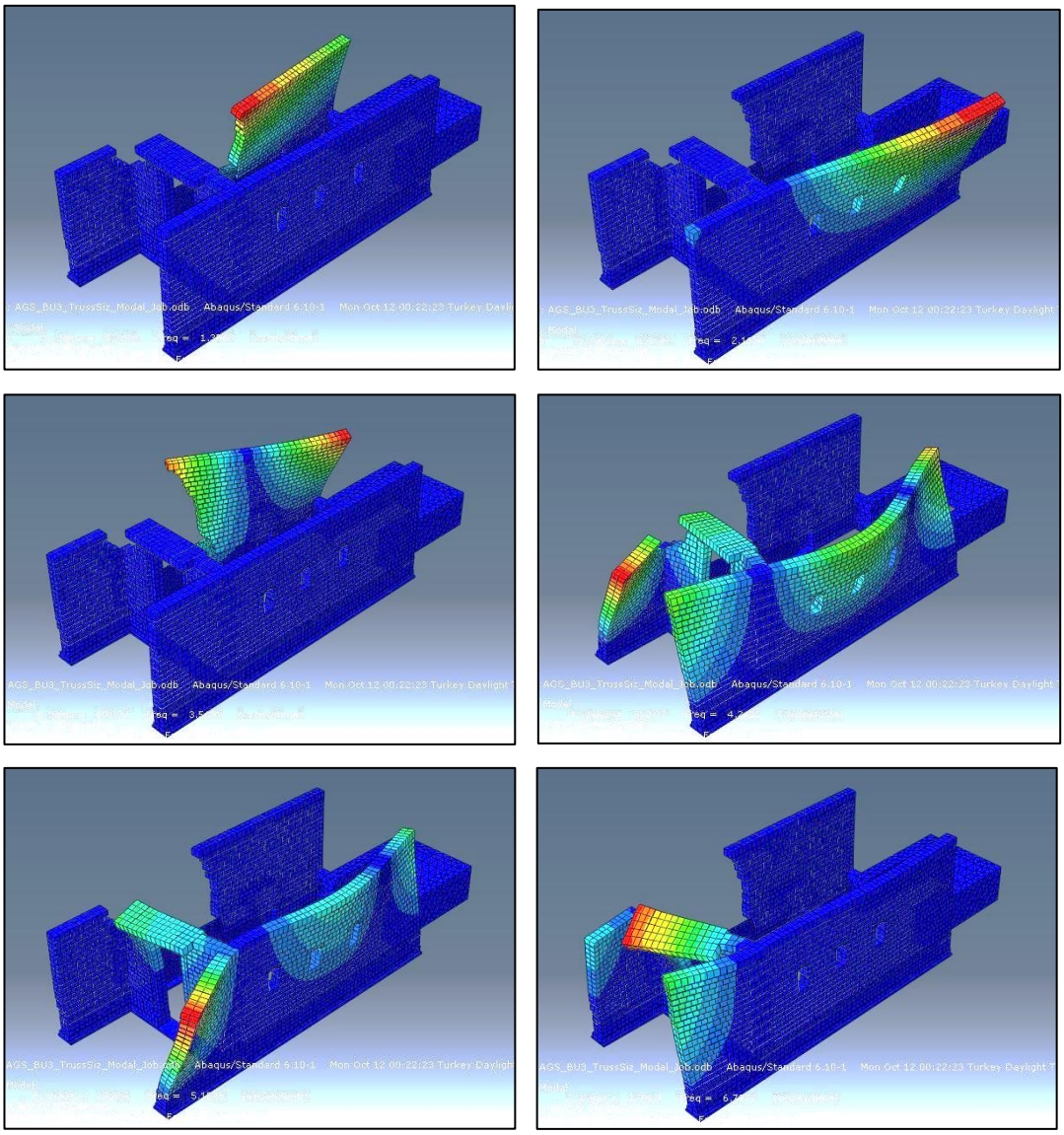

Figure 3.16: Mode shapes of the calibrated discrete element model. First mode is on the first row on the left, second mode on the right, third mode on the second row on the left and so on.

Since the geometrical information was known, the only parameters of calibration were modulus of elasticity and density of materials. The values of these properties belonging to various materials constituting the model that were determined during the calibration study are presented in Table 3.4.

Table 3.4: Material properties determined during calibration

	Density (kg/m^3)	**Modulus of Elasticity (MPa)**
Marble Blocks	2550	7100
North Wall Rubble	1800	620
South Wall Rubble	2000	3000
Andesite Blocks	2700	50000
Byzantine Era Crypt Blocks	2200	1000

Similarly with the linear elastic FEM model case, the determined material properties are merely hypothetical and the need for laboratory testing is clear; which is impossible due the current conservation status of the temple. Still, they point out some hints about the material condition of different sections of the temple. The most important material is certainly the temple's marble. Its low modulus of elasticity value may point out the material degradation, but it may also be a result of the flexibility generated by the iron connectors. Another point worth noting is the difference in the properties of the two rubble wall sections. Northern rubble wall is not covered like its southern counterpart, and it was not built as orderly; it's in a horrible condition. These factors seem to be reflecting their effects on the model as well, where very low elasticity modulus of northern wall suggests that it offers almost no real resistance to load.

The minor difference in the determined material properties in FEM and DEM is worth noting. This may be attributed to the geometrical differences in these models, where some details were dismissed in FEM, and also to the differences in modelling approaches, where the walls were modelled as a single entity in FEM and as made up of smaller elements in DEM.

Determination of these material properties are of critical importance, because not only will they be used in the evaluation of current structural capacity, but also in the studies presented in the next chapter where analyses are carried out for various strengthening proposals.

Apart from the calibration of material properties using structural modes, another verification study was carried out to properly model the tilting on the northern isolated wall. As stated in the introduction chapter, this northern isolated wall, the weakness of which was also revealed by the modal analysis (by its low period), is tilted by 3 degrees inwards, upon the rubble wall section that was used to replace missing stone layer. Even though it is tilted, the wall is in a relatively stable condition where increase in the tilt speculatively takes place in the long term. The vulnerability posed by the tilt may be exploited by an earthquake, but when at rest it does not collapse by itself. The complication with this task was in reflecting this behavior without a bias for collapse in the steady state. The model had to be modified in such a way that the tilt amount would hit the targeted value before the time history analysis step, but it would do so not while the tilt is increasing, but while it is in a steady state.

Even though without any intervention the straightly upwards modeled northern wall demonstrated a tilting pattern very similar to the actual structure, the tip displacement amount was less than a quarter of the actual amount. In order to achieve the desired tilt, the elements constituting the wall were leaned inwards for finite amounts adding up to half the desired inclination. The aim was to obtain the target tilt with the help of the gravity loading applied in the first step, before the time history analysis step was activated. It was observed that even though the wall would reach the tilt and top displacement amounts desired, it would never settle but continue tilting (in a linear way for some seconds) until it collapsed. In order to cope with this, taking into consideration the linear behavior in tilting of the wall, some selected elements in the desired corner were “pushed” back for five millimeters, increasing for five seconds linearly and then decreasing in the same

fashion until the "pushing" was terminated. The wall was observed to achieve a steady state at a top displacement value very close to the actual condition, after the termination of tilting and under the unchanging gravitational acceleration. This behavior was captured and shown in the Figure 3.16. The author would like the reader to note that this process required countless amounts of iterations both for the initial lean and the selection of "pushed" elements, and the amount and duration of "push" back.

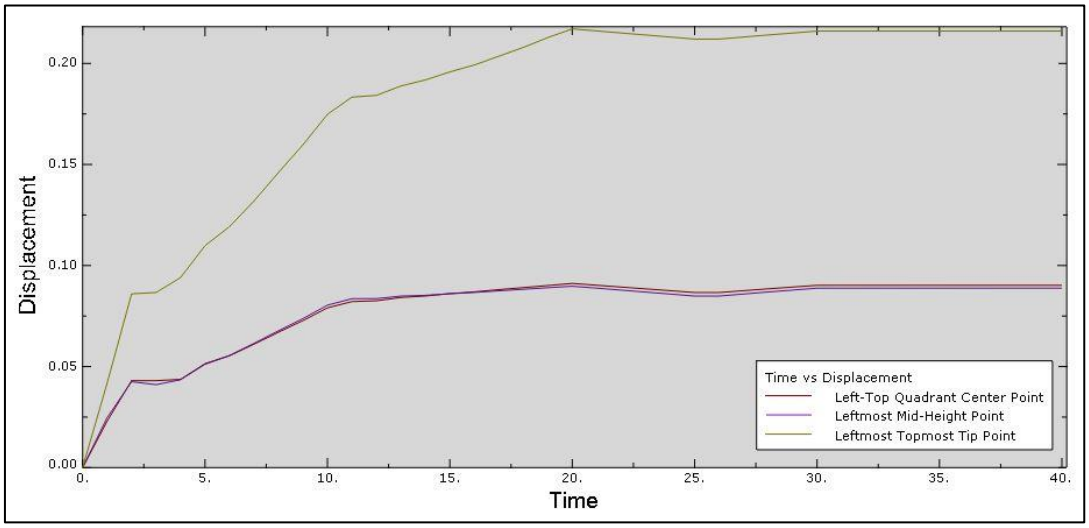

Figure 3.17: Time vs. Displacement graph of elements on the northern isolated wall's tilted end. Displacement of "Left-Top Quadrant Center Point" is from the element whose displacement amount was the main target.

Considering that the initial inwards lean was set at 29mm, its addition with the displacement shown in Figure 3.16 gives 51mm, which requires noting that while this value is quite close to the target of 52mm, the difference is negligible. Figure 3.17 shows the final state of the wall before the time history analysis. Also, on the Figure (3.16), note that "push" starts at 20th second, increasing until 25th second and then decays in a similar fashion for 5 more seconds where at 30th second it is terminated.

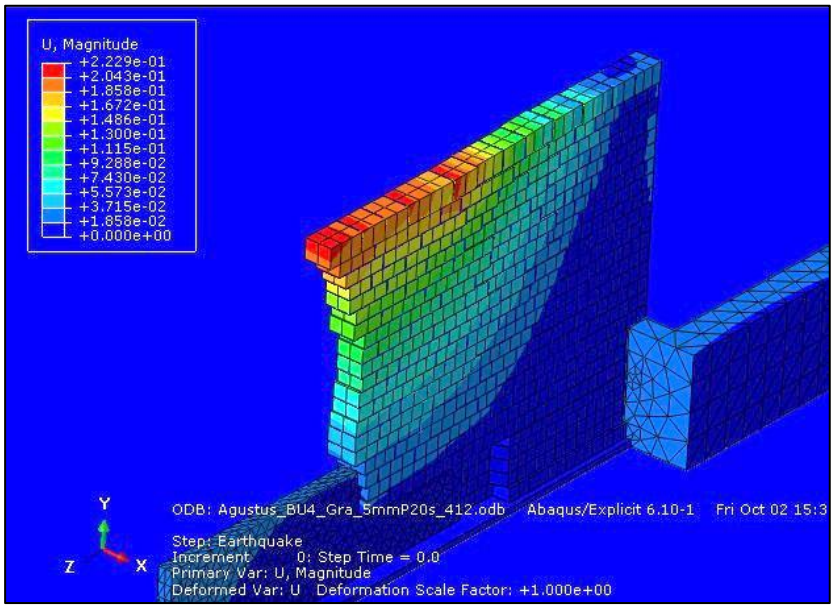

Figure 3.18: Northern isolated wall showing 22.29 cm displacement. Unique behavior of the actual wall where it resembles a folding paper leaf is mimicked accurately.

One final remark in this section is that instead of the 20 second gravitational loading mentioned in the previous section, a 40 second gravitational loading step was used for performance analyses discussed in the next section in order to be able to perform this verification before the time history analysis step.

3.4.3 Evaluation of Structural Capacity for Strengthening Proposals

The discrete element model of the temple, calibrated and modified as specified in the preceding section, was analyzed under the ground motion data selected as presented earlier in this chapter. Main purpose of conducting these analyses on the temple in its current form was to assess its collapse risk and determine the collapse mechanisms and sources. Analysis results were consequently used to determine the parts that require intervention.

First set of analyses were conducted with 475 year return period earthquake ground motions, namely ground motions No 412, 4547 and 5478.

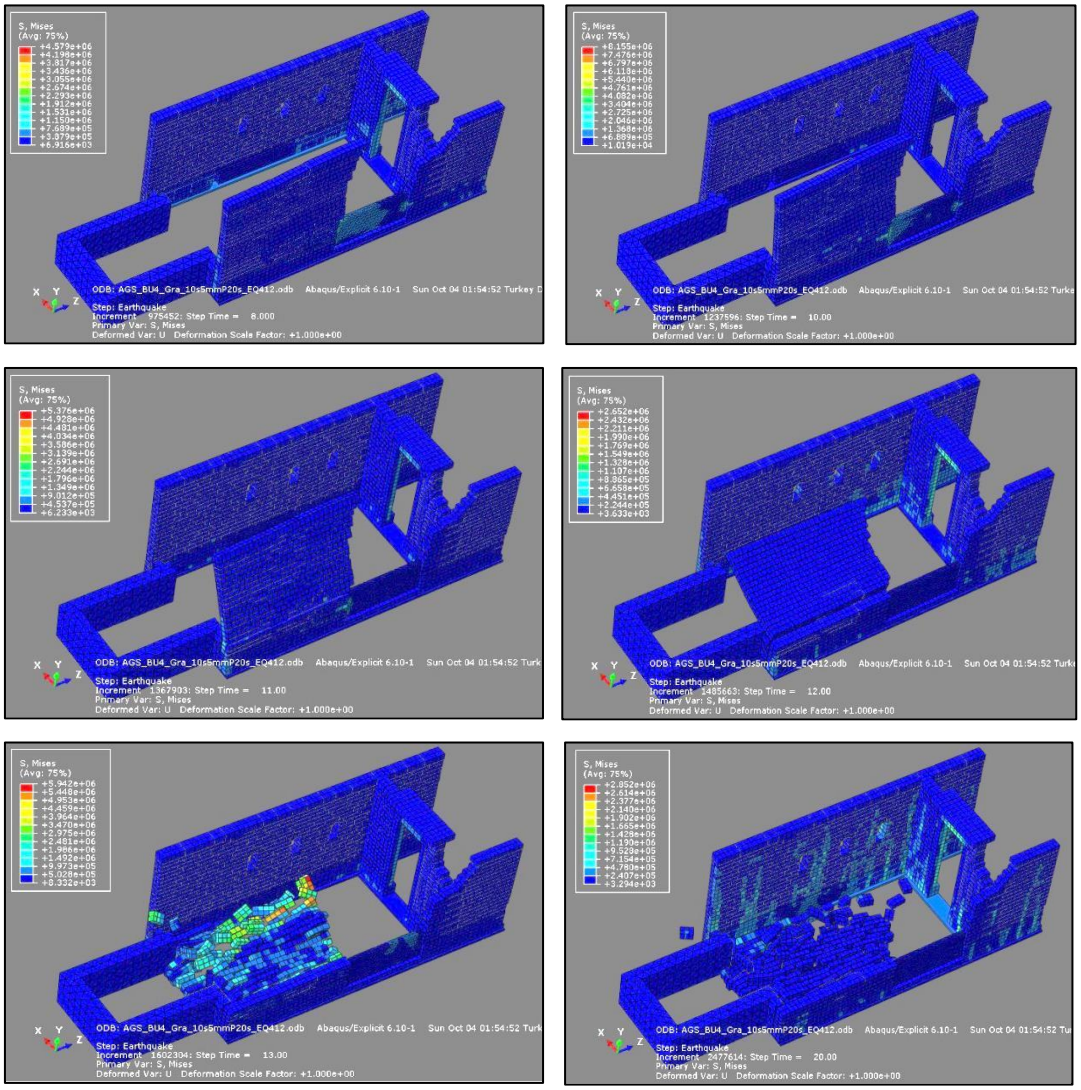

Figure 3.19: Collapse of the northern isolated wall as induced by EQ No 412

Excitation of the model provided by earthquake No 412 was enough to trigger instability of the already tilted northern isolated wall (Figure 3.18) where it crumbled on its tilted side, towards the interior of the temple. However, the damage was limited to this, and this earthquake caused no further damage on the other parts

of the structure. Observed stress values were also low. In any case, this analysis showed that the northern isolated wall, devoid of any out-of-plane support, can be overturned by a mild intensity earthquake.

Analyses carried out with earthquakes No 4547 and 5478 did not cause instability on the northern isolated wall, but furthered the tilt observed on its southern end, by 13 cm and 18 cm, respectively (Figure 3.19).

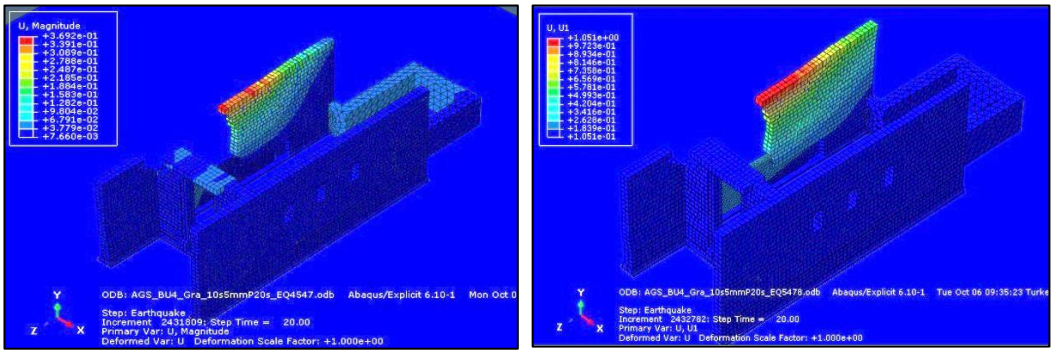

Figure 3.20: Deformations induced by earthquakes no 4547 (left) and 5478 (right)

Analysis with earthquake No 412-2475 yielded a result similar to its 475 year return period counterpart, where the tilted northern isolate wall collapsed inside the temple. The stone block layer where the overturning was initiated was also observed to be same.

Based on these results, a further investigation was initiated in order to examine the effect of Byzantine era crypt wall, since it was seen in the previous analyses that collapse of the northern isolated wall initiated from just above the layer supported by this short wall. These further analyses carried out with a record of Izmit 1999 earthquake also demonstrated further collapse mechanism of the temple.

Analysis carried out with this record and Byzantine era crypt present model showed that a stronger ground motion also causes the door frame to become unstable and collapse, along with the north wall (Figure 3.20). Instability of the door section resulted in not only the collapse of the ornamented lintel complex, but also the columns that supported it, possibly due to the defeat of almost nonexistent frictional force between the columns and the walls next to them.

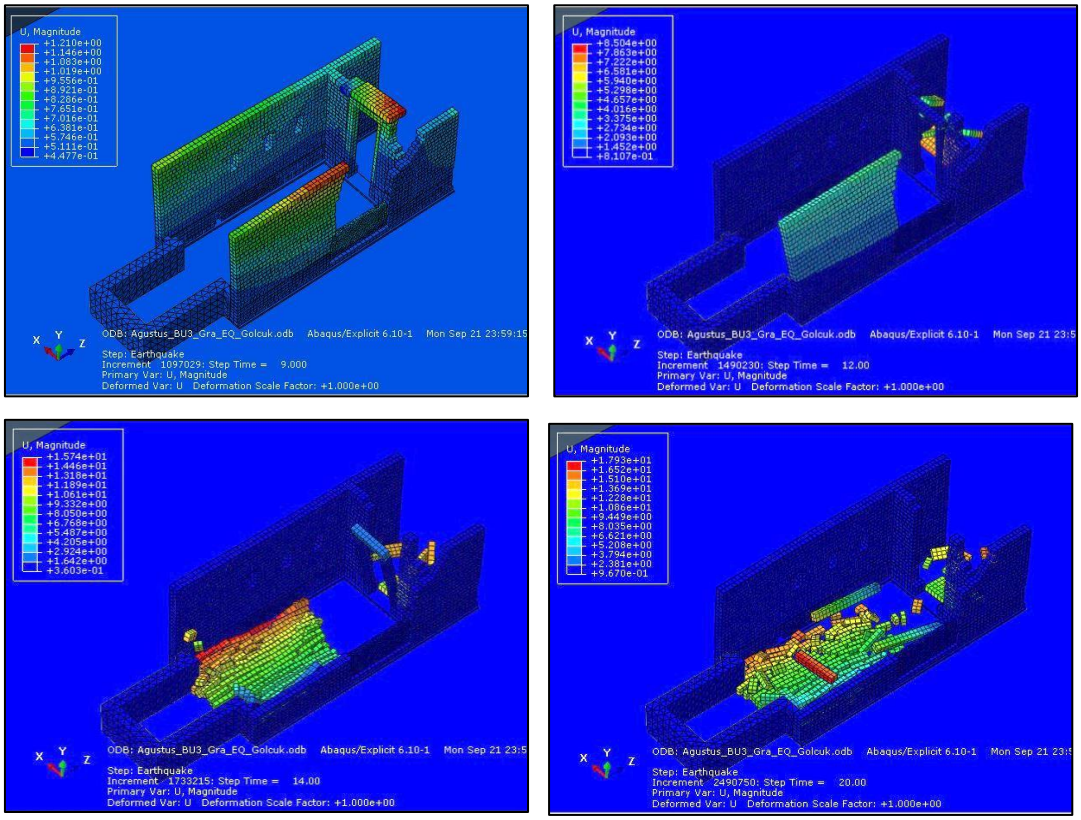

Figure 3.21: Collapse propagation under Izmit 1999 earthquake

Analysis case where the temple was excited with Izmit 1999 earthquake with Byzantine era crypt walls were removed, bore interesting results (Figure 3.21). It was observed that the in the absence of this short wall, the overturning started from a lower layer of blocks in the northern wall. Afterwards, top layers of the collapsing northern wall hit the southeastern wall. A combination of disturbing forces resulting

from this, and also the earthquake excitation cause the southeastern wall to disintegrate through the window openings. It is worth mentioning that a similar collapse of the door frame with the previous case where columns were toppled along with the ornamented lintel was also observed in this case.

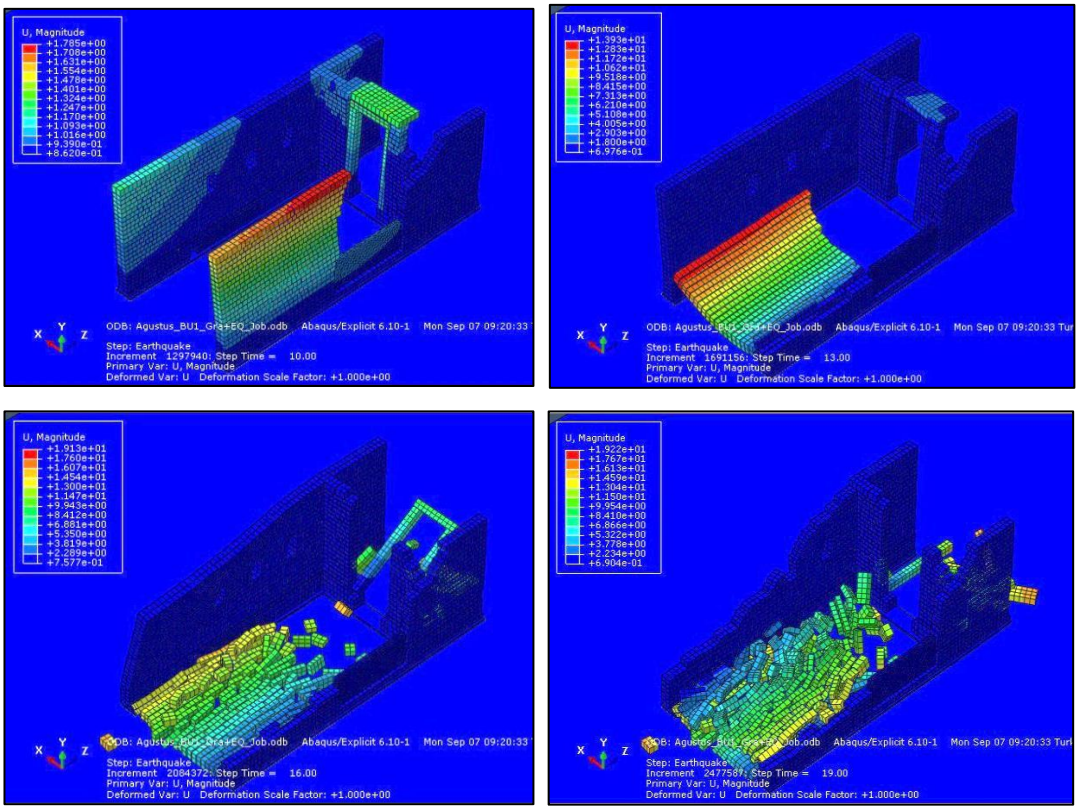

Figure 3.22: Collapse mechanism observed under Izmit 1999 earthquake excitation for the Byzantine era crypt removed case.

Comparison of these cases point out the difference that a small support can create for the longitudinal walls of the temple. With the second analysis, the collapse preventive effect of the relatively short Byzantine era crypt wall on the 10 meter high and approximately 28 meter long southeastern wall was observed clearly. This collapse preventive effect of a perpendicular support on the temple walls form the basis of one of the strengthening proposals laid out in the next chapter.

Another important point is the instability of the door lintel and frame shown with the Izmit 1999 analyses. Even though they remained intact in analyses conducted with other earthquake data, considering the inability to reflect the current deteriorated condition of the lintel as-is in the model, they can be considered under the risk of collapse and in the need of intervention. However their collapse mechanism may differ according to the state of iron connectors between the columns that constitute the frame and the walls. If they are intact, a higher resistance may be expected.

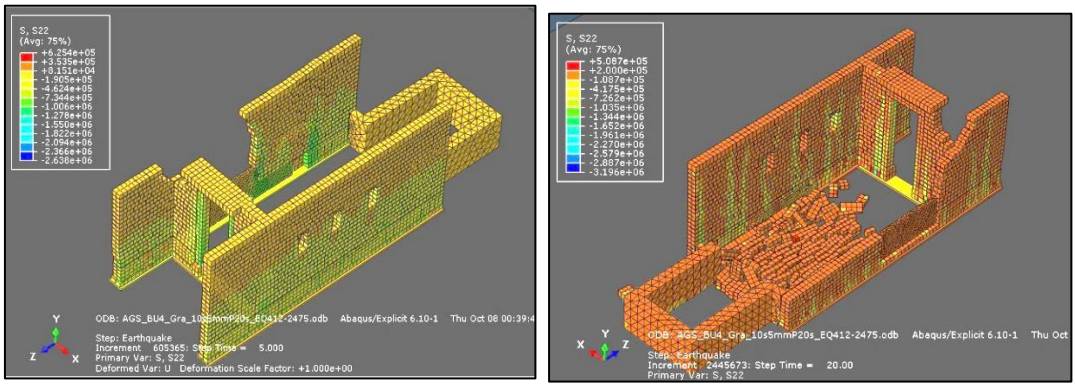

Figure 3.23: Vertical stress distributions observed on the model, (left) prior to north wall overturn, the 5th second into the analysis, and (right) at the end of the earthquake excitation.

Another evaluation of results was made from the point of stress concentrations. Stresses observed during the application of earthquake no 412 with 2475 years return period (highest intensity selected earthquake) never surpassed the 3-3.5 MPa compressive stress range, anywhere on the model. While this amount of compressive stress is far below critical for the marble blocks constituting the temple, it may be serious for the rubble wall section beneath the northern wall, from where the collapse initiates (Figure 3.22, left). Moreover, the presence of vertical stress concentrations revealed on the last frame may also give a hint as to the damage occurred on the northern wall back in 1834 leading to partial collapse.

Consequently, it can be derived that damage to the structure is not caused by compressive overloading on the materials, but separation of blocks and vertical cracks taking place during seismic action.

3.5 Results of Structural Identification Studies

In this chapter, the temple was analyzed in its current form, both with linear elastic finite element model, and with discrete element model. Both analyses showed a vulnerability with the northern isolated wall. While this vulnerability was indicated by a high amount of tensile stress occurring beneath this section, in the discrete element analysis the results showed that the northern isolated wall carried an eminent risk of collapse, prone to be triggered even by lower intensity ground motions. Discrete element analysis also allowed distinguishing the importance and effect of the out-of-plane support provided by the Byzantine era crypt wall, the collapse mechanism of the lateral walls, and also of the ornamented gate lintel. It was impossible to obtain these results from the linear elastic finite element analysis in SAP2000.

Consequently, analyses conducted in this chapter showed that the strengthening system proposals must focus on primarily on improving the seismic resistance of the northern isolated wall, which carries the foremost risk of collapse. Certainly a system generated to improve the overall behavior is even more desirable. In the next chapter, several proposals for the strengthening are laid out and analyzed in a similar manner.

CHAPTER 4

STRENGTHENING PROPOSALS FOR MONUMENTUM ANCYRANUM AND THEIR EVALUATION

With the temple structure being fully investigated and identified at the site with dynamic measurements and visual examination, along with the analytical model analyses in the virtual environment, the study was finalized by proposing strengthening options. The proposals are mostly focused on improving the seismic resistance of the northern isolated wall, the vulnerability of which was laid bare with the aforementioned investigations.

4.1 Proposed Strengthening Systems and Their Evaluation

Two strengthening proposals with two variations each are given in this study. These proposals were developed with the adoption of minimum possible intervention to the historical structure principle. In determination of the seismic performance of these proposals, discrete element model generated in ABAQUS software, used in the previous chapter, was modified with the addition of strengthening systems in their respective detail. Moreover, finite element model created in SAP2000 software was also employed in the performance check of the second proposal.

4.1.1 Rebuilding of the Northern Wall

This first strengthening proposal is inspired by the good performance of temple's southeastern wall in comparison to the northern isolated wall. The southeastern wall is connected to the gate section, providing it with the support required during seismic action. The effect of this support is transferred to the wall ends by means of connections between the layers. Accordingly, this strengthening proposal prescribes rebuilding of the destroyed section between the northern isolated wall and the remaining part of the northwestern wall connected to the gate section.

Two related discrete element models were created reflecting these conditions, making up the two variations of this proposal. The basic difference is the replacement of the rubble wall section halfway beneath the northern isolated wall. One variation considers this section replaced and other considers it to be left as-is. These variations are created in accordance with the concerns that the removal of the rubble wall section beneath the wall may prove very difficult and dangerous to the integrity of this section. In both variations, the rubble wall between the two sections of the northwestern wall is considered to be removed and replaced with the newly to-be-built wall. Moreover, the northern isolated wall is considered to be straightened back up with the help of a jack system, prior to the reconstruction. Replacement stones were considered to be between 1 to 2 meters in length, but mostly 1.5 meters. Those that are in the regular section have 0.45m height; the other layers are in agreement with their respective heights. The layout constituting the basis for these models and the corresponding proposals are provided in Figure 4.1.

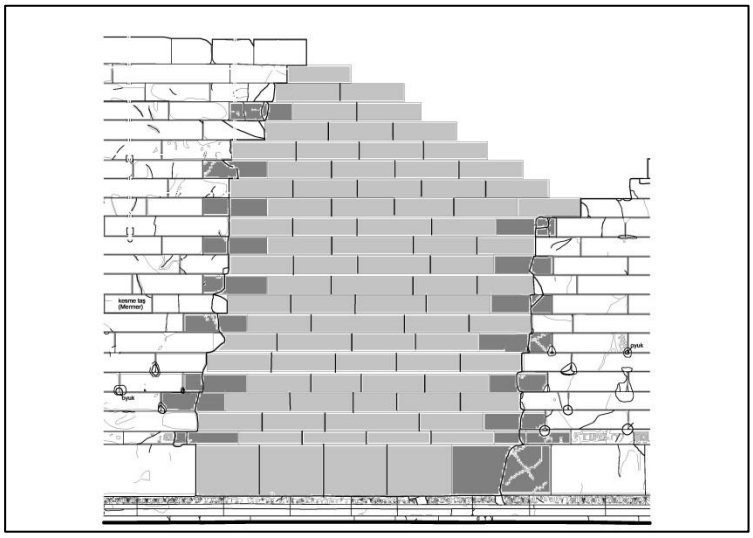

Figure 4.1: Reconstruction of the destroyed section of the northwestern wall. Original stones are colorless; those that are patched up are in dark grey and new stones in light grey

As seen in the Figure 4.1, realizing this proposal will require a patching up the broken blocks (dark grey blocks). Initially, replacement of the broken blocks were considered, however site investigations revealed this to be near impossible without causing damage to the wall, since especially the bottom layers are under compressive stress. Moreover, the iron braces will also resist the removal, and use of excessive force to remove them may also result in further damage. Therefore, patching up was the selected option necessary to ensure enough bonding between the existing sections and the new section to be built. Similar stone blocks were considered at the lower parts in agreement with the existing ones. The upper part of the wall was not fully reconstructed considering the minimum possible intervention principle; only adequate seismic performance enhancement was born in mind.

The first set of analyses was conducted with the model where the rubble wall layer beneath the northern isolated wall was not replaced. Results of the analyses carried out with earthquake no 412-2475 (Figure 4.2) showed that, this type of

strengthening is successful in preventing the collapsing of the northern isolated wall. Similar to the analysis case where no strengthening system was used in the previous chapter, the stress values are low, in the order of 1 to 2 MPa of compression. However, stress concentrations are observed at the edges of the wall where transition to the non-replaced rubble wall takes place (Figure 4.2, (a)). Displacement results also reveal the deficiency in the structure at this part, where the wall inclines up to 5-6cm above the non-replaced section (Figure 4.2 (b))

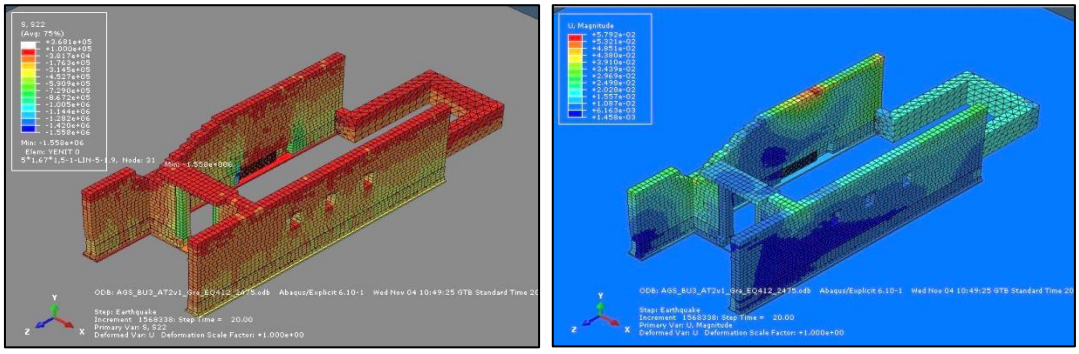

(a) (b)

Figure 4.2: Analysis results with earthquake no 412-2475, stress distributons (a) and displacements (b).

Figure 4.3 shows the modes of the structure with type of strengthening. The first mode of the structure still excites the northern isolated wall (the first bending mode); however, a significant drop in the period values can be observed, from 0.737s in the original model to 0.485 in this model. Southeastern wall's first bending period remained unchanged at 0.473s. Slight drops are observed in the third and fourth modal periods, from 0.280 to 0.237 and 0.236 to 0.230, respectively.

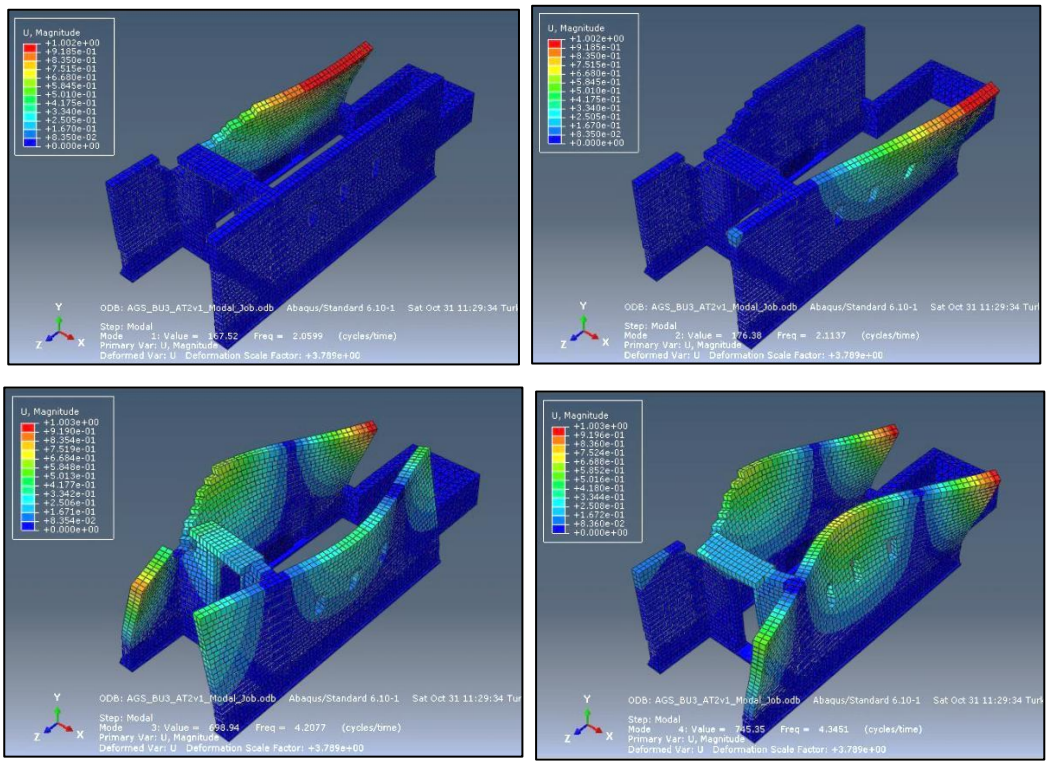

Figure 4.3: Mode shapes and modal periods of the model without stone block replacements. Period values are 0.485s, 0.473s, 0.237s and 0.230s.

These drops in period values point out to the extra restraint generated for the northern isolated wall with this system.

In addition to the test carried out with earthquake no 412-2475, another performance check was also carried out with Izmit 1999 earthquake record. The nonlinear time history analysis was carried out with the record, with independent applications where the horizontal component directions were interchanged.

The analyses yielded interesting results, where the structure avoided collapse in the application of earthquake with one set of directions, and lateral walls collapsing in the application of the earthquake with directions swapped. The collapse of the reinforced northwestern wall took place later than the original southeastern wall, a

few seconds after the termination of earthquake excitation. Related deformed model results are presented in Figure 4.4.

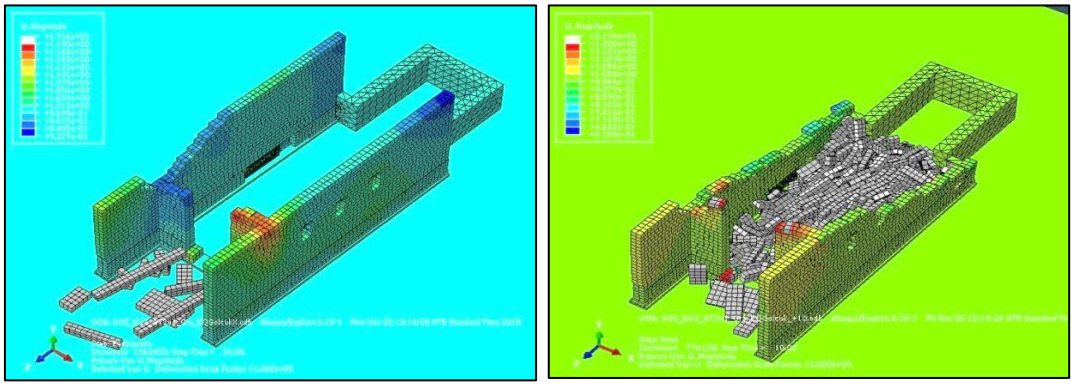

(a) (b)

Figure 4.4: Application of Izmit 1999 earthquake record. Lateral walls maintain integrity (a) and collapse almost completely (b).

Similarly with the original model, the ornamented door lintel was observed to collapse with these cases as well. Collectively, these analyses show that rebuilding of the destroyed section on the northern wall definitely increases the seismic performance of it. However, while the structure performs well in the case of ground motions up to a certain intensity, it may collapse completely when subjected to stronger excitations.

The influence of the non-replaced rubble wall section beneath the original northern isolated wall was also revealed by these analyses, where a slight inclination and displacement was observed at the top layer, facing inwards.

Consequently, another model was generated where the rubble wall was completely taken out and replaced with large blocks similar to the original ones at the bottom layers.

Modal analysis of this model showed even more restraint generated for the northwestern wall. The first mode of the structure, previously being the first bending mode of the northwestern wall, was replaced with the first bending mode of the southeastern wall, which remained unchanged (Figure 4.5). The other torsional modes showed a very slight decrease in their periods.

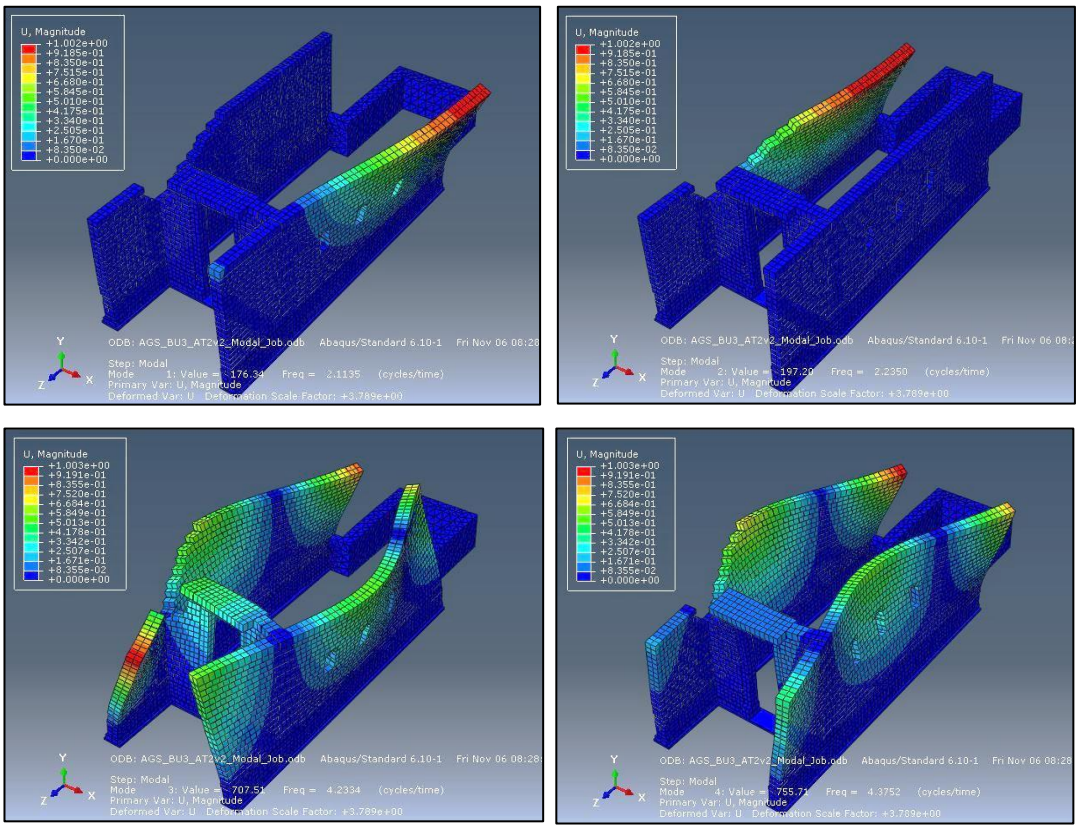

Figure 4.5: Mode shapes and modal periods of the model with stone block replacements. Period values are 0.473s, 0.447s, 0.236s and 0.228s.

Similarly with the previous case, nonlinear time history analyses were carried out to evaluate the performance of this proposal. Results of the analyses, again carried out with earthquake no 412-2475, showed that along with being able to sustain integrity of the structure, the alterations made with this model was successful in dispersing the stress concentrations taking place in the periphery of non-replaced rubble wall,

and the influence it had on the wall's inclination and top displacement (Figure 4.6, (b)). Dispersion of the stress concentrations here also leads to lower stresses observed on the structure, overall (Figure 4.6, (a)) where peak stress is around 1MPa, on the columns supporting the ornamented gate lintel.

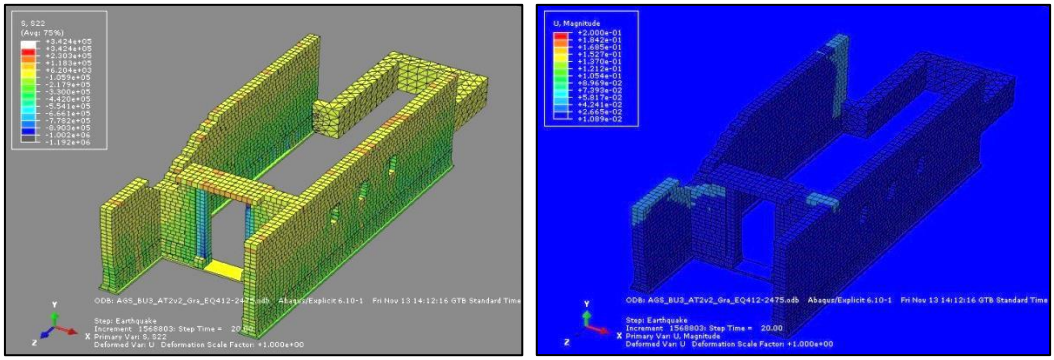

(a) (b)

Figure 4.6: Earthquake no 412-2475 excitation results, stress distributons (a) and displacements (b).

Performance evaluation carried out with Izmit 1999 record on this model, however, produced identical results with the previous case. Deformed models are presented in Figure 4.7. In the Figure 4.7 (b), the collapse sequence can be seen clearly, where while the northwestern wall is inclining prior to collapse, the southeastern wall has already collapsed. Considering the collapse mechanism is triggered from the window openings, this deficiency may be addressed as the culprit for the earthquake resistance capacity.

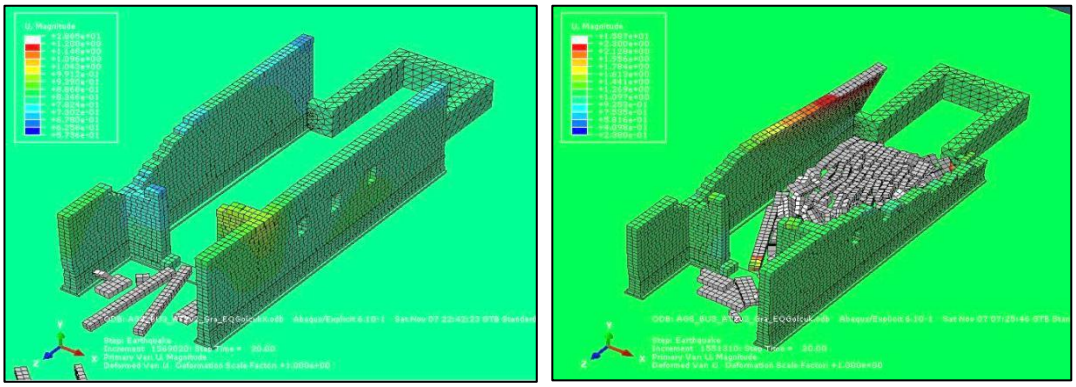

(a) (b)

Figure 4.7: Performance check and collapse mechanism observed under Izmit 1999 earthquake excitation. Lateral walls maintain integrity (a) and collapse in sequence, northwestern wall after northeastern wall (b).

Results obtained from both models demonstrate the increase earthquake resistance capacity of the northwestern wall. However, this local intervention does little to increase the seismic performance of the other parts of the structure. While the other parts maintain integrity by themselves up to a certain point, for higher intensities almost total collapse takes place. Considering the likelihood of this intense an earthquake taking place in the region is low, this strengthening proposal may be considered satisfactory.

In the real application of this proposal on the field, in order to be compatible with the construction technique employed in the original temple and as it is a requirement of ICOMOS Charter (2003), which states that “the value of an architectural heritage is not only in its appearance, but also in the integrity of all its components as a unique product of the specific building technology of its time”, “Opus Revinctum” method must be used in the reconstruction. Considering the difficulties in applying the traditional method of placing iron as the connector and pouring in molten lead resulting from the lack of labor experienced in the application of this method (basically nonexistent), and the dangerous nature of the materials used, a set of new options were laid down by Schueremans et al. (2003).

These options were designed to fulfill the very important requirement in order to achieve a robust connection, which is the encapsulation of the iron connector by lead. This will provide the required corrosion resistance, durability, and the necessary stiffness and strength to the joint.

1. Employing corrosion resistant steel: This is the most basic modern alteration that can be made to eliminate corrosion and negative effects induced by it. However even this is type of steel will not resist corrosion indefinitely, and may suffer from local corrosion. Therefore it is the best to make sure that the steel is covered fully by lead.

2. Application of epoxy with glass fiber bars: Glass fiber is a corrosion resistant material with a linear expansion value in the order of stone (12 μm/m°C), it also has high strength (500-1000 MPa) and relatively low stiffness (40000 MPa). Moreover, epoxy is a highly customizable material with low viscosity, a suitable filler material for the joints which also provides good adhesion, which means good transfer of loads. Good adhesion, however, presents a problem. It makes "reversibility", a criteria that must be satisfied in restoration works difficult, if not impossible. In addition, glass fiber bars fail in a brittle way when subjected to forces perpendicular to the direction of the fibers.

3. Utilization of titanium bars with mortar: Titanium has similar characteristics with glass fiber in terms of its expansion value (8.5 μm/m°C), stiffness (100000MPa) and strength (400-900MPa). Encasing it in mortar provides the necessary protection to provide adequate corrosion resistance. Working with mortar is also much easier than working with epoxy or molten lead. When these materials are utilized, care must be taken in the design process to obtain a joint that is weaker than the stones themselves so that the joint will not lead to the cracking of stones under excessive loading. One drawback is the high price of titanium; therefore usage of this combination is more suited to smaller restoration works.

4.1.2 Reassembly of the Opisthodomos Wall

The second method proposed for the strengthening of the temple was inspired by the seismic performance enhancing effect the Byzantine era crypt walls had on the southeastern lateral walls', as revealed by the analyses results given in Chapter 3. With this proposal, the opisthodomos wall, destroyed when the temple was converted into a church in the 6th century, is suggested to be reassembled in its former location, as a steel truss system. This truss system is supposed to support both the northwestern wall and the southeastern wall in their out-of-plane directions, forming and I shaped plan, resulting in a much more stable structure overall.

The system was designed to be light and slender, as a result of the related conservation committee decision on the Temple of Augustus that requests any permanent strengthening system to take up as small volume as possible. Built in its place left vacant by the destroyed opisthodmos wall, whose traces can still be seen on the lateral walls, the steel truss system is considered to be made up of 3 bays and 3 stories, with braces on each one. It is planned to constitute 2 such identical planar sections, placed at 1 meter away from each other. Middle and middle-bottom segments are designed to be left empty, without braces, in order to serve as a copy of the existing gate section and also allow sightseeing possible in the interior of the temple.

The performance of the temple with this modification was put to the test with a linear elastic model in SAP2000 software and also with the discrete element analyses in ABAQUS software. Prior to the generation of the aforementioned models, the element cross sections were determined with a preliminary hand calculation based on *Equivalent Earthquake Load Method*, defined in Turkish Earthquake Code (2007) Section 2.7 that considers the load generated by the northern isolated wall in the case of an earthquake.

Modal analyses in Chapter 3 and the ambient vibration measurements had resulted in a first period of ~0.75s for the northern isolated wall. Considering the seismic zone of Ankara as Zone 3 (which gives effective ground acceleration coefficient, A_0, as 0.2), and soil condition conservatively as Z3, the static lateral forces on the wall were calculated with the below formulas.

$$A(T)=A_0 * S(T) \quad (2)$$

Where A_0=0.2

I=1

S(T)=2.1 for T_A=0.15 sec. & T_B=0.6 sec.

A(T)=0.42

Reduction factor, R, for the wall was assumed as 1, to be on the safe side since the ductility of the wall was questionable. The total weight of the wall was calculated as:

$$W = \gamma * Volume * g \quad (3)$$

$W = 2.7\ ton/m^3 * 11m * 11m * 0.9m * 9.81m/s^2 = 2884.4\ kN$

$$V_t = (W * A(T))/R(T) \quad (4)$$

$V_t = 2884.4\ kN * 0.42 = 1211.3\ kN$

This calculated base shear was distributed to the height of the wall as a reverse wedge, and considered to be acting directly on the truss system. As a result of a simple conservative calculation, the sections of the truss were determined as:

1. Double channel section on the extreme ends in order to ease connection with the wall, with 0.3m outside depth and 0.2m outside width and 2.5cm uniform thickness,

2. 26ϕ3, 26ϕ2 and 26ϕ1 pipe sections for the intermediate columns and main beams, with thickness decreasing with height at each story,
3. 15ϕ1 for the top story braces and 15ϕ2 for the bottom two stories.

This proposal considers the tilted northern wall to be straightened back up with the help of a jack system, prior to its construction. A visualization of the proposal is provided in Figure 4.8 as a transverse cross sectional view.

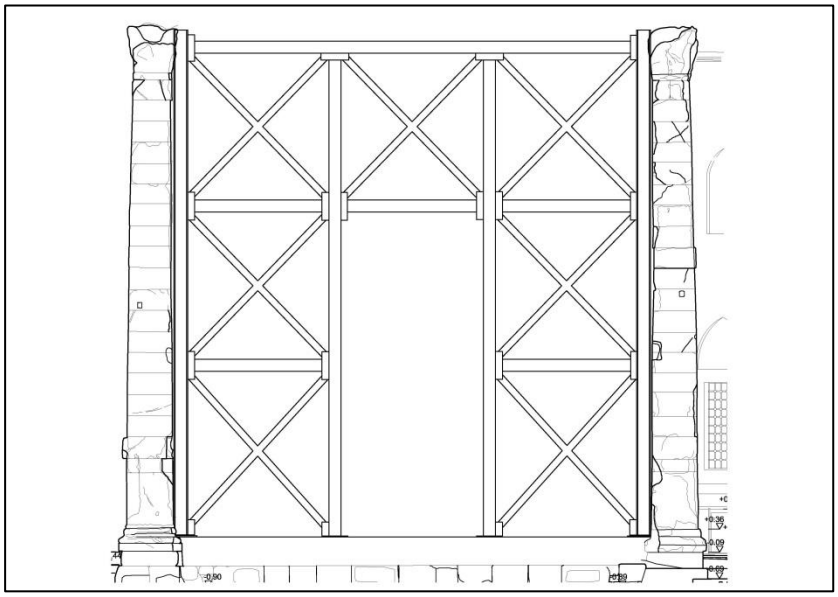

Figure 4.8: Visualization of the proposed truss system, opisthodomos axis.

The linear elastic model of the proposal was obtained with necessary modifications applied on the original model presented in Chapter 3. The truss system was connected to the walls by means of restrains in all directions. The system was tested by with response spectrum analysis, along with a time history analysis conducted with earthquake record no 412-2475. This model considers the rubble wall section beneath the northern isolated wall as not replaced. Analysis results from the response spectrum analysis are presented in Figure 4.9. Time-history analysis results are shown in Figure 4.10.

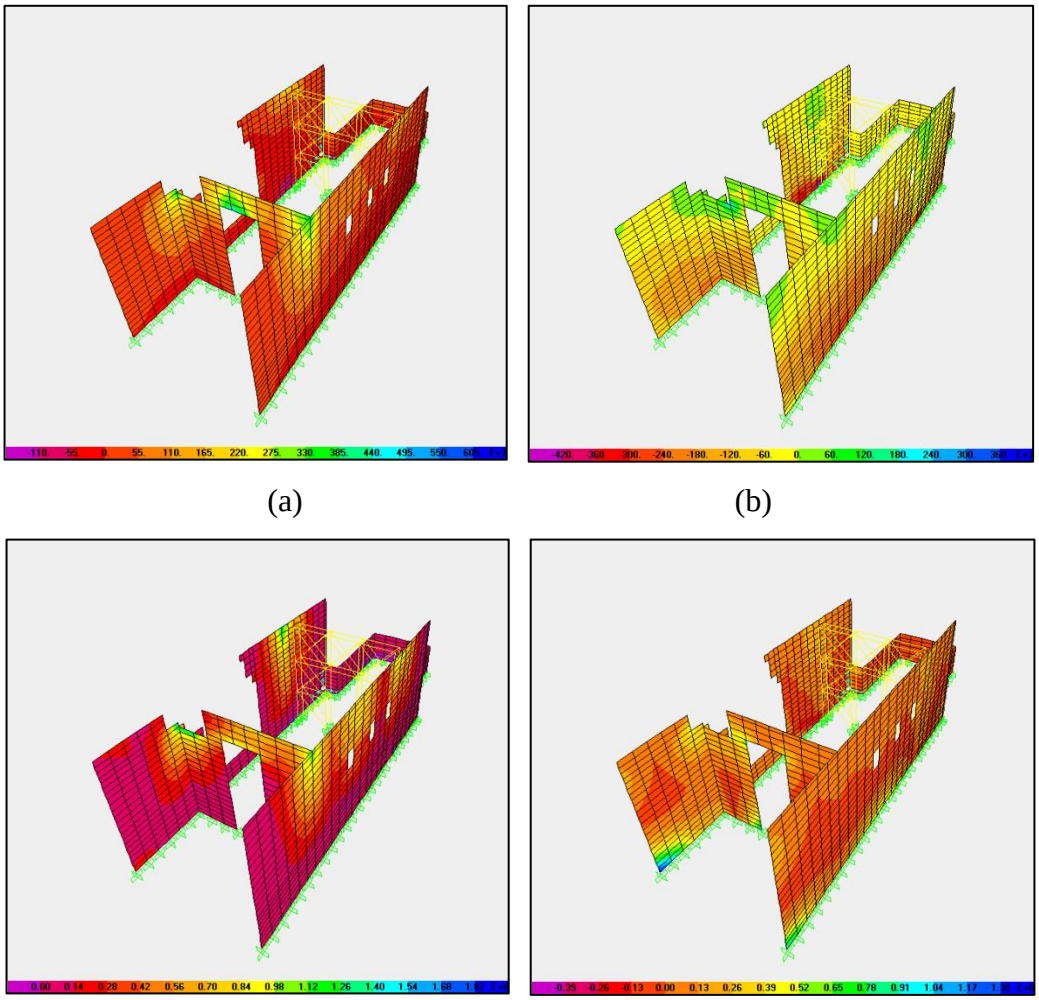

(a) (b)

(c) (d)

Figure 4.9: Response spectrum analysis results, with longitudinal direction application results S11 (a) and S22 (b) in top row, and transverse direction application results S11 (c) and S22 (d) in bottom row. Units in Pa.

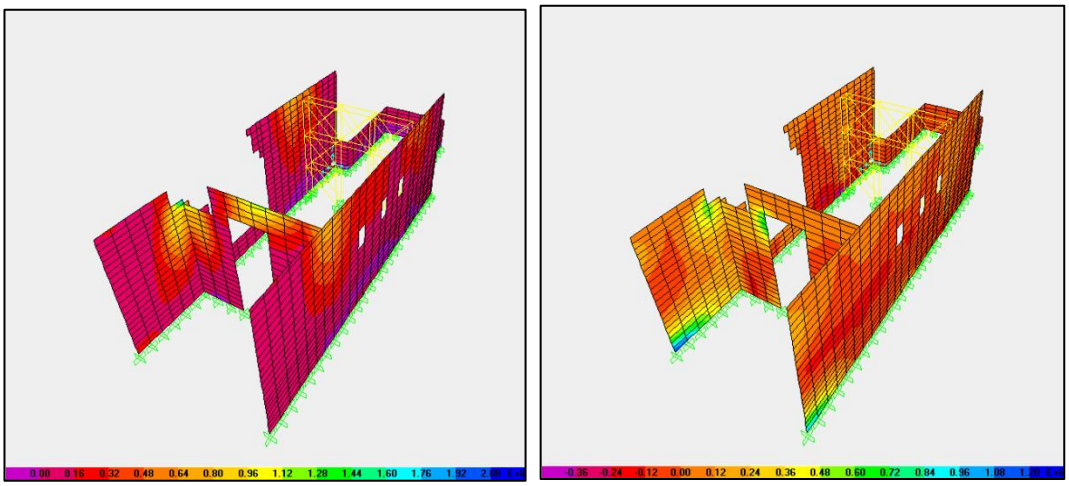

(a) (b)

Figure 4.10: Time-history analysis results with earthquake no 412-2475, S11(a) and S22 (b). Units are in Pa.

Linear elastic finite element model analysis results showed that the reassembly of the opisthodomos wall proposal was successful at dissipating the stress concentrations took place beneath the isolated northern wall in the original model, reducing it to the order of 200-300kPa tensile stress. Overall the model, tensile stresses reaching up to 1.5MPa was observed, but this type of model makes it impossible to make out the damage that this stress may induce. On the truss system, stress levels ranging from 25MPa in the double C sections to as low as 5MPa compressive stress on the braces were detected.

Some stress concentrations were also detected at the ornamented gate lintel, similar with the original model. However, its collapse risk or propagation could be revealed or made certain with this type of model. More detailed analyses were carried out in the discrete element model.

For the discrete element model created in ABAQUS, two different alternatives were considered. Similar to the previous proposal, they account for the rubble wall section halfway beneath the northern wall either left as-is, or replaced with large stone blocks similar to the existing ones. The connection of the truss system to the walls was again realized by means of constraints. These constraints were applied to the blocks in alternating pattern: On each wall, the topmost layer was constrained, and the next (one below) layer was left unconnected, only for the next layer to be connected again, and so on. Finally a shallow foundation was created similar to the existing one, placed at the surface with a depth of ~60 cm.

Figure 4.11 shows the mode shapes of the model where the rubble wall was left intact. The original first and second modes, which corresponded to the first bending modes of the northern isolated wall and the southeastern wall, were replaced with torsional modes of the northern isolated wall and that of the temple itself. Suppression of the original bending modes hints at the effectiveness of the support in generated by the truss system for these lateral walls. The modal periods for the first four modes were found as 0.255s (northern isolated wall torsion), 0.229s, 0.216s and 0.206s. When compared with the modal periods of the previous two proposals, a decrease in all values can be spotted. This can be attributed to the increase in stiffness with this proposal in comparison with the previous ones.

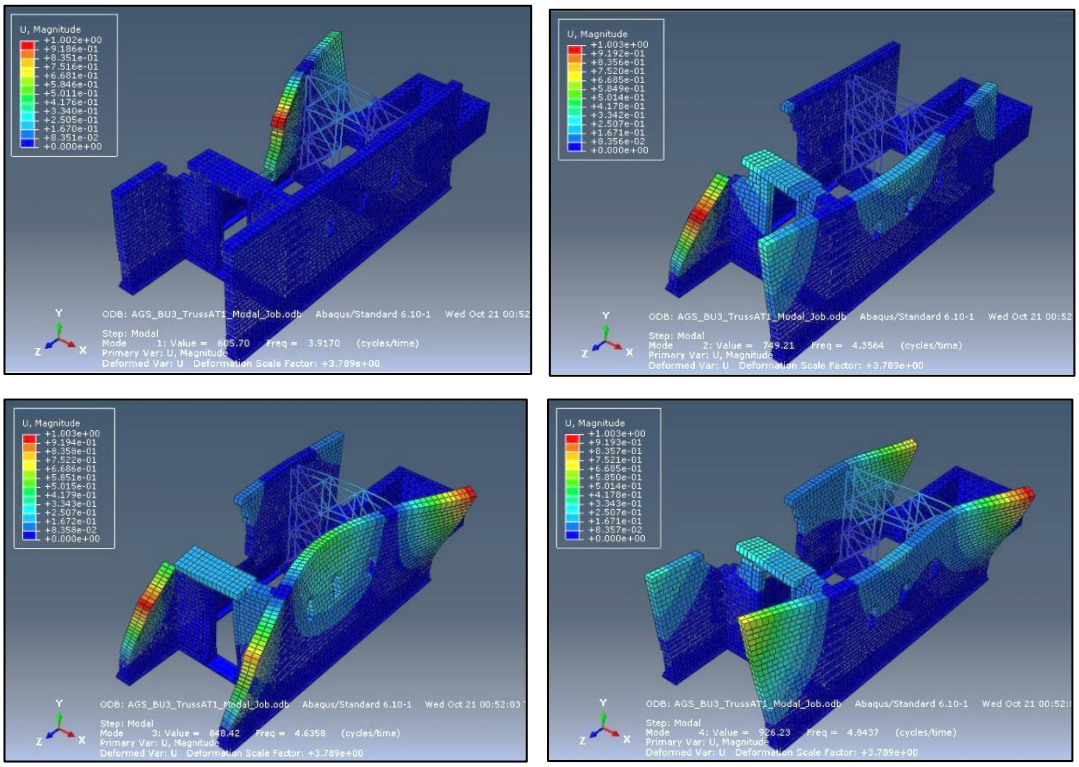

Figure 4.11: First four mode shapes of the strengthening proposal envisioning the construction of steel truss system without the rubble wall's replacement.

Time history analysis results of this model with earthquake no 412-2475 showed that the proposal is successful in preventing the collapse of the walls. However, due to lack of support beneath it, the southern end of the northern isolated wall again demonstrated the tilt problem; with the final displacement at the top layer occurring at around 15cm (Figure 4.12, (a)). Maximum compressive stresses occurred on the blocks remained at the order of 1 MPa, with some blocks at the upper layers experiencing small amounts of tension. On the truss system, low levels of stress were observed, in the order of 15 MPa (Figure 4.12, (b)).

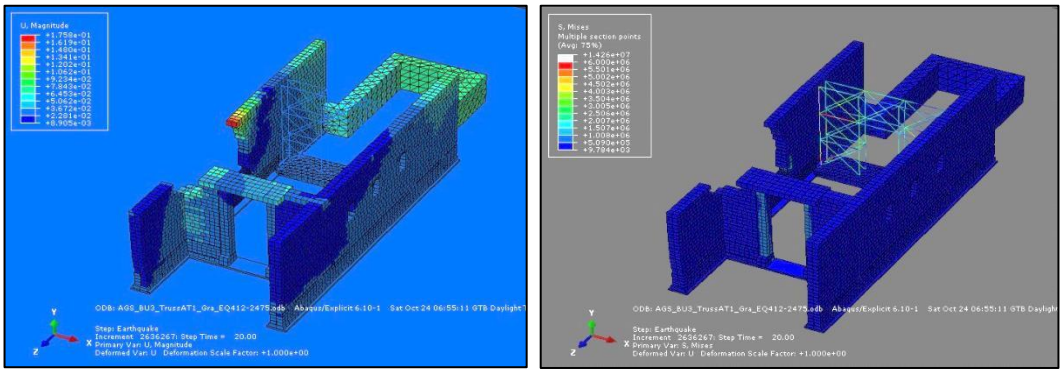

(a) (b)

Figure 4.12: Earthquake no 412-2475 excitation results, deformed model showing displacements (a) and stress distributions (b).

Following a similar approach with the previous proposals, the modal was subjected to 1999 Izmit earthquake for its performance evaluation. Contrary to the previous proposal's performance, the strengthening system was able to protect the lateral walls' integrity for this high intensity ground motion. A similar tilting of the northern wall was observed in both cases with the analysis carried out using earthquake no 412-2475. Deformed models are provided in the Figure 4.13.

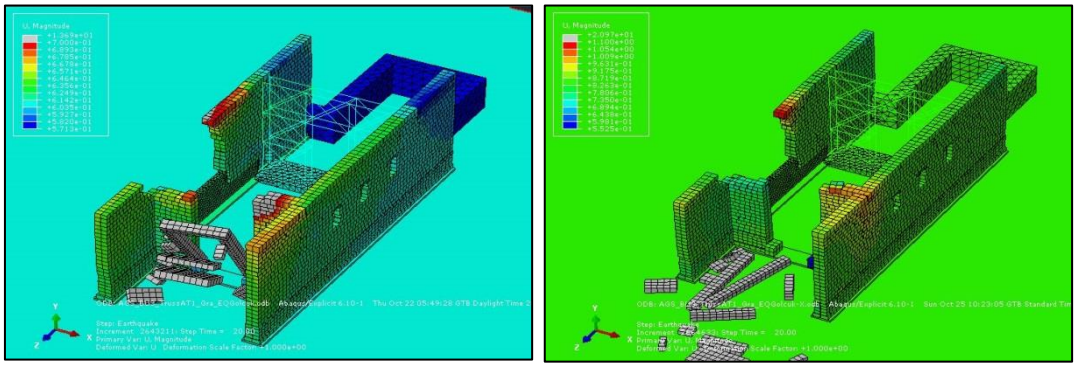

(a) (b)

Figure 4.13: Performance check results with Izmit 1999 earthquake excitation. The ornamented gate lintel shows some resistance, southern tip of the northern isolated wall tilted (a) and ornamented gate lintel collapsed, southern tip of the northern isolated wall tilted (b).

As briefly mentioned beforehand, in order to observe the effect of the replacement of the rubble wall part, only beneath the northern isolated wall, a corresponding model was created. In this model, the rubble wall was replaced with 3 large blocks of identical sizes. Prior to the time history analyses, the modes of the structure were obtained (Figure 4.14)

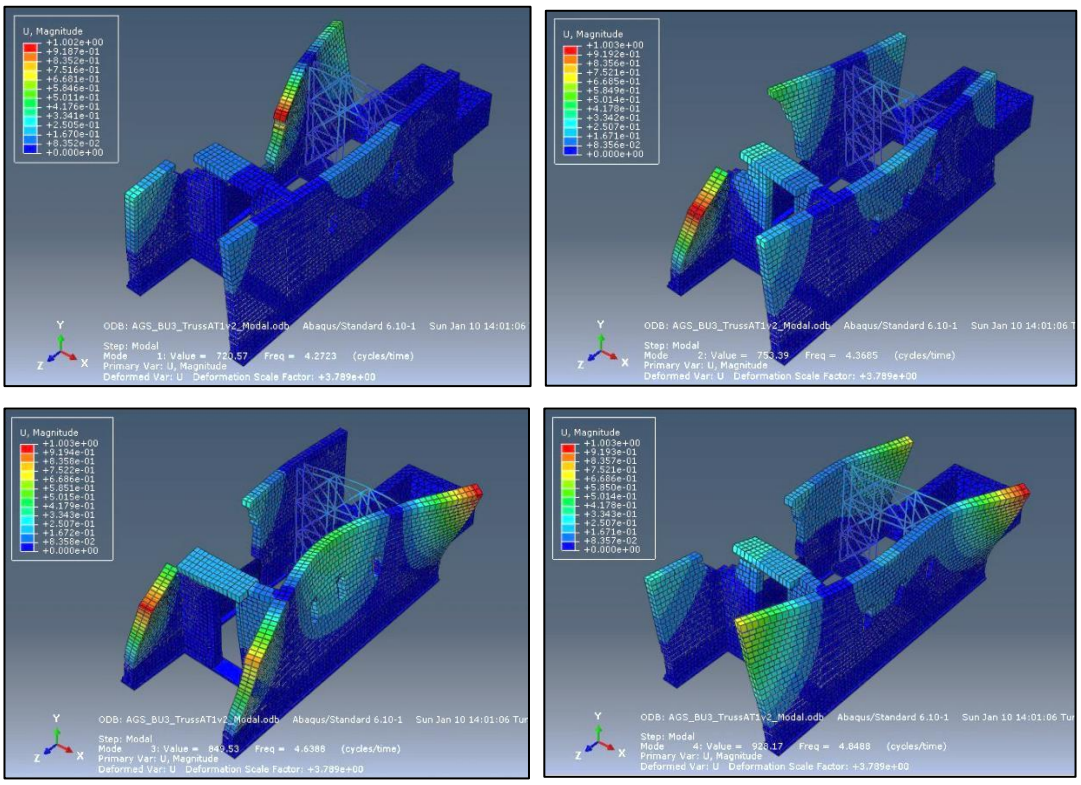

Figure 4.14: Mode shapes of the structure with rubble wall replacement and the truss system

Modal analysis yielded similar results, with slightly smaller modal periods, where a further notable decrease observed with the first mode which is solely related to the northern isolated wall, decreasing from 0.255s from the previous model to 0.234s in this one. Other period values remained almost the same: 0.229s, 0.215s, and 0.206s. This was expected since the change between two models is very local and only affects the northern isolated wall.

Using the same records as before, namely record no 412-2475 and Izmit 1999 record, a final set of time history analyses were conducted on this model. Results obtained from the analysis with record no 412-2475 showed that the replacement of the rubble wall beneath the northern isolated wall solved the tilting problem, similarly with the same case of the previous proposal. At the end of the analysis, ornamented gate lintel was deformed, but not collapsed. Gaps were formed at the extreme ends of the top layers, but collapse of block fall did not take place (Figure 4.15(a)). Stresses were calculated to be similar with the previous case (Figure 4.15(b)).

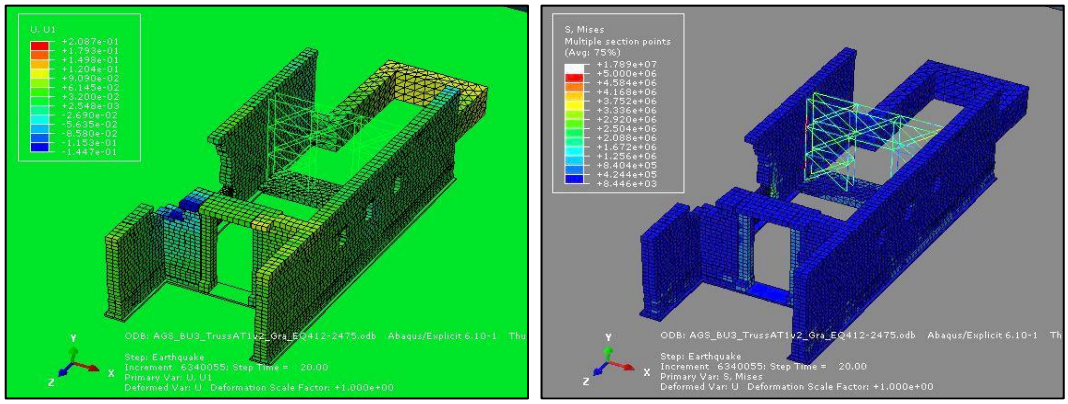

(a) (b)

Figure 4.15: Earthquake no 412-2475 excitation results: Displacements (a) and stress distributions (b).

Results of the analyses with the Izmit 1999 records yielded results that are similar, but somewhat better than the non-replacement counterpart of this model. Even though the ornamented gate lintel collapsed when the horizontal component directions of the earthquake were interchanged, it heavily deformed but avoided collapse in the initial directional setup (Figure 4.16 (a)). However, in real conditions, it would have surely collapsed, considering its deteriorated and damaged actual form. In both models, lateral walls again resisted collapse, and no

tilt took place in the northern isolated wall. Both results are presented in Figure 4.16.

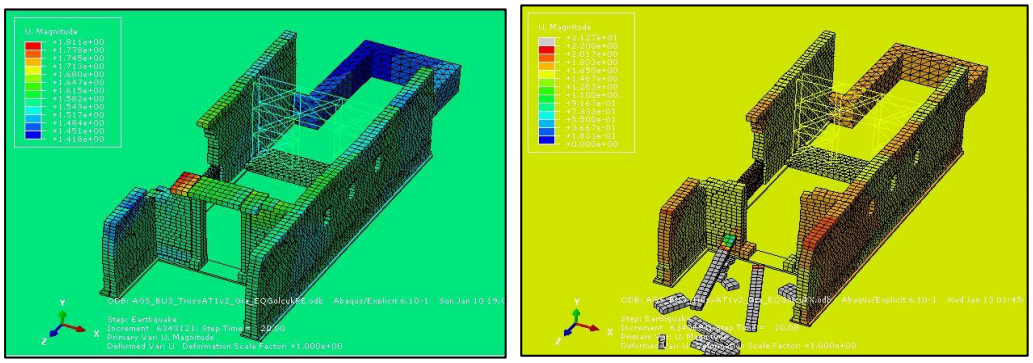

(a) (b)

Figure 4.16: Performance check results with Izmit 1999 earthquake excitation. The ornamented gate lintel resists collapse (a) and collapsed ornamented lintel, local dislocations at top layers (b).

The proposed strengthening system with the truss wall was successful in preventing the collapse of the structure, and was able to increase the overall stability as it is also connected to the southeastern wall. However, at the southwestern end of the northern isolated wall, the top layers extrude from the rest of the wall, and constitute a hazard for the visitors and also the temple wall itself. Even though they did not fall down as a result of the analyses, as inspected during the site visits, they are in a much deteriorated condition and there is a high chance that they will actually fall down in the case of a seismic activity. The reason to their stability during the analyses may be attributed to the "perfect" nature of the discrete element model, where it was impossible to imitate the small cracks and openings, also the tiny distances present at the actual case. Moreover, all blocks were again modelled as flawless rectangular parallelepipeds, which is again not the actual case. These issues result in a much higher contact surface and consequently, a higher restoring frictional force on the model, leading to stability not fully reflecting the truth.

Therefore, if this proposal is ever considered for actual implementation, those blocks must be restrained by means of steel braces connecting them to the rest of the blocks from their top faces. Another application might be the erection of a truss system similar to the proposed one, but on a much smaller scale, protruding from the interior and exterior of the wall to support these blocks. A final resort might be removal of these three most critical blocks. Even though it is not the best option, this will allow the investigation and better understanding of the brace system (Opus Revinctum). Conduction of material tests for further studies may also be possible with this option.

With the structural performance of the intervention methods laid out in this section, a superior overall seismic performance was observed with the installation of a truss wall at the opisthodomos wall location when compared to the northern wall rebuilding option. Moreover, in both cases, the tilting problem continued to manifest to a certain degree when the rubble wall beneath the northern isolated wall was not replaced.

In addition to the proposals and analyses presented in this section, another set of analyses were carried out with this proposal, where the tilted northern isolated wall was not assumed to straightened back to its original place. Details and results of this set of analyses can be found in Appendix B.

In Table 4.1, a comparison of the proposals from the conservation point of view is presented, complimentary to the structural evaluation comparisons given in this section. In this comparison, the principles laid out in ICOMOS Charter of Principles for the Analysis, Conservation and Structural Restoration of Architectural Heritage (2003) and Venice Charter (1964) was considered as a basis.

Table 4.1: Comparison table for intervention proposals from modern preservation concept point of view

		Venice Charter (1964)					2003 Recommendations
		Main aim of conservation, not to mask the historical features & evidence of ancient heritage	Article 6: No out of scale construction or modification allowed that will alter mass and color	Article 9: Preserve and reveal the aesthetic and historic value of the monument	Article 10: Modern techniques instead of traditional ones, with its effectiveness shown by scientific data	Article 12: Replacements must integrate harmoniously, but also must be distinguishable	Articles 3.5 & 3.9: Measures adopted should be reversible and kept at a minimum
Intervention Proposals	Northern Wall Rebuilding, **No** Rubble Wall Replacement	No such negative effect	Rebuilding is envisaged, but not out of scale	No adverse effect on aesthetic value	Uses traditional methods, with new material alternatives proposed, but tilting problem carries on	In harmony with existing structure, but different color blocks must be used	Reversibility may be difficult due to iron connectors and patching up of cracked blocks
	Northern Wall Rebuilding, **With** Rubble Wall Replacement	No such negative effect	Extensive rebuilding and replacement that may or may not be considered out of scale	No adverse effect on aesthetic value	Uses traditional methods, with new material alternatives proposed, no tilting problem	In harmony with existing structure, but different color blocks must be used	Difficult to reverse due to rubble wall replacement and iron connectors
	Opisthodomos Wall Reassembly **No** Rubble Wall Replacement	Designed as a large truss wall, but does not block view or hinder access	The large truss wall is an alteration	Truss wall has some adverse effect aesthetically	Modern technique with superiority shown by analyses; however, tilting problem continues	May be considered harmonious since built at the opisthodomos wall location	Truss wall may be dismantled but some intallation marks and holes will be left on the walls
	Opisthodomos Wall Reassembly, **With** Rubble Wall Replacement	Designed as a large truss wall, but does not block view or hinder access	Alteration induced by truss wall and also modification by means or replacement	Truss wall has some adverse effect aesthetically	Modern technique with superiority shown by analyses, and tilting problem ceases to exist	Replacement is harmonious and wall location can be considered appropriate	Similar with the above, but more difficult to completely remove due to rubble wall replacement

4.2 Considerations with the Ornamented Gate Lintel

The ornamented gate lintel on the southwestern gate section on the temple is in a damaged and deteriorated state. Moreover, even in the DEM analyses where it was modelled ignoring its cracks and defects, the lintel proved unstable and prone to collapse. It is considered that this section, previously tried to be intervened with metal straps, should be taken down in a controlled manner by means of cranes, and the state of damage and structural condition investigated. In the light of the existing information, as a remedy, the steel straps are to be removed and the lintel block, where loss of material is evident, should be patched up or replaced with a block with a similar property with the existing ones. Moreover, if the steel braces are corroded or nonexistent, they are to be recreated. As a part of the remedy, the existence of iron connectors between the gate columns and the walls are also to be investigated, since DEM analyses revealed a collapse propagation triggered by an instability in their behavior.

CHAPTER 5

DISCUSSION OF RESULTS AND CONCLUSIONS

In this thesis, a multistep approach was adopted for the structural analysis, evaluation and strengthening of the Temple of Augustus in Ankara. In the initial step, an identification study was carried out focused on the architectural and structural features of the structure. This was continued and enhanced with the site surveys aimed at capturing the behavior of the structure with ambient vibration measurements, collecting long time monitoring data, and also carrying out non-destructive tests to estimate the material conditions; in addition to understanding and discretizing the monument's geometry to the last detail by defining dimension of each piece also by looking at the as-built drawings. These studies were followed by the construction of analytical models, which were calibrated with the data obtained from the real structure. These models were used to determine the earthquake resistance capacity of the structure, along with its collapse mechanisms. At the final step, based on these results, a series of strengthening alternatives were proposed and their performances were evaluated under several selected earthquake records with the help of analytical models.

Investigations carried out at the site, especially those that focused on the damaged parts of the structure, verified that the method used in the construction of the temple, is indeed, "Opus Revinctum", where iron connectors would be placed in between the masonry units and encapsulated with molted lead. This was clearly indicated by the "slots" visible on the block surfaces, whose detection was made possible only by climbing the northern isolated wall. This special trait of the

structure provides it with extra robustness, and its presence was taken into consideration during the strengthening proposals.

Post processing of the measurements collected by the previously installed structural health monitoring system revealed the relation of the northern isolated wall's tilt, and the daily temperature cycles. However, considering that site visits also showed the contact between the emergency intervention system and the wall, it was discussed that these cycles were induced on the wall by the thermal expansion of the steel truss system, rather than by the wall itself.

Comparison of the ambient vibration measurements taken in this study with those taken as a part of a previous study by Turer and Eroglu (2006) indicated 41.3% and 13.4% drops in the northern isolated wall's modal periods. This decrease in the modal vibration periods were explained by the contact initiated between the wall and the emergency intervention system, resulting in restrains for the northern isolated wall.

A discrete element model was created using ABAQUS software featuring a high degree of geometrical accuracy where each single block was modelled individually with their actual sizes. This model, constituting ~1000 elements, successfully simulated the nonlinear behavior of the structure; allowing the detection of vulnerabilities and the collapse mechanism of the temple. Criticality and instability of the northern isolated wall was revealed and further studies were carried out accordingly.

The comparison of results obtained from discrete element analysis in ABAQUS and linear elastic analysis in SAP2000 for the models representing the current form of the structure revealed that for such type of structures, linear elastic models fail to realistically simulate and allow prediction of the post-cracking behavior and loss of stability. A model where elements are not modelled individually and friction in between stone blocks is not taken into consideration cannot generate an accurate

representation of the dissipation of energy and displacement. Outputs obtained from such a model will fail at pointing out to vulnerable and fragile areas, making an incorrect diagnosis of problems associated with a structure, and thus, making necessary intervention proposals inaccurate. With that being said, DEM analyses are also open for improvement. The blocks used in the models possess linear elastic properties, which were only determined through the model's calibration with actual vibration data at low deformations. Acquisition of related material properties along with friction characteristics from related tests conducted on actual material at a laboratory would definitely increase the accuracy of results. In this study, due to the special status of the temple, taking material samples and testing them in the lab was not possible. Moreover, since natural materials possess variable properties, there is always an accuracy margin with such analyses. Furthermore, cracking and possible crushing of the blocks during seismic action were not taken into consideration with the selected material model. Similarly, elements constituting the "Opus Revinctum" connections, namely the iron braces and the surrounding lead, were also not modelled. However, effects of braces having a big impact on the accuracy of analysis is arguable since their current condition and their exact layout is unknown; therefore, inaccurate modelling of braces geometrically and strength-wise may have led to unreliable results. Even though an optimization for mesh density was carried out in this study, a finer mesh would result in a better simulation of the actual case. All these issues also require an exceptional computational capacity and time, since the analyses carried out with parameters used in this study would still take more than a day to complete.

Two main strengthening proposals were brought forward, based on the performance evaluation results of the temple's current form. Each proposal had two variations, which are a) considering the removal and b) replacement of the rubble wall section beneath the northern isolated wall with marble blocks having similar sizes to existing blocks. Analyses results showed that both of the proposals were successful in increasing the temple's seismic performance. However, since the steel support system proposed to be installed at the old opisthodomos wall location will be

connected both to the northern and southeastern walls, increasing the overall capacity, it proved to be a better alternative compared to the "northwestern wall rebuilding" proposal. Moreover, even though the structure was unable to resist high intensity earthquake excitations of Mw=7.5 (Izmit 1999) with the "northwestern wall rebuilding" option, the steel truss system was able to provide the structure with enough support where lateral walls remained almost intact under the same severe earthquake loading conditions. In both strengthening cases (truss system at the opisthodomos wall location and northwestern wall rebuilding), the replacement of rubble wall affected the behavior of the northern isolated wall where the inward tilt would take place again, if the rubble wall was not replaced.

As a part of the study, along with the strengthening alternatives proposed for the lateral walls, a suggestion was also made for the prevention of collapse hazard of the ornamented door lintel. This suggestion envisaged the group of blocks constituting the ornamented lintel to be taken down, investigated and necessary replacements in the iron connectors and the blocks themselves carried out before its reinstallation on its original location back again.

It is considered that, along with a structural performance enhancing intervention to the structure focused on this study, the construction of a roof structure that will protect both the temple and also the invaluable carvings of *Res Gestae* is also an imminent requirement for the well-being of the temple and its riches. Moreover, finding a permanent solution for support with lime stone based footings and removal of existing temporary support with Portland cement base might be beneficial in the long run.

As for the proposals, the composite action between the steel truss wall proposed to be installed at the old opisthodomos wall location and old northern and southern walls will be necessary for shear transfer and rocking in the out-of-plane direction towards outside the temple. Thermal expansion of the proposed steel truss wall would also lead to some pull and push on the northern and southern walls on daily

and seasonal temperature cycles. Therefore, the steel used for the proposed truss wall system should be selected to have a low thermal expansion coefficient. Providing protection against direct sunlight would also be useful.

REFERENCES

ABAQUS 6.10 (2010). User's Manual. Dassault Systemes

ABAQUS 6.10 (2010). Theory Manual. Dassault Systemes

ABAQUS 6.10 (2010). Keywords Reference Manual. Dassault Systemes

American Society for Testing and Materials. C 597 – 02 Standard Test Method for Pulse Velocity Through Concrete (2002). http://doi.org/10.1520/C0597-09

Anadolu Medeniyetleri Müzesi. (2009). Retrieved December 22, 2015, from http://www.anadolumedeniyetlerimuzesi.gov.tr/belge/1-55043/augustus-tapinagi.html

Augustus, C. (14BC). Res Gestae Divi Augusti. Retrieved December 22, 2015, from http://www.livius.org/ra-rn/res_gestae/res_gestae01.html

AUTOCAD, 2013. AutoCAD Version 2013, Autodesk Inc.

Botteri, P., Fangi, G., & Trieste, U. (2000). the Ancyra Project : the Temple of Augustus and Rome in Ankara. *The International Archives of the Photogrammetry, Remote Sensing and Spatial Information Sciences*, *XXXIV*, 84–88.

Çördük, A. (2006). *Yunan ve Roma Mimarisindeki Yapı Teknikleri*. Ege Universitesi.

Dereli, H. (1949). *Ankara Anıdı Monumentum Ancyranum.* Milli Eğitim, Ankara.

Eck, W. (2007). *The age of Augustus* (2nd ed.). Oxford: Blackwell.

Ehrenberg, V., & Jones, A. H. M. (1976). *Documents Illustrating the Reigns of Augustus and Tiberius*.

Erberik, M. A., 2014. Analysis and Design of Structural Masonry Lecture Notes, Ankara, Turkey

Fowler, H. W., & Fowler, F. G. (1905). *The Works of Lucian of Samosata*. Oxford: The Clarendon Press.

Gliven, S. (2014). the Res Gestae Displaying of Augustus A Monument Image for All. *Journal of the Society of Architectural Historians*, *57*(1), 30–45.

Gökdemir, A., Demirel, C., Yeğin, Y., & Şimşek, Z. (2015). Ankara Temple (Monumentum Ancyranum/Temple of Augustus and Rome) restoration. *Case Studies in Construction Materials*, *2*, 55–65. http://doi.org/10.1016/j.cscm.2015.02.002

Greenhalgh, M. (2013). *From the Romans to the Railways The Fate of Antiquities in Asia Minor*. Canberra: Australian National University. Retrieved from http://www.brill.com/romans-railways

Hammond, N. G. L., & Walbank, F. W. (1972). A History of Macedonia: 336-167 B.C.

ICOMOS International Council on Monuments and Sites (2003). Principles for the Analysis, Conservation and Structural Restoration of Architectural Heritage. Victoria Falls, Zimbabwe

ICOMOS International Council on Monuments and Sites (1964). International Charter for the conservation and restoration of monuments and sites (The Venice Charter 1964). *IInd International Congress of Architects and Technicians of Historic Monuments*

Kadioğlu, S., & Akyol, A. A. (2008). Augustus tapinaği arkeometrik incelemeleri kapsaminda jeofizik çalişmalar. In *Kültür ve Turizm Bakanliği, Kültür Varlıkları ve Müzeler Genel Müdürlüğü, 25. Arkeometri Sonuçlari Toplantisi* (pp. 431–440).

Kadioğlu, Y. K., & Akyol, A. A. (2008). 2008 YILI ARKEOMETRİK ÇALIŞMALARI. *Kültür ve Turizm Bakanliği, Kültür Varlıkları ve Müzeler Genel Müdürlüğü, 25. Arkeometri Sonuçlari Toplantisi*, 441–458.

Kázmér, M., Major, B., Hariyadi, A., & Pramumijoyo, Subagyo Haryana, Y. D. (2010). Living with earthquakes – development and usage of earthquake-resistant construction methods in European and Asian Antiquity. *Geophysical Research Abstracts*, *12*(EGU2010-14244).

Krencker & Shede *(1936). Der Tempel in Ankara*

Laurenço, P. B. (1998). Experimental and Numerical Issues in the Modelling of the Mechanical Behaviour of Masonry. *Structural Analysis of Historical Constructions II*.

Livy (1976). *Rome and the Mediterranean*. (H. Bettison, Trans.). London: Penguin Classics

Marino, M., Neri, F., Maria, A. D. E., & Borri, A. (2014). Experimental Data of Friction Coefficients for some Types of Masonry and its Correlation with an Index of Quality Masonry (IQM). In *Second European Conference on Earthquake Engineering and Seismology* (pp. 1–12).

MATLAB, 2013. MATLABR2013B, MathWorks Inc.

Mistler, M., Butenweg, C., & Meskouris, K. (2006). Modelling methods of historic masonry buildings under seismic excitation. *J Seismol*, (10:497–510). http://doi.org/10.1007/s10950-006-9033-z

NEHRP Consultants Joint Venture. (2011). Selecting and Scaling Earthquake Ground Motions for Performing Response-History Analyses, (NIST GCR 11-917-15).

Nguyen, T. N., & Gjørven, A. (2012). Seismisk analyse / dimensjonering av beholdere / tank.

Perrot, G. & Guillaume, E. (1872) *Exploration archeologique de la Galatie et la Bithynie*

Rankin, D. (2002). *Celts and the Classical World*.

Roca, P., Cervera, M., Gariup, G., and Pela, L. (2010). Structural Analysis of Masonry Historical Constructions. Classical and Advanced Approaches. *Archives of Computational Methods in Engineering*; 17: 299-325

Rose, M. (2000). Central Turkey's Four Capitals. Retrieved December 23, 2015, from archive.archeology.org/online/features/turkey/

Rubene, S., & Vilnitis, M. (2014). Use of the Schmidt Rebound Hammer for Non Destructive Concrete Structure Testing in Field / Wykorzystanie Młotka Schmidta Do Nieniszczących Badań Konstrukcji Betonowych W Praktyce. *Technical Transactions Civil Engineering / Czasopismo Techniczne Budownictwo*, (1-B/2014).

SAP2000, 2011. Structural and Earthquake Engineering Software Version 15.0, CSI.

Schueremans, L., Ignoul, S., Lembrechts, P., Vandewalle, B., Van Gamert, D., & Van Balen, K. (2003). Metal anchors in lead, fundamental approach and alternatives. In *Proceedings of the Sixth International Conference on Materials Science and Restoration* (pp. 333–340). Karlsruhe.

Sezen, H., & Dogangun, A. (2012). Seismic Performance of Historical and Monumental Structures. *Earthquake Engineering, Prof. Halil Sezen (Ed.)*.

Sezen, H., Firat, G. Y., & Sozen, M. A. (2003). Investigation of the performance of monumental structures during the 1999 Kocaeli and Düzce earthquakes. In *Fifth National Conference on Earthquake Engineering*. Istanbul, Turkey.

Swarney, P. (2003). The Accomplishments of Augustus (Res Gestae Divi Augusti). Retrieved from http://www.yorku.ca/pswarney/3130/rg2003-2.htm

Texier, C. (1839) *Description de L'Asie Mineurel*

The Augustus Temple of Ankara. (n.d.). Retrieved December 22, 2015, from https://www.kultur.gov.tr/EN,39515/the-augustus-temple-of-ankara.html

Turkish Ministry of Public Works and Settlement (2007). *Specification for Structures to be Built in Disaster Areas*. TEC2007, Ankara, Turkey

Türer, A., 2013. Structural Health Monitoring Lecture Notes, Ankara, Turkey

Ural, A., & Uslu, S. (2013). Shear tests on stone masonry walls with metal connectors. *European Journal of Environmental and Civil Engineering*.

Vitruvius. (15BC). De Architectura Libri. Retrieved June 5, 2015, from http://www.vitruvius.be

APPENDIX A

PHOTOGRAPHIC ARCHIVE OF THE TEMPLE

A collection of pictures taken at the site, showing its most recent form where the emergency intervention system is present, is provided in this appendix.

Figure A.1: General view from southern vantage point

Figure A.2: General view from the eastern vantage point, holes are visible all around the wall

Figure A.3: General view from the northern vantage point, the northern isolated wall in the front

(a) (b)

Figure A.4: View of the temple interior; from the crypt wall to the gate section (a) and vice versa (b)

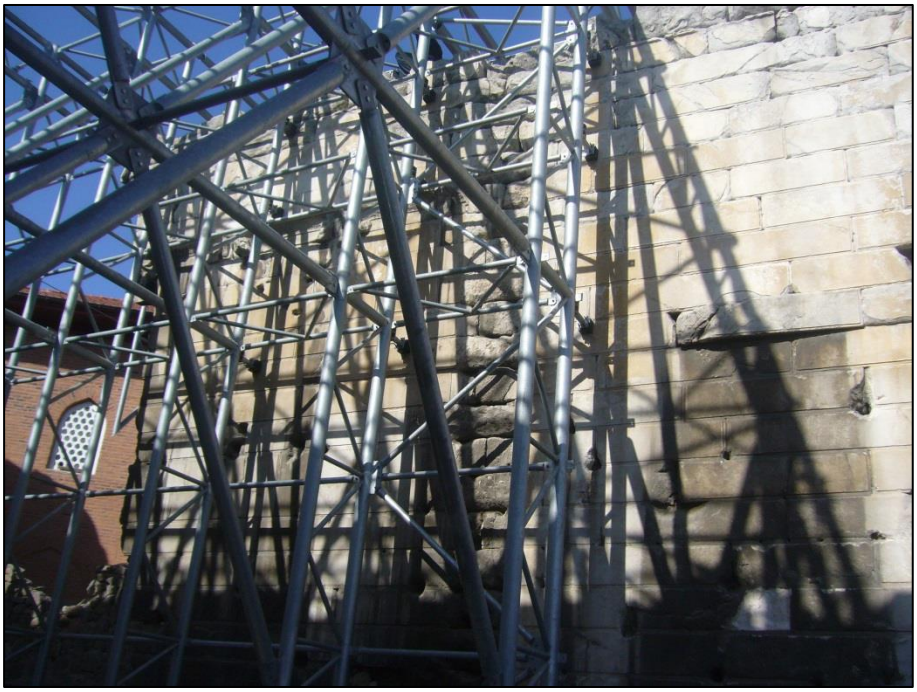

Figure A.5: Northern isolated wall as seen from inside the temple

(a) (b)

Figure A.6: Northern isolated wall, seen from inside (a) and outside (b) the temple

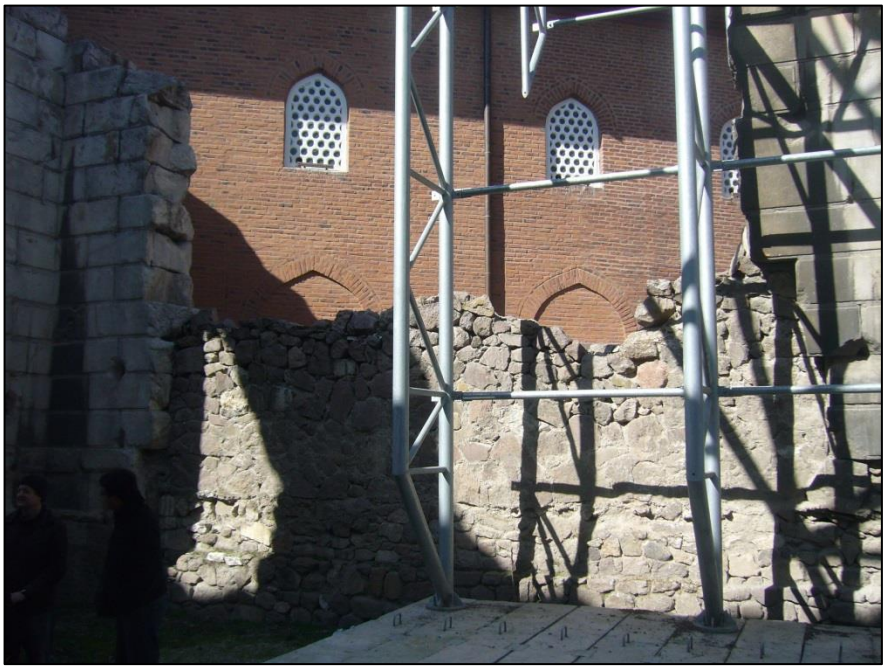

Figure A.7: Rubble wall between the remaining parts of the northwestern wall

Figure A.8: Location of the removed opisthodomos wall, where the deformations left from the removal operation are visible

Figure A.9: Temple from atop the northern isolated wall, looking at the intersection of the southeastern wall and the gate section. The slots where most probably the ancient wooden beams were placed are visible.

Figure A.10: Windows on the southeastern wall and the solar panel of SHM system

APPENDIX B

ADDITIONAL ANALYSES WITH TRUSS SYSTEM

A final set of analyses were carried out that considers the truss wall mentioned in the second strengthening proposal to be constructed without the straightening of the northern isolated wall back to its original position. In this model, the truss wall was modelled compatible with the tilt observed on the wall, and the corresponding displacement of ~0.52 m at the top layer. In accordance with the consideration that it would not be possible for the northern isolated wall to be brought back to its original position, the rubble wall was also left untouched.

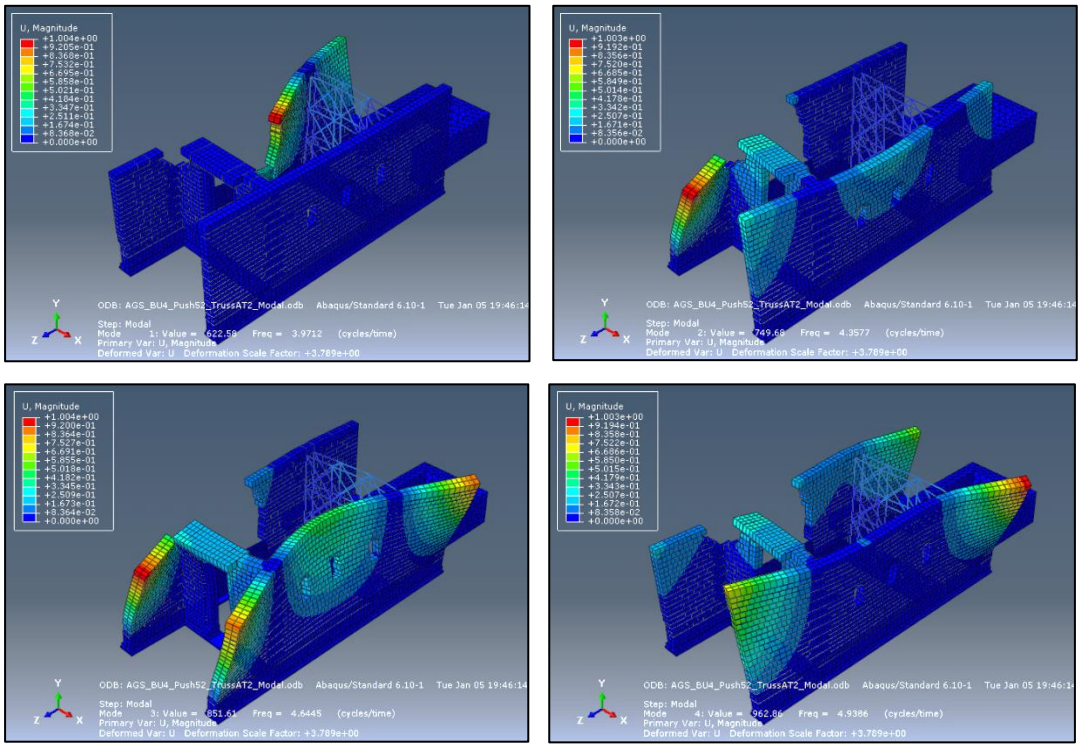

Figure B.1: Mode shapes of the structure with the tilted northern wall and and truss wall modelled as inclined in accordance with it.

The mode shapes of the model are given in Figure B.1. The modal periods were obtained as 0.252, 0.229, 0.215 and 0.202 seconds, which are very similar with the modal periods of this model's straightened north wall counterpart, presented in Section 4.1.2.

This model was also analyzed with the selected ground motion records by means of time-history analysis similar to the previous other analyses. Results obtained from the analysis with record no 412-2475 showed in this model's case that the north wall's maximum tilting of 0.52 m was further progressed by ~0.08 m by the earthquake excitation and reached up to ~0.60 m, but collapse did not take place. The ornamented gate lintel did not collapse, but deformed. Gaps formed between the blocks at the top layers, especially at the wall ends. Similarly with the previous cases, the maximum compressive stresses on the blocks remained in the order of 1 MPa, and small amounts of tension (less than 200 kPa) were observed on some blocks at the top layers. The permanent stresses observed on the truss system demonstrated a small increase where up to ~30 MPa was observed. The deformation and stress results are provided in Figure B.2 (a) and (b).

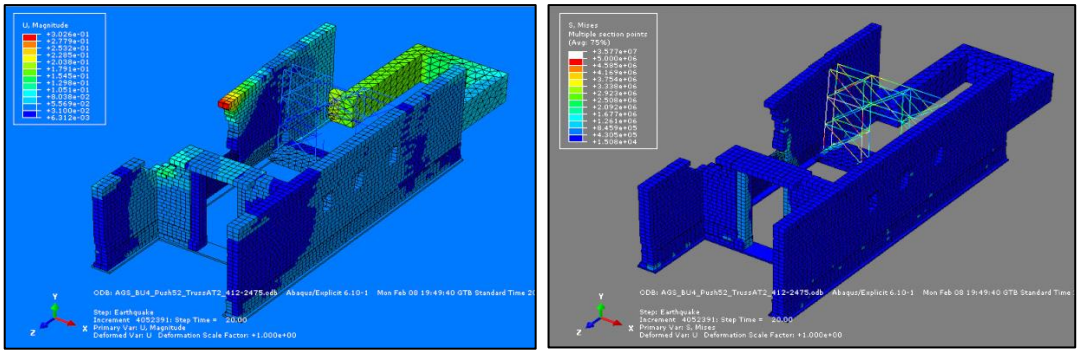

(a) (b)

Figure B.2: Results with earthquake no 412-2475 excitation: Displacements (a) and stress distributions (b).

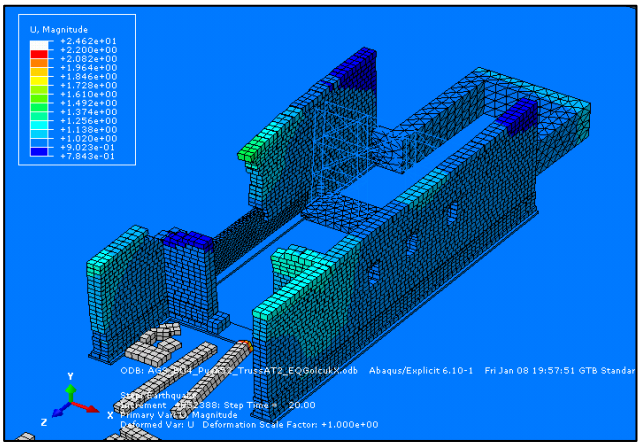

Figure B.3: Performance check result with Izmit 1999 earthquake excitation. The southern tip of the northern isolated wall displays increased tilt and the ornamented lintel is collapsed.

Performance analysis results with the Izmit 1999 record a similar result with the cases where the northern isolated wall was considered to be straightened back to vertical position. Despite the collapse of the ornamented gate lintel, the rest of the structure (Figure B.3) showed a good overall resistance against this intense earthquake. However, even though the blocks at the western end of the northern isolated wall resisted collapse, they are expected to collapse in the real case, due to reasons previously explained in section 4.1.2.

Results of these analyses showed that the "opisthodomos wall reassembly" proposal is very successful in preventing the structure's collapse, even if the earthquake loading is applied without straightening the northern isolated wall back to vertical position. However, it should also be noted that each large earthquake would generate cracks, dislocated stones, residual forces in structural members, and permanent deformations.